AD-A175 006 ASYMPTOTIC SOLUTIONS TO COMPRESSIBLE LAMINAR BOUNDARY-LAYER SOLUTIONS FOR (U) TORONTO UNIV DOWNSVIEW (ONTARIO) INST FOR AEROSPACE STUDIES B Y WANG ET AL AUG 86 UTIAS-310 1/1

UNCLASSIFIED F/G 20/4 NL

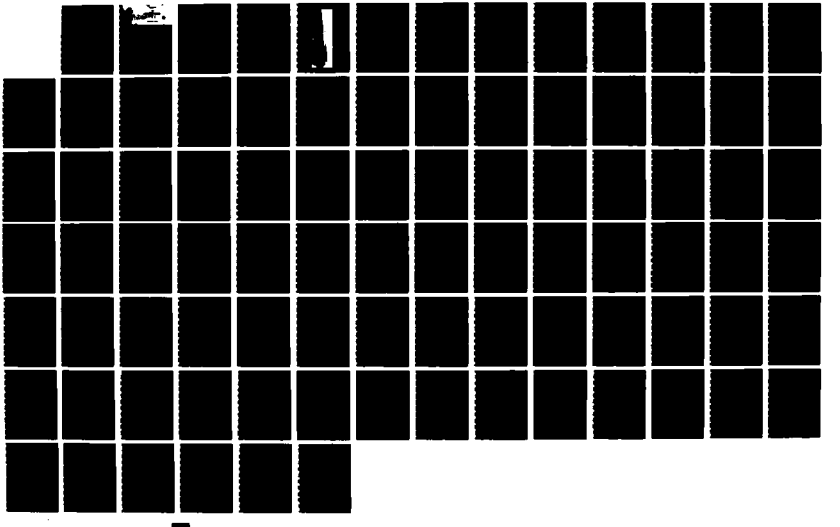

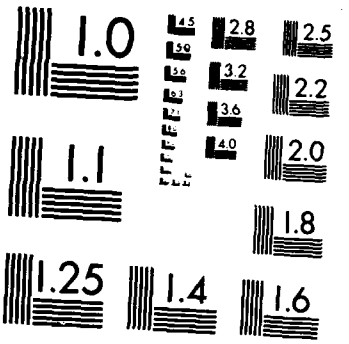

INSTITUTE
FOR
AEROSPACE STUDIES

UNIVERSITY OF TORONTO

ASYMPTOTIC SOLUTIONS TO COMPRESSIBLE LAMINAR BOUNDARY-LAYER SOLUTIONS FOR DUSTY-GAS FLOW OVER A SEMI-INFINITE FLAT PLATE

by

B. Y. Wang and I. I. Glass

August 1986

UTIAS Report No. 310
CN ISSN 0082-5255

UNCLASSIFIED

TY CLASSIFICATION OF THIS PAGE (When Data Entered)

REPORT DOCUMENTATION PAGE

READ INSTRUCTIONS BEFORE COMPLETING FORM

1. REPORT NUMBER **AFOSR-TR- 86-2165**	2. GOVT ACCESSION NO.
3. RECIPIENT'S CATALOG NUMBER	
4. TITLE (and Subtitle) ASYMPTOTIC SOLUTIONS TO COMPRESSIBLE LAMINAR BOUNDARY-LAYER EQUATIONS FOR DUSTY-GAS FLOW OVER A SEMI-INFINITE FLAT PLATE	5. TYPE OF REPORT & PERIOD COVERED Interim
	6. PERFORMING ORG. REPORT NUMBER UTIAS Report No. 310
7. AUTHOR(s) B. Y. Wang and I. I. Glass	8. CONTRACT OR GRANT NUMBER(s) F-AFOSR-82-0096
9. PERFORMING ORGANIZATION NAME AND ADDRESS University of Toronto, Institute for Aerospace Studies, 4925 Dufferin Street, Downsview, Ontario, Canada, M3H 5T6	10. PROGRAM ELEMENT, PROJECT, TASK AREA & WORK UNIT NUMBERS 61102F 2307/A1
11. CONTROLLING OFFICE NAME AND ADDRESS Air Force Office of Scientific Research/NA, Bldg. 410, Bolling Air Force Base, DC 20332, U.S.A.	12. REPORT DATE
	13. NUMBER OF PAGES
14. MONITORING AGENCY NAME & ADDRESS (if different from Controlling Office) same as 11	15. SECURITY CLASS. (of this report) UNCLASSIFIED
	15a. DECLASSIFICATION/DOWNGRADING SCHEDULE

16. DISTRIBUTION STATEMENT (of this Report)

Approved for public release; distribution unlimited.

17. DISTRIBUTION STATEMENT (of the abstract entered in Block 20, if different from Report)

18. SUPPLEMENTARY NOTES

DEC 1 2 1986

19. KEY WORDS (Continue on reverse side if necessary and identify by block number)

1. Dusty-gas flows; 2. Two-phase flows; 3. Boundary-layer flows; 4. Partial-differential equations; 5. Numerical analysis.

20. ABSTRACT (Continue on reverse side if necessary and identify by block number)

An asymptotic analysis is given of the compressible, laminar boundary-layer flow of a dilute gas-particle mixture over a semi-infinite flat plate. The analysis extends existing work by considering more realistic drag and heat-transfer relations than those provided by Stokes. A more general viscosity-temperature expression is also incorporated into the analysis. The

Continued

DD FORM 1 JAN 73 1473

UNCLASSIFIED

SECURITY CLASSIFICATION OF THIS PAGE (When Data Entered)

solution involves a series expansion in terms of the slip parameter of the particles. The numerical results, including the zeroth and first-order approximations for the gas and particle phases, are presented for the two limiting regimes: the large-slip limit near the leading edge and the small-slip limit far downstream. Significant effects on the flow produced by the particles with Stokes' and non-Stokes' relations are studied and clarified. The effects of some nondimensional similarity parameters, such as the Reynolds, Prandtl and Eckert numbers, on the two-phase boundary-layer flow are discussed. Key words:

PLATE 1: ILLUSTRATION OF A DUSTY-GAS BOUNDARY LAYER. THE PHOTOS SHOW THE AIR-SAND BOUNDARY-LAYER DEVELOPMENT STARTING FROM THE SHORE OF THE GULF OF AQUABA, JORDAN, AS VIEWED FROM EILAT, ISRAEL (PHOTOS BY I. I. GLASS).

ASYMPTOTIC SOLUTIONS TO COMPRESSIBLE LAMINAR BOUNDARY-LAYER EQUATIONS FOR DUSTY-GAS FLOW OVER A SEMI-INFINITE FLAT PLATE

by

B. Y. Wang and I. I. Glass

Submitted February, 1986

August, 1986

UTIAS Report No. 310
CN ISSN 0082-5255

Acknowledgements

We are pleased to express our thanks to Prof. J. J. Gottlieb and Dr. W. S. Liu for their constructive review of the manuscript and many useful suggestions.

One of us (B. Y. Wang) is grateful to the Institute of Mechanics, Academia Sinica, Beijing, China, and to UTIAS for the opportunity to do research work during 1984-1986.

The financial assistance received from the Natural Sciences and Engineering Research Council under grant No. A1647, the U.S. Air Force under grant AF-AFOSR-82-0096, the Defence Nuclear Agency under contract DNA 001-85-C-0368, and the Defence Research Establishment, Suffield (DRES), is acknowledged with thanks.

Abstract

An asymptotic analysis is given of the compressible, laminar boundary-layer flow of a dilute gas-particle mixture over a semi-infinite flat plate. The analysis extends existing work by considering more realistic drag and heat-transfer relations than those provided by Stokes. A more general viscosity-temperature expression is also incorporated into the analysis. The solution involves a series expansion in terms of the slip parameter of the particles. The numerical results, including the zeroth and first-order approximations for the gas and particle phases, are presented for the two limiting regimes: the large-slip limit near the leading edge and the small-slip limit far downstream. Significant effects on the flow produced by the particles with Stokes' and non-Stokes' relations are studied and clarified. The effects of some nondimensional similarity parameters, such as the Reynolds, Prandtl and Eckert numbers, on the two-phase boundary-layer flow are discussed.

Table of Contents

Notation

a_1	coefficient in Eqs. (5.4) and (5.20)
a_2	coefficient in Eq. (5.4)
b_1	coefficient in Eqs. (5.5) and (5.21)
b_2	coefficient in Eq. (5.5)
c_1	coefficient in Eqs. (5.6) and (5.22)
c_2	coefficient in Eq. (5.6)
c_p	specific heat of a gas at constant pressure
c_s	specific heat of a particle material
c_v	specific heat of a gas at constant volume
C_D	drag coefficient for a sphere in viscous flows
C_{D_o}	Stokesian drag coefficient for a sphere in viscous flows
d	particle diameter
D	normalized drag coefficient
Dx	x-component of the drag force per unit volume acting on the gas
Dy	y-component of the drag force per unit volume acting on the gas
Ec	gas Eckert number based on freestream temperature
f	transformation function for gas velocity
f_p	transformation function for particle velocity
$F^{(1)}$	first-order function defined in Eq. (3.34)
k	heat conductivity of a gas
M	Mach number
Nu	Nusselt number based on particle diameter
p	gas static pressure
Pr	gas Prandtl number

$\dot{q}_w$	rate of heat transfer at the wall
Q	total heat transfer per unit volume to gas from particles
R	gas constant
Re_p	particle Reynolds number based on freestream velocity and particle diameter
Re_s	slip Reynolds number based on particle slip velocity and particle diameter
Re_∞	flow Reynolds number based on freestream velocity and velocity-equilibrium length
S	Sutherland constant
T	gas static temperature
T_p	particle temperature
T_s	temperature defect between gas and particles
u	x-component of gas velocity
u_p	x-component of particle velocity
u_s	x-component of particle slip velocity
$U^{(1)}$	first-order velocity of gas, defined in Eq. (3.35)
v	y-component of gas velocity
v_p	y-component of particle velocity
v_s	y-component of particle slip velocity
x	horizontal coordinate along the wall
y	vertical coordinate normal to the wall

Greek Symbols

α	ratio of specific heats of two phases
β	mass loading ratio of particles
γ	ratio of specific heats of gas
δ	boundary-layer displacement thickness
η	similarity variable for boundary-layer solutions

$\Theta^{(1)}$	first-order temperature of gas, defined in Eq. (3.36)
λ_∞^*	velocity-equilibrium length
μ	dynamic viscosity of gas
ν	kinematic viscosity of gas
ρ	density of gas phase
ρ_p	density of particle phase
ρ_s	density of particle material
τ_v	velocity-equilibrium time
τ_T	temperature-equilibrium time
τ_w	shear stress at the wall
ϕ	dissipation function due to the relative motion of particles in a gas
ψ_p	stream function for particle phase

Subscripts

w	wall conditions
∞	freestream conditions
o	reference values

Superscripts

*	dimensional quantities
(0)	zeroth-order quantities
(1)	first-order quantities
'	first-order derivative with respect to similarity variable η
"	second-order derivative with respect to similarity variable η
—	modified properties for gas-particle mixture

1.0 INTRODUCTION

1.1 Motivation for the Present Study

Gas and solid-particle flows are encountered in many different fields. Typical examples occurring in nature are dust storms, forest-fire smoke and the dispersion of solid pollutants in the atmosphere. Many processes in industry utilize gas-particle flows, such as transportation of pulverized materials in pneumatic conveyors, separation and classification of particles in cyclone or other separators, fluidization in chemical reactors, and combustion of powdered fuels in combustion chambers. In addition, gas flows with suspended solid particles have various applications in science and engineering, for example, satellite drag, ablation, MHD generators, solid propellant rockets, laser-Doppler anemometry and blast waves moving over the Earth's surface.

For some applications in pipe or nozzle flows and flows over bodies, the behaviour of such two-phase flows at a solid surface is extremely important. Hence, it is necessary to study boundary-layer flows of a gas-particle mixture. From solutions of gas boundary-layer equations, it is possible to determine the effects of solid particles on the boundary-layer characteristics, say, shear stress, heat transfer and boundary-layer growth.

The problem considered in this report is the laminar boundary-layer flow over a semi-infinite flat plate in a compressible gas containing uniform, spherical solid particles. This study provides basic physical insight into the flow of such a two-phase system, even though the solution is for a relatively straightforward problem. Moreover, as a parallel study, the asymptotic solution can be used to compare with finite-difference solutions and to verify independently the correctness of the finite-difference scheme [1].

1.2 Previous Work

Several authors have worked on the problems of two-phase boundary-layer flows. Most of these analyses were based on the assumption of an incompressible fluid [2-16]. Singleton [17] first treated the case of a compressible dusty-gas boundary-layer flow. He derived the governing equations and obtained asymptotic solutions for two limiting regimes: the large-slip regime near the leading edge and the small-slip regime far downstream. However, he assumed Stokes' relation for the drag force and heat transfer, which is valid only for the case where the particle slip Reynolds number is of order unity. He developed his governing equations assuming that the gas viscosity-temperature relation has the special form of $\mu^*/\mu^*_\infty = \sqrt{T^*/T^*_\infty}$, and gave his solutions for the case where the Prandtl and Eckert numbers of the gas are equal to unity.

1.3 Present Study

The present analysis will extend Singleton's analysis to the more general problem of compressible laminar dusty-gas boundary-layer flows over a semi-infinite flat plate. It will present the basic equations under conditions that the drag and heat transfer between the two phases may have different relevant forms instead of Stokes' relation and that the power index in the expression for the viscosity coefficient can have arbitrary values from 0.5 to 1.0. The paper will give the numerical results in the two limiting regions at several values of the Prandtl number, Eckert number, Reynolds number and the viscosity power index.

1.4 Basic Assumptions

The basic assumptions are as follows:

(1) The gas is perfect. The specific heats of the gas are constant. The Prandtl number of the gas is constant. The viscosity and heat conductivity of the gas have a power-law relation with the gas temperature.

(2) The solid particles are rigid spheres of uniform size. The number density of particles is sufficiently high to treat the particle phase as a continuum. However, the particles are also sufficiently dilute to consider them as non-interacting.

(3) The particles have no random motions and therefore the particle phase does not contribute to the static pressure of the two-phase system.

(4) The volume fraction of the particle phase is assumed as negligible. This implies that the coefficient of viscosity for the gas-particle mixture can be taken as the viscosity of the gas phase alone.

(5) The specific heat of the particle material is constant. Its thermal conductivity is much larger than that of the gas and hence the temperature inside each particle can be assumed uniform.

(6) There is no radiative heat transfer from one particle to another. There is no chemical reaction, no coagulation, no phase change in the two-phase system. There is no particle deposition on the surface of the plate.

(7) Only the processes of drag and heat transfer couple the particles to the gas. The drag coefficient and the Nusselt number for a single sphere in a viscous flow are assumed valid for the particle cloud. Other force interaction terms, such as lift, buoyancy and gravity, are neglected.

(8) There is no dry friction as the particles slide along the wall. The slowing down of the particle motion is only due to the gas whose velocity decreases to zero at the wall.

(9) The two-phase flow is steady. The flow Reynolds number is sufficiently high so that a laminar boundary-layer forms on the surface of the flat plate, but lower than a critical value so that no transition to turbulence occurs.

(10) The usual boundary-layer assumptions are still valid for the two-phase system and consequently the variation of pressure across the boundary layer can be neglected. In addition, for the flat-plate problem, there is no pressure gradient in the external flow. The particle phase and gas phase in the external flow are in equilibrium.

2.0 GOVERNING EQUATIONS AND BOUNDARY CONDITIONS

2.1 Governing Equations

Let x^* and y^* be the distance along and normal to the wall, respectively. The origin is fixed at the leading edge of the plate. The geometry of the problem is sketched in Fig. 1. The conservation equations for steady two-dimensional laminar boundary-layer flows of a compressible gas-particle mixture over a semi-infinite flat plate are as follows:

For the gas phase:

Continuity:

$$\frac{\partial}{\partial x^*} \rho^* u^* + \frac{\partial}{\partial y^*} \rho^* v^* = 0 \tag{2.1}$$

Momentum:

$$\rho^* \left(u^* \frac{\partial u^*}{\partial x^*} + v^* \frac{\partial u^*}{\partial y^*}\right) = \frac{\partial}{\partial y^*} \left(\mu^* \frac{\partial u^*}{\partial y^*}\right) + Dx \tag{2.2}$$

Energy:

$$\rho^* c_p^* \left(u^* \frac{\partial T^*}{\partial x^*} + v^* \frac{\partial T^*}{\partial y^*}\right) = \frac{\partial}{\partial y^*} \left(k^* \frac{\partial T^*}{\partial y^*}\right) + \mu^* \left(\frac{\partial u^*}{\partial y^*}\right)^2 + \phi + Q \tag{2.3}$$

State:

$$p^* = \rho^* R^* T^* \tag{2.4}$$

For the particle phase:

Continuity:

$$\frac{\partial}{\partial x^*} \rho_p^* u_p^* + \frac{\partial}{\partial y^*} \rho_p^* v_p^* = 0 \tag{2.5}$$

x-momentum:

$$\rho_p^* \left(u_p^* \frac{\partial u_p^*}{\partial x^*} + v_p^* \frac{\partial u_p^*}{\partial y^*}\right) = -Dx \tag{2.6}$$

y-momentum:

$$\rho_p^* \left(u_p^* \frac{\partial v_p^*}{\partial x^*} + v_p^* \frac{\partial v_p^*}{\partial y^*}\right) = -Dy \tag{2.7}$$

Energy:

$$\rho_p^* c_s^* \left(u_p^* \frac{\partial T_p^*}{\partial x^*} + v_p^* \frac{\partial T_p^*}{\partial y^*}\right) = -Q \tag{2.8}$$

In Eqs. (2.1)-(2.8), the interaction terms between the gas and particles can be expressed by (see Appendix):

$$Dx = \rho_p^* \frac{u_p^* - u^*}{\tau_v^*} D \tag{2.9}$$

$$Dy = \rho_p^* \frac{v_p^* - v^*}{\tau_v^*} D \tag{2.10}$$

$$\phi = (u_p^* - u^*)Dx + (v_p^* - v^*)Dy \tag{2.11}$$

$$Q = \rho_p^* c_s^* \frac{T_p^* - T^*}{\tau_t^*} \frac{Nu}{2} \tag{2.12}$$

where

$$D = \frac{C_D}{C_{D_o}} \tag{2.13}$$

$$C_{D_0} = \frac{24}{Re_s} \tag{2.14}$$

$$\tau_v^* = \frac{\rho_s^* \, d^{*2}}{18\mu^*} \tag{2.15}$$

$$\tau_T^* = \frac{\rho_s^* \, d^{*2}}{12k^*} c_s^* \tag{2.16}$$

Here, D represents the real drag coefficient C_D normalized by the Stokesian drag coefficient C_{D0} and Nu is the Nusselt number based on the particle diameter. According to the assumption (7), D and Nu determine the gas-particle interaction. When the interaction law between the gas and particles just has the Stokes form, D = 1.0 and Nu = 2.0. It is well known that the Stokes relation is valid only for small slip Reynolds number of order unity. In general, D and Nu are both functions of the Reynolds number and Prandtl number. From the definition of slip Reynolds number and Prandtl number,

$$Re_s = \frac{\rho^* \sqrt{(u_p^* - u^*)^2 + (v_p^* - v^*)^2} \, d^*}{\mu^*} \tag{2.17}$$

$$Pr = \frac{c_p^* \, \mu^*}{k^*} \tag{2.18}$$

The local equilibrium-time parameters, τ_v^* and τ_T^*, are a measure of the relaxation process. For example, the velocity equilibrium time τ_v^* is the time elapsed for a particle to reduce its relative velocity to e^{-1} of its original value if the force accelerating (or decelerating) the particle toward the gas velocity is given by the Stokes drag. These two local parameters are functions of the local gas temeprature since the viscosity coefficient μ^* and the heat conductivity k^* are functions of the gas temperature. It is convenient to introduce an equilibrium length λ_∞^*, which is based on the freestream parameters:

$$\lambda_\infty^* = \frac{\rho_s^* \, d^{*2}}{18\mu_\infty^*} u_\infty^* \tag{2.19}$$

The two-phase relaxation process takes place throughout the equilibrium length. Therefore, it is reasonable to choose λ_∞^* as the characteristic length of the dusty-gas boundary-layer problem. Then the equilibrium-time parameters can be expressed in the form

$$\tau_v^* = \frac{\lambda_\infty^*}{u_\infty^*} \cdot \frac{\mu_\infty^*}{\mu^*} \tag{2.20}$$

$$\tau_T^* = \frac{3}{2} Pr \frac{c_s^*}{c_p^*} \cdot \frac{\lambda_\infty^*}{u_\infty^*} \cdot \frac{\mu_\infty^*}{\mu^*} \tag{2.21}$$

Thus, the basic boundary-layer equations (2.1)-(2.8) become

$$\frac{\partial}{\partial x^*} \rho^* u^* + \frac{\partial}{\partial y^*} \rho^* v^* = 0 \tag{2.22}$$

$$\rho^* \left(u^* \frac{\partial u^*}{\partial x^*} + v^* \frac{\partial u^*}{\partial y^*}\right) = \frac{\partial}{\partial y^*} \left(\mu^* \frac{\partial u^*}{\partial y^*}\right) + \rho_p^* (u_p^* - u^*) \frac{u_\infty^*}{\lambda_\infty^*} \frac{\mu^*}{\mu_\infty^*} D \tag{2.23}$$

$$\rho^* \left(u^* \frac{\partial T^*}{\partial x^*} + v^* \frac{\partial T^*}{\partial y^*}\right) = \frac{1}{Pr} \frac{\partial}{\partial y^*} \left(\mu^* \frac{\partial T^*}{\partial y^*}\right) + \frac{\mu^*}{c_p^*} \left(\frac{\partial u^*}{\partial y^*}\right)^2$$

$$+ \frac{\rho_p^*}{c_p^*} \left[(u_p^* - u^*)^2 + (v_p^* - v^*)^2\right] \frac{u_\infty^*}{\lambda_\infty^*} \frac{\mu^*}{\mu_\infty^*} D$$

$$+ \frac{1}{3Pr} \rho_p^* (T_p^* - T^*) \frac{u_\infty^*}{\lambda_\infty^*} \frac{\mu^*}{\mu_\infty^*} Nu \tag{2.24}$$

$$p^* = \rho^* R^* T^* \tag{2.25}$$

$$\frac{\partial}{\partial x^*} \rho_p^* u_p^* + \frac{\partial}{\partial y^*} \rho_p^* v_p^* = 0 \tag{2.26}$$

$$u_p^* \frac{\partial u_p^*}{\partial x^*} + v_p^* \frac{\partial u_p^*}{\partial y^*} = -(u_p^* - u^*) \frac{u_\infty^*}{\lambda_\infty^*} \frac{\mu^*}{\mu_\infty^*} D \tag{2.27}$$

$$u_p^* \frac{\partial v_p^*}{\partial x^*} + v_p^* \frac{\partial v_p^*}{\partial y^*} = -(v_p^* - v^*) \frac{u_\infty^*}{\lambda_\infty^*} \frac{\mu^*}{\mu_\infty^*} D \tag{2.28}$$

$$u_p^* \frac{\partial T_p^*}{\partial x^*} + v_p^* \frac{\partial T_p^*}{\partial y^*} = -\frac{\alpha}{3Pr} (T_p^* - T^*) \frac{u_\infty^*}{\lambda_\infty^*} \frac{\mu^*}{\mu_\infty^*} Nu \tag{2.29}$$

where α is the ratio of specific heats of the two particles:

$$\alpha = \frac{c_p^*}{c_s^*} \tag{2.30}$$

For boundary-layer flows, the normal component of velocity is usually a small quantity. It means that the contribution of the normal velocity is often neglected compared with the tangential velocity. Then, the expression for the slip Reynolds number, Eq. (2.17), becomes

$$Re_s = \frac{\rho^* |u_p^* - u^*| d^*}{\mu^*} \tag{2.31}$$

and the gas energy equation (2.24) reduces to

$$\rho^* \left(u^* \frac{\partial T^*}{\partial x^*} + v^* \frac{\partial T^*}{\partial y^*}\right) = \frac{1}{Pr} \frac{\partial}{\partial y^*} \left(\mu^* \frac{\partial T^*}{\partial y^*}\right) + \frac{\mu^*}{c_p^*} \left(\frac{\partial u^*}{\partial y^*}\right)^2$$

$$+ \frac{\rho_p^*}{c_p^*} (u_p^* - u^*)^2 \frac{u_\infty^*}{\lambda_\infty^*} \frac{\mu^*}{\mu_\infty^*} D + \frac{\rho_p^*}{3Pr} (T_p^* - T^*) \frac{u_\infty^*}{\lambda_\infty^*} \frac{\mu^*}{\mu_\infty^*} Nu \tag{2.32}$$

In order to obtain a closed set of equations, it is required to specify the expression for $\mu^*(T)$. From the standpoint of kinetic theory of gases, the most exact relation for the viscosity of a perfect gas is Sutherland's form [18]:

$$\frac{\mu^*}{\mu_0^*} = \frac{T_0^* + S^*}{T^* + S^*} \left(\frac{T^*}{T_0^*}\right)^{3/2} \tag{2.33}$$

where S^* is the Sutherland constant. This form of Sutherland's relation, however, is not suitable for the series-expansion method which is used in the present analysis. The other viscosity form used in many analytical solutions to the boundary-layer equations is of power form, which is written as

$$\frac{\mu^*}{\mu_\infty^*} = \left(\frac{T^*}{T_\infty^*}\right)^\omega \tag{2.34}$$

where ω is the power index which lies between 0.5 and 1.0. This relation for the gas viscosity is readily applied to the series-expansion method, as shown later.

From the basic assumption (10), the pressure is constant throughout the boundary layer:

$$p^* = \text{constant} \tag{2.35}$$

With this condition (2.35) and the gas state equation (2.25), the gas density can be expressed in terms of the gas temperature:

$$\frac{\rho^*}{\rho^*_\infty} = \frac{T^*_\infty}{T^*} \tag{2.36}$$

Substituting Eq. (2.36) into the basic equations (2.22), (2.23), (2.26)-(2.29) and (2.32) with the power relation for the gas viscosity (2.34), the following equations are obtained:

$$T^*\left(\frac{\partial u^*}{\partial x^*} + \frac{\partial v^*}{\partial y^*}\right) = u^* \frac{\partial T^*}{\partial x^*} + v^* \frac{\partial T^*}{\partial y^*} \tag{2.37}$$

$$u^* \frac{\partial u^*}{\partial x^*} + v^* \frac{\partial u^*}{\partial y^*} = \nu^*_\infty \left(\frac{T^*}{T^*_\infty}\right) \frac{\partial}{\partial y^*} \left[\left(\frac{T^*}{T^*_\infty}\right)^\omega \frac{\partial u^*}{\partial y^*}\right] + \frac{\rho^*_p}{\rho^*_\infty} (u^*_p - u^*) \frac{u^*_\infty}{\lambda^*_\infty} \left(\frac{T^*}{T^*_\infty}\right)^{\omega+1} D \tag{2.38}$$

$$u^* \frac{\partial T^*}{\partial x^*} + v^* \frac{\partial T^*}{\partial y^*} = \frac{\nu^*_\infty}{Pr} \left(\frac{T^*}{T^*_\infty}\right) \frac{\partial}{\partial y^*} \left[\left(\frac{T^*}{T^*_\infty}\right)^\omega \frac{\partial T^*}{\partial y^*}\right] + \frac{\nu^*_\infty}{c^*_p} \left(\frac{T^*}{T^*_\infty}\right)^{\omega+1} \left(\frac{\partial u^*}{\partial y^*}\right)^2$$

$$+ \frac{\rho^*_p}{\rho^*_\infty c^*_p} (u^*_p - u^*)^2 \frac{u^*_\infty}{\lambda^*_\infty} \left(\frac{T^*}{T^*_\infty}\right)^{\omega+1} D + \frac{1}{3Pr} \frac{\rho^*_p}{\rho^*_\infty} (T^*_p - T^*) \frac{u^*_\infty}{\lambda^*_\infty} \left(\frac{T^*}{T^*_\infty}\right)^{\omega+1} Nu \tag{2.39}$$

$$\frac{\partial}{\partial x^*} \rho^*_p u^*_p + \frac{\partial}{\partial y^*} \rho^*_p v^*_p = 0 \tag{2.40}$$

$$u^*_p \frac{\partial u^*_p}{\partial x^*} + v^*_p \frac{\partial u^*_p}{\partial y^*} = -(u^*_p - u^*) \frac{u^*_\infty}{\lambda^*_\infty} \left(\frac{T^*}{T^*_\infty}\right)^\omega D \tag{2.41}$$

$$u_p^* \frac{\partial v_p^*}{\partial x^*} + v_p^* \frac{\partial v_p^*}{\partial y^*} = -(v_p^* - v^*) \frac{u_\infty^*}{\lambda_\infty^*} \left(\frac{T^*}{T_\infty^*}\right)^\omega D \qquad (2.42)$$

$$u_p^* \frac{\partial T_p^*}{\partial x^*} + v_p^* \frac{\partial T_p^*}{\partial y^*} = -\frac{\alpha}{3Pr} (T_p^* - T^*) \frac{u_\infty^*}{\lambda_\infty^*} \left(\frac{T^*}{T_\infty^*}\right)^\omega Nu \qquad (2.43)$$

Under the conditions of $\omega = 0.5$, $D = 1.0$ and $Nu = 2.0$, the equations (2.37)-(2.43) reduce to those derived by Singleton [17].

Physically, the boundary-layer flow-field of a two-phase mixture can be divided into three distinct regions (see Fig. 1). These regions are divided according to the nondimensional slip parameter x^*/λ_∞^* as follows: the large-slip region ($x^*/\lambda_\infty^* << 1$), the moderate-slip region ($x^*/\lambda_\infty^* \sim 1$), and the small-slip region ($x^*/\lambda_\infty^* >> 1$). Following Singleton [17], a small-parameter expansion method was used to solve the boundary-layer equations for dusty gases. Only the asymptotic solutions in the two limiting regimes can be obtained by this perturbation technique: the large-slip approximation for the near leading-edge solution and the small-slip approximation for the far-downstream solution, respectively. Clearly, the large-slip regime is characterized by a frozen flow where the gas and the particles move independently, while the small-slip regime is characterized by an equilibrium flow where the gas and the particles move together (see Fig. 2).

2.2 Boundary Conditions

The boundary conditions for the gas phase are:

(1) At the wall, there is neither slip in velocity nor jump in temperature:

$$u^*(x^*, 0) = 0, \qquad v^*(x^*, 0) = 0, \qquad T^*(x^*, 0) = T_w^* \qquad (2.44)$$

(2) As y^* approaches infinity, the flow parameters must match those in the external flow or the freestream:

$$u^*(x^*, \infty) = u_\infty^*, \qquad T^*(x^*, \infty) = T_\infty^* \qquad (2.45)$$

The boundary conditions for the particle phase are:

(1) At the wall, there is no mass transfer

$$v_p^*(x^*, 0) = 0 \tag{2.46}$$

(2) As y^* approaches infinity, the flow parameters must match their freestream values:

$$u_p^*(x^*, \infty) = u_{p_\infty}^*, \qquad T_p^*(x^*, \infty) = T_{p_\infty}^*, \qquad \rho_p^*(x^*, \infty) = \rho_{p_\infty}^* \tag{2.47}$$

Since the particles and gas are assumed to be in equilibrium in the external flow, the freestream parameters for the particle phase can be readily determined as

$$u_{p_\infty}^* = u_\infty^*, \qquad T_{p_\infty}^* = T_\infty^*, \qquad \rho_{p_\infty}^* = \beta\rho_\infty^* \tag{2.48}$$

where β is the mass loading ratio of the particles. Otherwise, the two-phase external flow must be solved first in order to obtain the outer boundary conditions for the particle phase if the particles are not in equilibrium with the gas in the freestream.

3.0 LARGE-SLIP APPROXIMATION

3.1 Transformation of Boundary-Layer Equations

For the large-slip region, it is convenient to define a stream function ψ_p for the particle phase:

$$\rho_p^* u_p^* = \rho_{p_\infty}^* \frac{\partial \psi_p^*}{\partial y^*} \tag{3.1}$$

$$\rho_p^* v_p^* = -\rho_{p_\infty}^* \frac{\partial \psi_p^*}{\partial x^*} \tag{3.2}$$

Then the continuity equation for the particle phase, Eq. (2.40), is satisfied automatically.

In this region, the following nondimensional flow variables and function transformation are chosen:

$$x = \frac{x^*}{\lambda_\infty^*}, \qquad \eta = \sqrt{\frac{u_\infty^*}{2\nu_\infty^* x^*}}\, y^* \tag{3.3}$$

$$u = \frac{u^*}{u_\infty^*}, \qquad v = \sqrt{\frac{2x^*}{\nu_\infty^* u_\infty^*}}\, v^*, \qquad T = \frac{T^*}{T_\infty^*}, \qquad \rho = \frac{\rho^*}{\rho_\infty^*} \tag{3.4}$$

$$f = \eta u - v, \qquad f_p = \sqrt{\frac{1}{2\nu_\infty^* u_\infty^* x^*}}\, \psi^*_p \tag{3.5}$$

$$\rho_p = \frac{\rho_p^*}{\rho_{p_\infty}^*} = \frac{\rho_p^*}{\beta\rho_\infty^*}, \qquad T_p = \frac{T_p^*}{T_\infty^*} \tag{3.6}$$

$$\mu = \frac{\mu^*}{\mu_\infty^*} \tag{3.7}$$

With Eqs. (3.1)-(3.3) and (3.5)-(3.6), the particle velocities can be expressed as

$$u_p^* = u_\infty^* \left[\frac{1}{\rho_p} \frac{\partial f_p}{\partial \eta}\right] \tag{3.8}$$

$$v_p^* = \frac{\sqrt{2\nu_\infty^* u_\infty^* x^*}}{\lambda_\infty^*} \left[\frac{1}{\rho_p} \left(\frac{\partial f_p}{\partial x} + \frac{f}{2x} - \frac{\eta}{2x} \frac{\partial f_p}{\partial \eta}\right)\right] \tag{3.9}$$

Substituting the above expressions, the basic equations (2.37)-(2.39) and (2.41-(2.43) are transformed into the following form:

$$T\left(\frac{\partial u}{\partial x} + \frac{u}{2x} - \frac{1}{2x} \frac{\partial f}{\partial \eta}\right) = u \frac{\partial T}{\partial x} - \frac{f}{2x} \frac{\partial T}{\partial \eta} \tag{3.10}$$

$$u \frac{\partial u}{\partial x} - \frac{f}{2x} \frac{\partial u}{\partial \eta} = \frac{T}{2x} \frac{\partial}{\partial \eta} \left(T^\omega \frac{\partial u}{\partial \eta}\right) + \beta T^{\omega+1} \left(\frac{\partial f_p}{\partial \eta} - \rho_p u\right) D \tag{3.11}$$

$$\frac{\partial u}{\partial x} + \frac{u}{2x} - \frac{1}{2x}\frac{\partial f}{\partial \eta} = \frac{1}{2xPr}\frac{\partial}{\partial \eta}\left(T^{\omega}\frac{\partial T}{\partial \eta}\right) + \frac{Ec}{2x}T^{\omega}\left(\frac{\partial u}{\partial \eta}\right)^2 + \beta Ec\frac{T^{\omega}}{\rho_p}\left(\frac{\partial f_p}{\partial \eta} - \rho_p u\right)^2 D$$

$$+ \frac{\beta}{3Pr}\rho_p T^{\omega}(T_p - T)Nu \qquad (3.12)$$

$$\frac{\partial f_p}{\partial \eta}\left[\rho_p\left(\frac{\partial^2 f_p}{\partial x\,\partial \eta} - \frac{\eta}{2x}\frac{\partial^2 f_p}{\partial \eta^2}\right) - \frac{\partial f_p}{\partial \eta}\left(\frac{\partial \rho_p}{\partial x} - \frac{\eta}{2x}\frac{\partial \rho_p}{\partial \eta}\right)\right]$$

$$- \left(\frac{\partial f_p}{\partial x} + \frac{f_p}{2x} - \frac{\eta}{2x}\frac{\partial f_p}{\partial \eta}\right)\left(\rho_p\frac{\partial^2 f_p}{\partial \eta^2} - \frac{\partial \rho_p}{\partial \eta}\frac{\partial f_p}{\partial \eta}\right)$$

$$= -\rho_p{}^2 T^{\omega}\left(\frac{\partial f_p}{\partial \eta} - \rho_p u\right)D \qquad (3.13)$$

$$-\rho_p\frac{\partial f_p}{\partial \eta}\left(\frac{\partial^2 f_p}{\partial x^2} + \frac{1}{x}\frac{\partial f_p}{\partial x} - \frac{f_p}{4x^2} - \frac{\eta}{2x}\frac{\partial^2 f_p}{\partial x\,\partial \eta} + \frac{\eta}{4x^2}\frac{\partial f_p}{\partial \eta}\right)$$

$$+ \left(\frac{\partial f_p}{\partial \eta}\frac{\partial \rho_p}{\partial x} - \frac{\partial f_p}{\partial x}\frac{\partial \rho_p}{\partial \eta} - \frac{f_p}{2x}\frac{\partial \rho_p}{\partial \eta}\right)\left(\frac{\partial f_p}{\partial x} + \frac{f_p}{2x} - \frac{\eta}{2x}\frac{\partial f_p}{\partial \eta}\right)$$

$$+ \rho_p\left(\frac{\partial f_p}{\partial x} + \frac{f_p}{2x}\right)\left(\frac{\partial^2 f_p}{\partial x\,\partial \eta} - \frac{\eta}{2x}\frac{\partial^2 f_p}{\partial \eta^2}\right) = \rho_p{}^2 T^{\omega}\left(\frac{\partial f_p}{\partial x} + \frac{f_p}{2x} - \frac{\eta}{2x}\frac{\partial f_p}{\partial \eta} + \frac{\eta}{2x}\rho_p u - \frac{f}{2x}\rho_p\right)D \qquad (3.14)$$

$$\frac{\partial f_p}{\partial \eta}\frac{\partial T_p}{\partial x} - \frac{\partial T_p}{\partial \eta}\left(\frac{\partial f_p}{\partial x} + \frac{f_p}{2x}\right) = -\frac{\alpha}{3Pr}\rho_p T^{\omega}(T_p - T)Nu \qquad (3.15)$$

where Ec is the gas Eckert number based on the freestream temperature,

$$Ec = \frac{u_{\infty}^{*2}}{c_p^{*}\,T_{\infty}^{*}} = (\gamma - 1)M_{\infty}^2 \qquad (3.16)$$

3.2 Expansion in Terms of the Slip Parameter (x^*/λ_{∞}^*)

The following expansion in terms of the slip parameter (x^*/λ_{∞}^*) is made:

$$f(x, \eta) = f^{(0)}(\eta) + xf^{(1)}(\eta) + \ldots$$

$$u(x, \eta) = u^{(0)}(\eta) + xu^{(1)}(\eta) + \ldots$$

$$T(x, \eta) = T^{(0)}(\eta) + xT^{(1)}(\eta) + \ldots \tag{3.17}$$

$$f_p(x, \eta) = f_p^{(0)}(\eta) + xf_p^{(1)}(\eta) + \ldots$$

$$T_p(x, \eta) = T_p^{(0)}(\eta) + xT_p^{(1)}(\eta) + \ldots$$

$$\rho_p(x, \eta) = \rho_p^{(0)}(\eta) + x\rho_p^{(1)}(\eta) + \ldots$$

Putting the expansion (3.17) into Eqs. (3.10)-(3.15) and equating coefficients of $(x)^n$ where $n = 0, 1, \ldots$, the zeroth and first-order equations for the large-slip limit are obtained as follows.

The zeroth-order problem is:

$$f^{(0)'} - \frac{T^{(0)'}}{T^{(0)}} f^{(0)} - u^{(0)} = 0 \tag{3.18}$$

$$u^{(0)''} + \left(\frac{f^{(0)}}{T^{(0)\omega+1}} + \omega \frac{T^{(0)'}}{T^{(0)}}\right)u^{(0)'} = 0 \tag{3.19}$$

$$T^{(0)''} + \left(\mathrm{Pr} \frac{f^{(0)}}{T^{(0)\omega+1}} + \omega \frac{T^{(0)'}}{T^{(0)}}\right)T^{(0)'} + \mathrm{Ec}\ \mathrm{Pr}\left(u^{(0)'}\right)^2 = 0 \tag{3.20}$$

$$f_p^{(0)} = \eta \tag{3.21}$$

$$T_p^{(0)} = 1 \tag{3.22}$$

$$\rho_p^{(0)} = 1 \tag{3.23}$$

with the boundary conditions

$$f^{(0)}(0) = 0; \quad u^{(0)}(0) = 0; \quad u^{(0)}(\infty) = 1; \quad T^{(0)}(0) = T_w; \quad T^{(0)}(\infty) = 1 \tag{3.24}$$

$$f_p^{(0)}(0) = 0; \quad f_p^{(0)'}(\infty) = 1; \quad T_p^{(0)}(\infty) = 1; \quad \rho_p^{(0)}(\infty) = 1 \tag{3.25}$$

In fact, the equations for the particle phase, (3.21)-(3.23), are algebraic expressions which represent the zeroth-order solution for the particles. The boundary conditions (3.25) were already used in Eqs. (3.21)-(3.23).

The first-order problem is

$$f^{(1)'} - \frac{T^{(0)'}}{T^{(0)}} f^{(1)} - 3u^{(1)} + \left(2u^{(0)} + \frac{T^{(0)'}}{T^{(0)}} f^{(0)}\right) \frac{T^{(1)'}}{T^{(0)}} - \frac{f^{(0)}}{T^{(0)}} T^{(1)'} = 0 \tag{3.26}$$

$$u^{(1)''} + \left(\frac{f^{(0)}}{T^{(0)^{\omega+1}}} + \omega \frac{T^{(0)'}}{T^{(0)}}\right)u^{(1)'} - 2 \frac{u^{(0)}}{T^{(0)^{\omega+1}}} u^{(1)} - \left[(\omega+1) \frac{f^{(0)}u^{(0)'}}{T^{(0)^{\omega+2}}}\right.$$

$$\left. + \omega \frac{T^{(0)'}u^{(0)'}}{T^{(0)^2}}\right]T^{(1)} + \omega \frac{u^{(0)'}}{T^{(0)}} T^{(1)'} + \frac{u^{(0)'}}{T^{(0)^{\omega+1}}} f^{(1)}$$

$$= -2\beta(1 - u^{(0)})D \tag{3.27}$$

$$T^{(1)''} + \left(Pr \frac{f^{(0)}}{T^{(0)^{\omega+1}}} + 2\omega \frac{T^{(0)'}}{T^{(0)}}\right)T^{(1)'} - \left[(\omega+1)Pr \frac{f^{(0)}T^{(0)'}}{T^{(0)^{\omega+2}}} + \omega\left(\frac{T^{(0)'}}{T^{(0)}}\right)^2\right.$$

$$\left. + 2Pr \frac{u^{(0)}}{T^{(0)^{\omega+1}}}\right]T^{(1)} + 2EcPr\left(u^{(0)'}u^{(1)'}\right) + Pr \frac{T^{(0)'}}{T^{(0)^{\omega+1}}} f^{(1)}$$

$$= -2\beta EcPr(1-u^{(0)})^2 D - \frac{2}{3} \beta(1 - T^{(0)})Nu \tag{3.28}$$

$$\eta^2\rho_p^{(1)'} - 2\eta\rho_p^{(1)} = \eta f_p^{(1)'} - 3f_p^{(1)} - 2T^{(0)^\omega}(\eta - f^{(0)})D \tag{3.29}$$

$$\eta^2 f_p^{(1)''} - 3\eta f_p^{(1)'} + 3f_p^{(1)} = -2T^{(0)^\omega}(\eta u^{(0)} - f^{(0)})D \tag{3.30}$$

$$\eta T_p^{(1)'} - 2T_p^{(1)} = -\frac{2\alpha}{3Pr} T^{(0)^\omega}(T^{(0)} - 1)Nu \tag{3.31}$$

where the normalized drag coefficient D and the Nusselt number Nu are given by their zeroth-order approximations. The boundary conditions are:

$$f^{(1)}(0) = 0; \quad u^{(1)}(0) = 0; \quad u^{(1)}(\infty) = 0; \quad T^{(1)}(0) = 0; \quad T^{(1)}(\infty) = 0 \tag{3.32}$$

$$f_p^{(1)}(0) = 0; \quad f_p^{(1)'}(\infty) = 0; \quad T_p^{(1)}(\infty) = 0; \quad \rho_p^{(1)}(\infty) = 0 \tag{3.33}$$

From the first-order approximate equations, Eqs. (3.26)-(3.31), it is seen that the loading ratio of the particles β appears oly in the equations for the gas phase, i.e., Eqs. (3.26)-(3.28). In addition, it is possible to yet a more general solution which is suitable for any value of the loading ratio, by introducing the new variables:

$$F^{(1)}(\eta) = f^{(1)}(\eta)/\beta \tag{3.34}$$

$$U^{(1)}(\eta) = u^{(1)}(\eta)/\beta \tag{3.35}$$

$$(1)(\eta) = T^{(1)}(\eta)/\beta \tag{3.36}$$

Substituting the expressions (3.34)-(3.36) into Eqs. (3.26)-(3.28), the first-order equations for the gas phase become

$$F^{(1)'} - \frac{T^{(0)'}}{T^{(0)}} F^{(1)} = 3U^{(1)} - \left(2u^{(0)} + \frac{T^{(0)'}}{T^{(0)}} f^{(0)}\right) \frac{(1)}{T^{(0)}} + \frac{f^{(0)}}{T^{(0)}} \quad (1)' \tag{3.37}$$

$$U^{(1)''} + \left(\frac{f^{(0)}}{T^{(0)^{\omega+1}}} + \omega \frac{T^{(0)'}}{T^{(0)}}\right)U^{(1)'} - 2 \frac{u^{(0)}}{T^{(0)^{\omega+1}}} U^{(1)}$$

Continued

$$= \left[(\omega+1)\frac{f^{(0)}u^{(0)'}}{T^{(0)\omega+2}} + \omega\frac{T^{(0)'}u^{(0)'}}{T^{(0)2}}\right]\Theta^{(1)} - \omega\frac{u^{(0)'}}{T^{(0)}}\Theta^{(1)'}$$

$$- \frac{u^{(0)'}}{T^{(0)\omega+1}}F^{(1)} - 2(1-u^{(0)})D \tag{3.38}$$

$$\Theta^{(1)''} + \left(Pr\frac{f^{(0)}}{T^{(0)\omega+1}} + 2\omega\frac{T^{(0)'}}{T^{(0)}}\right)\Theta^{(1)'} - \left[(\omega+1)Pr\frac{f^{(0)}T^{(0)'}}{T^{(0)\omega+2}} + 2Pr\frac{u^{(0)}}{T^{(0)\omega+1}}\right]\Theta^{(1)}$$

$$= -2EcPr(u^{(0)'}U^{(1)'}) - Pr\frac{T^{(0)'}}{T^{(0)\omega+1}}F^{(1)} - 2EcPr(1-u^{(0)})^2D - \frac{2}{3}(1-T^{(0)})Nu \tag{3.39}$$

Similarly, the boundary conditions (3.32) take the form

$$F^{(1)}(0) = 0; \quad U^{(1)}(0) = 0; \quad U^{(1)}(\infty) = 0; \quad \Theta^{(1)}(0) = 0; \quad \Theta^{(1)}(\infty) = 0 \tag{3.40}$$

3.3 First-Order Problem and Interaction Terms

From Eqs. (3.18)-(3.23) and (3.26)-(3.31), it is found that the interaction terms between the gas and particles appear only in the first-order approximation. In other words, the zeroth-order equations can be solved without knowing the interaction relation between the two phases. However, in order to obtain the first-order solution, appropriate expressions for the drag and heat transfer between the two phases should be given.

As mentioned before, when solid particles move through a gas at very low relative velocities, that is, when $Re_s \lesssim 1$, the Stokesian form can be applied. For the case where Stokes' relation applies, then $D = 1.0$ and $Nu = 2.0$. When the relative, or slip, velocities between the particles and the gas increase to a higher value, Stokes' relation is not valid. Therefore, a relevant form for the interaction should be assumed for the non-Stokesian case. In the case of larger slip velocities, it may be

reasonable to apply the following drag and heat-transfer relations [19, 20]:

$$C_D = 0.48 + 28\ Re_s^{-0.85} \tag{3.41}$$

$$Nu = 2.0 + 0.6\ Pr^{1/3}\ Re_s^{1/2} \tag{3.42}$$

The drag coefficient C_D and Nusselt number Nu for the non-Stokesian case in this analysis, given by Eqs. (3.41) and (3.42), are functions of the slip Reynolds number Re_s as well as the Prandtl number Pr. Comparing the non-Stokes and the Stokes relations indicates that these two cases are in agreement only for the slip Reynolds number of order unity or less. As the slip Reynolds number becomes larger than unity, the Stokes relation underestimates the drag and heat-transfer between the gas and the particles. In general, the non-Stokes relation agrees with the standard drag curve [21] much better than the Stokes relation. Correspondingly, the normalized drag coefficient is

$$D = \frac{1}{50} Re_s + \frac{7}{6} Re_s^{0.15} \tag{3.43}$$

In the series-expansion method, the slip Reynolds number Re_s should be expanded just as the other quantities. Neglecting the first-order small quantities, the slip Reynolds number can be expressed as

$$Re_s = Re_p \frac{1 - u^{(0)}}{T^{(0)^{\omega+1}}} \tag{3.44}$$

where Re_p is the particle Reynolds number based on the freestream velocity

$$Re_p = \frac{\rho_\infty^* u_\infty^* d^*}{\mu_\infty^*} \tag{3.45}$$

The zeroth-order approximations for D and Nu can be obtained by substituting Eq. (3.44) into Eqs. (3.42) and (3.43). Then the first-order equations can be solved numerically. The equations for the gas phase, Eqs. (3.26)-(3.28), consist of second-order, ordinary-differential, simultaneous equations with two-point boundary values, similar to the case of the zeroth-order equations for the gas phase. The solution to the equations for the particle phase, Eqs. (3.29)-(3.31), can be obtained in the integral form:

$$\rho_p^{(1)} = -2\eta^2 \int_{\infty}^{\eta} \frac{T(0)^{\omega}}{x^4} (x - f^{(0)})Ddx - \eta^2 \int_{\infty}^{\eta} \frac{T(0)^{\omega}}{x^4} (xu^{(0)} - f^{(0)})Ddx$$

$$+ \int_{\infty}^{\eta} \frac{T(0)^{\omega}}{x^2} (xu^{(0)} - f^{(0)})Ddx \qquad (3.46)$$

$$f_p^{(1)'} = -3\eta^2 \int_{\infty}^{\eta} \frac{T(0)^{\omega}}{x^4} (xu^{(0)} - f^{(0)})Ddx + \int_{\infty}^{\eta} \frac{T(0)^{\omega}}{x^2} (xu^{(0)} - f^{(0)})Ddx \qquad (3.47)$$

$$f_p^{(1)} = -\eta^3 \int_{\infty}^{\eta} \frac{T(0)^{\omega}}{x^3} (xu^{(0)} - f^{(0)})Ddx + \eta \int_{\infty}^{\eta} \frac{T(0)^{\omega}}{x^2} (xu^{(0)} - f^{(0)})Ddx \qquad (3.48)$$

$$T_p^{(1)} = -\frac{2\alpha}{3Pr} \int_{\infty}^{\eta} \frac{T(0)^{\omega}}{x^3} (T^{(0)} - 1)Nu\, dx \qquad (3.49)$$

The quantity $f_p^{(1)'} = df_p^{(1)}/d\eta$, given by (3.47), can be used to give the first-order approximation of the tangential velocity for the particle phase, $u_p^{(1)}$. From Eq. (3.8), the x-component of particle velocity can be given by the derivative of the transformation function $f_p(\eta)$:

$$u_p = \frac{1}{\rho_p} \frac{\partial f_p}{\partial \eta} \qquad (3.50)$$

In addition, in the large-slip limit, the nondimensional density of the particle phase, ρ_p, is of order unity since the zeroth-order solution is $\rho_p^{(0)} = 1$, i.e., Eq. (3.23). Substituting Eqs. (3.17), (3.21) and (3.23), Eq. (3.50) yields the series-expansion form as

$$u_p = 1 + x(f_p^{(1)'} - \rho_p^{(1)}) + \ldots \qquad (3.51)$$

Clearly, the first and second terms in Eq. (3.51), represent respectively the zeroth and first-order approximation of the tangential particle velocity u_p.

4.0 SMALL-SLIP APPROXIMATION

4.1 Basic Equations in Terms of Slip Quantities

For the small-slip region, it is convenient to employ slip quantities as dependent variables since they are small quantities of first order with respect to the slip parameter (λ^*_∞/x^*). The slip quantities are defined as

$$u^*_s = u^*_p - u^*, \qquad v^*_s = v^*_p - v^*, \qquad T^*_s = T^*_p - T^* \tag{4.1}$$

Putting Eq. (4.1) into the basic equations (2.37)-(2.43) and making some algebraic manipulation results in

$$T^*\left(\frac{\partial u^*}{\partial x^*} + \frac{\partial v^*}{\partial y^*}\right) = u^* \frac{\partial T^*}{\partial x^*} + v^* \frac{\partial T^*}{\partial y^*} \tag{4.2}$$

$$\rho^*_p\left(\frac{\partial u^*_s}{\partial x^*} + \frac{\partial v^*_s}{\partial y^*} + \frac{\partial u^*}{\partial x^*} + \frac{\partial v^*}{\partial y^*}\right) + u^*_s \frac{\partial \rho^*_p}{\partial x^*} + v^*_s \frac{\partial \rho^*_p}{\partial y^*} + u^* \frac{\partial \rho^*_p}{\partial x^*} + v^* \frac{\partial \rho^*_p}{\partial y^*} = 0 \tag{4.3}$$

$$\frac{\rho^*_p}{\rho^*}\left(u^*_s \frac{\partial u^*}{\partial x^*} + v^*_s \frac{\partial u^*}{\partial y^*} + u^* \frac{\partial u^*_s}{\partial x^*} + v^* \frac{\partial u^*_s}{\partial y^*} + u^*_s \frac{\partial u^*_s}{\partial x^*} + v^*_s \frac{\partial u^*_s}{\partial y^*}\right)$$

$$+ \left(1 + \frac{\rho^*_p}{\rho^*}\right)\left(u^* \frac{\partial u^*}{\partial x^*} + v^* \frac{\partial u^*}{\partial y^*}\right) - \frac{\mu^*_\infty}{\rho^*} \frac{\partial}{\partial y^*}\left[\left(\frac{T^*}{T^*_\infty}\right)^\omega \frac{\partial u^*}{\partial y^*}\right] = 0 \tag{4.4}$$

$$u^*_s \frac{\partial u^*}{\partial x^*} + v^*_s \frac{\partial u^*}{\partial y^*} + u^* \frac{\partial u^*_s}{\partial x^*} + v^* \frac{\partial u^*_s}{\partial y^*} + u^*_s \frac{\partial u^*_s}{\partial x^*} + v^*_s \frac{\partial u^*_s}{\partial y^*} + \frac{\mu^*_\infty}{\rho^*} \frac{\partial}{\partial y^*}\left[\left(\frac{T^*}{T^*_\infty}\right)^\omega \frac{\partial u^*}{\partial y^*}\right]$$

$$= -\frac{u^*_\infty}{\lambda^*_\infty}\left(1 + \frac{\rho^*_p}{\rho^*}\right)\left(\frac{T^*}{T^*_\infty}\right)^\omega u^*_s \tag{4.5}$$

$$u^*_s \frac{\partial v^*}{\partial x^*} + v^*_s \frac{\partial v^*}{\partial y^*} + u^* \frac{\partial v^*_s}{\partial x^*} + v^* \frac{\partial v^*_s}{\partial y^*} + u^*_s \frac{\partial v^*_s}{\partial x^*} + v^*_s \frac{\partial v^*_s}{\partial y^*} + u^* \frac{\partial v^*}{\partial x^*} + v^* \frac{\partial v^*}{\partial y^*}$$

Continued

$$= - \frac{u_\infty^*}{\lambda_\infty^*} \left(\frac{T^*}{T_\infty^*}\right)^\omega v_s^* \tag{4.6}$$

$$\frac{\rho_p^* c_s^*}{\rho^* c_p^*} \left(u_s^* \frac{\partial T^*}{\partial x^*} + v_s^* \frac{\partial T^*}{\partial y^*} + u^* \frac{\partial T_s^*}{\partial x^*} + v^* \frac{\partial T_s^*}{\partial y^*} + u_s^* \frac{\partial T_s^*}{\partial x^*} + v_s^* \frac{\partial T_s^*}{\partial y^*}\right)$$

$$+ \left(1 + \frac{\rho_p^* c_s^*}{\rho^* c_p^*}\right)\left(u^* \frac{\partial T^*}{\partial x^*} + v^* \frac{\partial T^*}{\partial y^*}\right) - \frac{1}{Pr} \frac{\mu_\infty^*}{\rho^*} \frac{\partial}{\partial y^*} \left[\left(\frac{T^*}{T_\infty^*}\right)^\omega \frac{\partial T^*}{\partial y^*}\right] - \frac{1}{c_p^*} \frac{\mu_\infty^*}{\rho^*} \left(\frac{T^*}{T_\infty^*}\right)^\omega \left(\frac{\partial u^*}{\partial y^*}\right)^2$$

$$= \frac{\rho_p^*}{\rho^* c_p^*} \frac{u_\infty^*}{\lambda_\infty^*} \left(\frac{T^*}{T_\infty^*}\right)^\omega u_s^{*2} \tag{4.7}$$

$$u_s^* \frac{\partial T^*}{\partial x^*} + v_s^* \frac{\partial T^*}{\partial y^*} + u^* \frac{\partial T_s^*}{\partial x^*} + v^* \frac{\partial T_s^*}{\partial y^*} + u_s^* \frac{\partial T_s^*}{\partial x^*} + v_s^* \frac{\partial T_s^*}{\partial y^*}$$

$$+ \frac{1}{Pr} \frac{\mu_\infty^*}{\rho^*} \frac{\partial}{\partial y^*} \left[\left(\frac{T^*}{T_\infty^*}\right)^\omega \frac{\partial T^*}{\partial y^*}\right] + \frac{\mu_\infty^*}{\rho^* c_p^*} \left(\frac{T^*}{T_\infty^*}\right)^\omega \left(\frac{\partial u^*}{\partial y^*}\right)^2$$

$$= - \frac{\rho_p^*}{\rho^* c_p^*} \frac{u_\infty^*}{\lambda_\infty^*} \left(\frac{T^*}{T_\infty^*}\right)^\omega u_s^{*2} - \frac{2\alpha}{3Pr} \frac{u_\infty^*}{\lambda_\infty^*} \left(1 + \frac{\rho_p^* c_s^*}{\rho^* c_p^*}\right)\left(\frac{T^*}{T_\infty^*}\right)^\omega T_s^* \tag{4.8}$$

The conditions of D = 1.0 and Nu = 2.0 are already employed in Eqs. (4.2)-(4.8), since the slip velocities are always small quantities in the small-slip region.

4.2 Transformation of Basic Equations

Let

$$u = \frac{u^*}{u_\infty^*}, \qquad v = \sqrt{\frac{2(1+\beta)x^*}{v_\infty^* u_\infty^*}}\, v^*, \qquad T = \frac{T^*}{T_\infty^*}, \qquad \rho = \frac{\rho^*}{\rho_\infty^*} = \frac{T_\infty^*}{T^*} \tag{4.9}$$

$$u_s = \frac{u_s^*}{u_\infty^*}, \qquad v_s = \sqrt{\frac{2(1+\beta)x^*}{v_\infty^* u_\infty^*}}\, v_s^*, \qquad T_s = \frac{T_s^*}{T_\infty^*}, \qquad \rho_p = \frac{\rho_p^*}{\rho_{p_\infty}^*} = \frac{\rho_p^*}{\beta\rho_\infty^*} \tag{4.10}$$

and

$$x = \frac{x^*}{\lambda_\infty^*}, \qquad \eta = \sqrt{\frac{(1+\beta)u_\infty^*}{2\nu_\infty^* x^*}}\, y^*, \qquad f = \eta u - v \tag{4.11}$$

$$\mu = \frac{\mu^*}{\mu_\infty^*} \tag{4.12}$$

As in the large-slip limit, substituting Eqs. (4.9)-(4.12) into Eqs. (4.2)-(4.8), the dimensionless basic equations can be obtained:

$$T\frac{\partial u}{\partial x} + \frac{u}{2x}T - \frac{T}{2x}\frac{\partial f}{\partial \eta} - u\frac{\partial T}{\partial x} + \frac{f}{2x}\frac{\partial T}{\partial \eta} = 0 \tag{4.13}$$

$$\rho_p\left(\frac{\partial u_s}{\partial x} - \frac{\eta}{2x}\frac{\partial u_s}{\partial \eta} + \frac{1}{2x}\frac{\partial v_s}{\partial \eta} + \frac{\partial u}{\partial x} + \frac{u}{2x} - \frac{1}{2x}\frac{\partial f}{\partial \eta}\right) + u_s\frac{\partial \rho_p}{\partial x} - \frac{\eta}{2x}u_s\frac{\partial \rho_p}{\partial \eta}$$

$$+ \frac{v_s}{2x}\frac{\partial \rho_p}{\partial \eta} + u\frac{\partial \rho_p}{\partial x} - \frac{f}{2x}\frac{\partial \rho_p}{\partial \eta} = 0 \tag{4.14}$$

$$\beta\rho_p T\left(u_s\frac{\partial u}{\partial x} - \frac{\eta}{2x}u_s\frac{\partial u}{\partial \eta} + \frac{v_s}{2x}\frac{\partial u}{\partial \eta} + u\frac{\partial u_s}{\partial x} - \frac{f}{2x}\frac{\partial u_s}{\partial \eta} + u_s\frac{\partial u_s}{\partial x} - \frac{\eta}{2x}u_s\frac{\partial u_s}{\partial \eta}\right.$$

$$\left. + \frac{v_s}{2x}\frac{\partial u_s}{\partial \eta}\right) + (1+\beta\rho_p T)\left(u\frac{\partial u}{\partial x} - \frac{f}{2x}\frac{\partial u}{\partial \eta}\right) - \frac{1+\beta}{2x}T\frac{\partial}{\partial \eta}\left(T^\omega\frac{\partial u}{\partial \eta}\right) = 0 \tag{4.15}$$

$$u_s\frac{\partial u}{\partial x} - \frac{\eta}{2x}u_s\frac{\partial u}{\partial \eta} + \frac{v_s}{2x}\frac{\partial u}{\partial \eta} + u\frac{\partial u_s}{\partial x} - \frac{f}{2x}\frac{\partial u_s}{\partial \eta} + u_s\frac{\partial u_s}{\partial x} - \frac{\eta}{2x}u_s\frac{\partial u_s}{\partial \eta}$$

$$+ \frac{v_s}{2x}\frac{\partial u_s}{\partial \eta} + \frac{1+\beta}{2x}T\frac{\partial}{\partial \eta}\left(T^\omega\frac{\partial u}{\partial \eta}\right) = -(1+\beta\rho_p T)T^4 u_s \tag{4.16}$$

$$\eta u \frac{\partial u}{\partial x} - u \frac{\partial f}{\partial x} - \frac{\eta}{2x} u^2 - \frac{\eta}{2x} f \frac{\partial u}{\partial \eta} + \frac{f}{2x} \frac{\partial f}{\partial \eta} + u_s \frac{\partial v_s}{\partial x} - u_s \frac{\eta}{2x} \frac{\partial v_s}{\partial \eta} + \frac{v_s}{2x} \frac{\partial v_s}{\partial \eta} - \frac{u_s v_s}{2x}$$

$$+ \eta u_s \frac{\partial u}{\partial x} - u_s \frac{\partial f}{\partial x} - \frac{\eta^2}{2x} u_s \frac{\partial u}{\partial \eta} + \frac{\eta}{2x} u_s \frac{\partial f}{\partial \eta} - \frac{\eta}{x} u u_s + \frac{f}{2x} u_s + \frac{\eta}{2x} v_s \frac{\partial u}{\partial \eta}$$

$$- \frac{v_s}{2x} \frac{\partial f}{\partial \eta} + u \frac{\partial v_s}{\partial x} - \frac{f}{2x} \frac{\partial v_s}{\partial \eta} = -T^{\omega} v_s \qquad (4.17)$$

$$\beta \rho_p T \left(u_s \frac{\partial T}{\partial x} - \frac{\eta}{2x} u_s \frac{\partial T}{\partial \eta} + \frac{v_s}{2x} \frac{\partial T}{\partial \eta} + u \frac{\partial T_s}{\partial x} - \frac{f}{2x} \frac{\partial T_s}{\partial \eta} + u_s \frac{\partial T_s}{\partial x} - \frac{\eta}{2x} u_s \frac{\partial T_s}{\partial \eta} \right.$$

$$\left. + \frac{v_s}{2x} \frac{\partial T_s}{\partial \eta} \right) + (\alpha + \beta \rho_p T) \left(u \frac{\partial T}{\partial x} - \frac{f}{2x} \frac{\partial T}{\partial \eta} \right) - \frac{\alpha}{Pr} \frac{1+\beta}{2x} T \frac{\partial}{\partial \eta} \left(T^{\omega} \frac{\partial T}{\partial \eta} \right)$$

$$- \alpha Ec \frac{1+\beta}{2x} T^{\omega+1} \left(\frac{\partial u}{\partial \eta} \right)^2 = \alpha Ec \beta \rho_p T^{\omega+1} u_s^2 \qquad (4.18)$$

$$u_s \frac{\partial T}{\partial x} - \frac{\eta}{2x} u_s \frac{\partial T}{\partial \eta} + \frac{v_s}{2x} \frac{\partial T}{\partial \eta} + u \frac{\partial T_s}{\partial x} - \frac{f}{2x} \frac{\partial T_s}{\partial \eta} + u_s \frac{\partial T_s}{\partial x} - \frac{\eta}{2x} u_s \frac{\partial T_s}{\partial \eta} + \frac{v_s}{2x} \frac{\partial T_s}{\partial \eta}$$

$$+ \frac{1+\beta}{2x} \frac{T}{Pr} \frac{\partial}{\partial \eta} \left(T^{\omega} \frac{\partial T}{\partial \eta} \right) + Ec \frac{1+\beta}{2x} T^{\omega+1} \left(\frac{\partial u}{\partial \eta} \right)^2$$

$$= -Ec \beta \rho_p T^{\omega+1} u_s^2 - \frac{2}{3Pr} (\alpha + \beta \rho_p T) T^{\omega} T_s \qquad (4.19)$$

4.3 Expansion in Terms of the Slip Parameter (λ_∞^*/x^*)

In the small-slip lilmit, perturbation expansions are made in terms of λ_∞^*/x^*:

$$f(x, \eta) = f^{(0)}(\eta) + \frac{1}{x} f^{(1)}(\eta) + \ldots$$

$$u(x, \eta) = u^{(0)}(\eta) + \frac{1}{x} u^{(1)}(\eta) + \ldots$$

$$T(x, \eta) = T^{(0)}(\eta) + \frac{1}{x} T^{(1)}(\eta) + \ldots$$

$$u_s(x, \eta) = \frac{1}{x} u_s^{(1)}(\eta) + \ldots \tag{4.20}$$

$$v_s(x, \eta) = \frac{1}{x} v_s^{(1)}(\eta) + \ldots$$

$$T_s(x, \eta) = \frac{1}{x} T_s^{(1)}(\eta) + \ldots$$

$$\rho_p(x, \eta) = \rho_p^{(0)}(\eta) + \frac{1}{x} \rho_p^{(1)}(\eta) + \ldots$$

where $x = x^*/\lambda_\infty^*$ is the nondimensional slip parameter.

Then, the small-slip approximation for the zeroth-order problem leads to

$$f^{(0)\prime} - \frac{T^{(0)\prime}}{T^{(0)}} f^{(0)} - u^{(0)} = 0 \tag{4.21}$$

$$u^{(0)\prime\prime} + \left(\frac{f^{(0)}}{T^{(0)^{\omega+1}}} + \omega \frac{T^{(0)\prime}}{T^{(0)}}\right) u^{(0)\prime} = 0 \tag{4.22}$$

$$T^{(0)\prime\prime} + \left(\mathrm{Pr} \frac{1 + \beta/\alpha}{1+\beta} \frac{f^{(0)}}{T^{(0)^{\omega+1}}} + \omega \frac{T^{(0)\prime}}{T^{(0)}}\right) T^{(0)\prime} + \mathrm{EcPr}\left(u^{(0)\prime}\right)^2 = 0 \tag{4.23}$$

$$\rho_p^{(0)} = \frac{1}{T^{(0)}} \tag{4.24}$$

with the boundary conditions

$$f^{(0)}(0) = 0; \quad u^{(0)}(0) = 0; \quad u^{(0)}(\infty) = 1; \quad T^{(0)}(0) = T_w; \quad T^{(0)}(\infty) = 1 \tag{4.25}$$

For the small-slip approximation, the zeroth-order solutions of the particle velocity and temperature are the same as those for the gas and the first-order solutions are given by the first-order slip quantities. The zeroth-order density for the particle phase is given by Eq. (4.24). The boundary condition for the particle phase density

$$\rho_p^{(0)}(\infty) = 1 \tag{4.26}$$

has been used during the derivation of Eq. (4.24).

The first-order equations for $f^{(1)}$, $u^{(1)}$, $T^{(1)}$ and $\rho^{(1)}$ are given by

$$f^{(1)'} - \frac{T(0)'}{T^{(0)}} f^{(1)} = - \frac{T(0)'}{T(0)^2} f^{(0)} T^{(1)} + 2 \frac{u^{(0)}}{T^{(0)}} T^{(1)} + \frac{f^{(0)}}{T^{(0)}} T^{(1)'} - u^{(1)} \tag{4.27}$$

$$u^{(1)''} + \frac{f^{(0)} + \omega T^{(0)} {}^{\omega} T^{(0)'}}{T^{(0)^{\omega+1}}} u^{(1)'} + \frac{2u^{(0)}}{T^{(0)^{\omega+1}}} u^{(1)}$$

$$= \frac{\beta}{1+\beta} \frac{1}{T^{(0)^{\omega+1}}} \left[\frac{\eta u^{(0)^2} u^{(0)'}}{2T^{(0)^{\omega}}} - 2 \frac{f^{(0)} u^{(0)} u^{(0)'}}{T^{(0)^{\omega}}} + (\omega-1) \frac{f^{(0)^2} T^{(0)'} u^{(0)'}}{T^{(0)^{\omega+1}}} \right.$$

$$\left. + \frac{f^{(0)^3} u^{(0)'}}{2T^{(0)^{2\omega+1}}} \right] - \frac{u^{(0)'}}{T^{(0)^{\omega+1}}} f^{(1)} - \frac{\beta}{1+\beta} \frac{f^{(0)} u^{(0)'}}{T^{(0)^{\omega+1}}} \left(\frac{T^{(1)}}{T^{(0)}} + T^{(0)} \rho_p^{(1)} \right)$$

$$+ \omega \frac{T^{(0)'} u^{(0)'}}{T^{(0)^2}} T^{(1)} + (\omega+1) \frac{f^{(0)} u^{(0)'}}{T^{(0)^{\omega+2}}} T^{(1)} - \omega \frac{u^{(0)'}}{T^{(0)}} T^{(1)'} \tag{4.28}$$

$$T^{(1)''} + \left(Pr \frac{1 + \beta/\alpha}{1+\beta} f^{(0)} + 2\omega T^{(0)} {}^{\omega} T^{(0)'} \right) \frac{T^{(0)'}}{T^{(0)^{\omega+1}}} + \left[2Pr \frac{1 + \beta/\alpha}{1+\beta} u^{(0)} \right.$$

Continued

$$- \Pr \frac{\omega(1 + \beta/\alpha) + 1}{1+\beta} \frac{T(0)'}{T(0)} f(0) - \omega \frac{T(0)'^2}{T(0)^{1-\omega}}] \frac{T(1)}{T(0)^{\omega+1}}$$

$$= \Pr \frac{\beta/\alpha}{1+\beta} \frac{1}{T(0)^{\omega+1}} [\frac{\eta u(0)^2 T(0)'}{2T(0)^{\omega}} - \frac{f(0) u(0) T(0)'}{2T(0)^{\omega}} + \frac{3(2\omega-1)\Pr/\alpha - 2}{4} \frac{f(0)^2 T(0)'^2}{T(0)^{\omega+1}}$$

$$- \frac{9\Pr}{4\alpha} \frac{f(0) u(0) T(0)'}{T(0)^{\omega}} + \frac{3\Pr^2}{4\alpha} \frac{1 + \beta/\alpha}{1+\beta} \frac{f(0)^3 T(0)'}{T(0)^{2\omega+1}} + \frac{3Ec\Pr^2}{4\alpha} \frac{f(0)^2 u(0)'^2}{T(0)^{\omega}}]$$

$$- Ec\Pr \frac{\beta}{1+\beta} \frac{f(0)^2 u(0)'^2}{2T(0)^{2\omega+1}} - \Pr \frac{1 + \beta/\alpha}{1+\beta} \frac{T(0)'}{T(0)^{\omega+1}} f(1) - \Pr \frac{\beta/\alpha}{1+\beta} \frac{f(0) T(0)'}{T(0)^{\omega}} \rho_p^{(1)}$$

$$- 2Ec\Pr(u(0)' u(1)') \tag{4.29}$$

$$f(0) \rho_p^{(1)'} + (2u(0) + \frac{T(0)'}{T(0)} f(0)) \rho_p^{(1)}$$

$$= - \frac{f(0) u(0)'}{T(0)^{\omega+1}} + \frac{\eta u(0) u(0)'}{T(0)^{\omega+1}} + \frac{\omega-2}{2} \frac{f(0) u(0) T(0)'}{T(0)^{\omega+2}} + \omega \frac{f(0)^2 T(0)'^2}{T(0)^{\omega+3}}$$

$$+ \frac{1}{2} [\Pr \frac{1 + \beta/\alpha}{1+\beta} \frac{f(0) T(0)'}{T(0)^{\omega+1}} + Ec\Pr(u(0)')^2] \frac{f(0)^2}{T(0)^{\omega+2}} - \frac{\omega+1}{2} \frac{\eta u(0)^2 T(0)'}{T(0)^{\omega+2}}$$

$$+ \frac{f(0) T(0)'}{T(0)^3} T(1) - 2 \frac{u(0)}{T(0)^2} T(1) - \frac{f(0)}{T(0)^2} T(1)' \tag{4.30}$$

with the boundary conditions

$$f^{(1)}(0) = 0; \quad u^{(1)}(0) = 0; \quad u^{(1)}(\infty) = 1; \quad T^{(1)}(0) = 0; \quad T^{(1)}(\infty) = 0 \tag{4.31}$$

The first-order problem in the small-slip limit is determined by the second-order, ordinary-differential, simultaneous equations with two-point boundary values. In this aspect, it is similar to the first-order problem in the large-slip limit. But the solution to the above equations (4.27)-(4.30) is difficult to obtain, since these equations are too complex and have high coupling. In addition, Eq. (4.30) has a singular point at $\eta = 0$. Moreover, as pointed out by Singleton [17], regardless of the choice of $u^{(1)}(0)$ and $T^{(1)}(0)$, the resulting solutions to $u^{(1)}(\eta)$ and $T^{(1)}(\eta)$ from Eqs. (4.28) and (4.29) always approach zero as η approaches infinity, making it impossible to pick out the correct solutions. Therefore, in this analysis, it was not attempted to obtain the first-order solutions to Eqs. (4.27)-(4.30) but just the zeroth-order solutions to Eqs. (4.21)-(4.24) which are of more practical interest. The first-order problem for the particle velocity and temperature are readily obtained. With the series expansion (4.20), the slip quantities of first order are given as

$$u_s^{(1)} = \frac{f(0)u(0)'}{2T(0)^{\omega}} \tag{4.32}$$

$$v_s^{(1)} = \frac{1}{2T(0)^{\omega}} \left(\eta u(0)^2 + \eta f(0)u(0)' - f(0)u(0) - \frac{T(0)'}{T(0)} f(0)^2\right) \tag{4.33}$$

$$T_s^{(1)} = \frac{3Pr}{4\alpha} \frac{f(0)T(0)'}{T(0)^{\omega}} \tag{4.34}$$

Equations (4.32)-(4.34) are not differential but algebraic equations. The values of three slip quantities $u_s^{(1)}$, $v_s^{(1)}$ and $T_s^{(1)}$ at any given point are determined from the zeroth-order solutions for the gas phase.

5.0 RESULTS AND DISCUSSIONS

The zeroth and first-order equations for the large-slip and small-slip limits can be solved numerically. They are a system of nonlinear, second-order, ordinary-differential equations. The corresponding boundary conditions are specified at the two end points, i.e., at the wall and the outer edge of the boundary layer. Mathematically, it is a two-point boundary-value problem and it can be solved by Gear's method [22].

5.1 Large-Slip Limit

From Eqs. (3.18)-(3.20), the zeroth-order problem for the gas phase in the large-slip limit is as simple as that for the boundary-layer flow of a pure gas without particles. Therefore, as for the conventional viscous flows of a pure gas, the Reynolds number, the Prandtl number, the Eckert number and the viscosity power index are important controlling parameters in the analysis of compressible, laminar, boundary-layer flows of a gas-particle mixture. The numerical solutions of Eqs. (3.18)-(3.20) are given in Figs. 3 to 5 and the influence of the parameters Pr, Ec and ω on the flow properties are shown in these figures and it is seen that their effects are relatively small. Here, it is not necessary to discuss the zeroth-order solutions for the gas phase in detail since it is the same as the similarity solution for the flat-plate boundary layer of a pure gas. Similarly, the zeroth-order solutions for the particle phase are readily obtained. Equations (3.21)-(3.23) indicate that, in the zeroth-order approximation, the particle motion in the boundary layer remains uniform. All the zeroth-order flow quantities for the particle phase (density, velocity and temperature) are the same as those in the freestream or the external flow. This is due to the fact that both the gas and the particles move independently of each other in the zeroth-order problem. The influence of the particles on the flow properties is prevalent only in the first or higher order solutions. It is a major feature of the two-phase boundary-layer flows in the large-slip region.

Figures 6 to 8 show the first-order solutions for the gas phase, i.e., the solutions to Eqs. (3.37)-(3.39). They are the numerical results for the Stokes case and the effects of Ec, Pr and ω are significant this time. For the first-order problem, the same value of the flow parameters Pr, Ec, ω and T_w were chosen as in the zeroth-order problem where Pr = 0.69-1.0, Ec = 0.1-1.0, ω = 0.5-1.0 and T_w = 0.5. For the non-Stokes case, the numerical results with Pr = 0.69, Ec = 1.0, ω = 0.67 and T_w = 0.5 are presented in Fig. 9. They cover quite a wide range of the particle Reynolds number (Re_p = 0.1-100.0) and the changes are very significant. For the particle phase, the first-order solution can be obtained by numerically integrating Eqs. (3.46)-(3.49). The results for the Stokes case with α = 1.0 are given in Figs. 10 to 12. It is seen that significant changes occur in ρ_p and $T_p^{(1)}$ with ω, Pr and Ec and in $f_p^{(1)}$ with Pr and Ec. The results for the non-Stokes case are shown in Fig. 13 where the changes with Re_p are even more significant. The computations for the particle phase is carried out under the same conditions as those for the gas phase.

By comparing the results for the non-Stokes case with those for the Stokes case, it is seen that the results based on the Stokes relation are reasonable qualitatively. They present the similar tendency of variations in the flow properties, such as velocity and temperature. However, they are not correct quantitatively, especially for the large particle Reynolds number, as expected. Nevertheless, this comparatively simple case of the Stokes relation is still considered in many analyses of dusty-gas flows

since it is useful for understanding the main characteristics of two-phase flow phenomena.

From the solution to the first-order problem, it was found that there exist significant differences in the first-order flow profiles between the two phases. For instance, the first-order velocity of the gas is positive and, while passing across the boundary layer from the outer edge to the wall, it increases first to a maximum value and then decreases to zero (see Fig. 7). By contrast, the first-order velocity of the particles is negative and its magnitude increases monotonically from the outer edge of the boundary layer to the wall (c.f. Fig. 11). This arises from the fact that the mechanisms of motion for the two phases are not the same. There are two kinds of forces exerted on the gas: the viscous force by the gas and the drag force by the particles. For the particle phase, however, only the drag force of the gas influences its motion. Therefore, after entering the boundary layer at the leading edge, the gas decreases immediately its tangential velocity from the freestream value at the outer edge to zero velocity at the wall due to viscosity. Since the density of the particle material is much greater than the gas density, the particles cannot accommodate this rapid deceleration but tend to slip through the gas as they decelerate. It takes some time for the particles and gas to adjust to an equilibrium state. It implies that in the large-slip region near the leading edge, the gas has small deviation from the pure-gas boundary-layer flow while the particles have small deviation from their original state of uniform motion in the freestream. The particles are 'frozen'. This situation is justified by the zeroth-order solution, which represents the complete frozen-flow limit. The relaxation process takes place throughout the equilibrium length λ_∞^*. In the meantime, owing to the slip velocity, the drag force arises between the two phases and then the first-order flow is induced by this gas-particle interaction. The gas is accelerated and the particles are retarded. This is the reason why the two phases have their first-order velocities in opposite directions. While traversing the boundary layer from the outer edge to the wall, the slip velocity increases and then the first-order velocity for the two phases both increase first in the region near the outer edge, since the drag force is proportional to the slip velocity. The first-order velocity of the particles continues to increase in magnitude on approaching the wall, since the particle motion is driven only by the drag force. However, for the gas phase, in the region near the wall where the velocity gradient for the gas is great, the viscous force prevails and the no-slip condition at the wall forces the gas velocity to go to zero. Thus, the first-order velocity of the gas decreases in the inner boundary layer and vanishes at the wall. A similar argument is valid for the first-order temperature profile by employing the correspondence of the temperature to the velocity, the heat conductivity to the viscosity and the heat transfer to the drag force.

Finally, for boundary-layer analyses, there are three characteristic quantities of interest: the shear stress at the wall τ_w^*, the heat-transfer rate at the wall $\dot{q}_w^*$, and the displacmeent thickness δ^*. As usual, they are

determined from the flow profiles of the gas phase:

$$\tau_w^* = \left(\mu_w^* \frac{\partial u^*}{\partial y^*}\right)_w, \quad \dot{q}_w^* = -\left(k^* \frac{\partial T^*}{\partial y^*}\right)_w, \quad \delta^* = \int_0^\infty \left(1 - \frac{\rho^* u^*}{\rho_\infty^* u_\infty^*}\right) dy^* \tag{5.1}$$

It is convenient to introduce the following nondimensional characteristic quantities:

$$\tau_w = \frac{\tau_w^*}{\rho_\infty^* u_\infty^{*2}} \sqrt{Re_\infty}, \quad \dot{q}_w = \frac{\dot{q}_w^*}{k_\infty^* T_\infty^*} \frac{\lambda_\infty^*}{\sqrt{Re_\infty}}, \quad \delta = \frac{\delta^*}{\lambda_\infty^*} \sqrt{Re_\infty} \tag{5.2}$$

where Re_λ is the flow Reynolds number based on the freestream velocity u_∞^* and the velocity-equilibrium length λ_∞^*,

$$Re_\infty = \frac{\rho_\infty^* u_\infty^* \lambda_\infty^*}{\mu_\infty^*} \tag{5.3}$$

Then, the nondimensional boundary-layer characteristics can be expressed as:

$$\tau_w = \frac{\mu_w}{\sqrt{x}} a_1 (1 + x\beta a_2 + \ldots) \tag{5.4}$$

$$\dot{q}_w = -\frac{\mu_w}{\sqrt{x}} b_1 (1 + x\beta b_2 + \ldots) \tag{5.5}$$

$$\delta = \sqrt{x}\, c_1 (1 + x\beta c_2 + \ldots) \tag{5.6}$$

where μ_w is the nondimensional viscosity of the gas at the wall

$$\mu_w = T_w^\omega \tag{5.7}$$

and the coefficients a_1, a_2, b_1, b_2, c_1 and c_2 are given by

$$a_1 = u^{(0)'}(0), \qquad a_2 = \frac{u^{(1)'}(0)}{u^{(0)'}(0)} \tag{5.8}$$

$$b_1 = T^{(0)'}(0), \qquad b_2 = \frac{T^{(1)'}(0)}{T^{(0)'}(0)} \tag{5.9}$$

$$c_1 = \int_0^\infty \left(1 - \frac{u^{(0)}}{T^{(0)}}\right) d\eta, \qquad c_2 = \int_0^\infty \frac{u^{(0)}T^{(1)} - T^{(0)}u^{(1)}}{T^{(0)2}}\, d\eta \tag{5.10}$$

From the above relations, it is known that the coefficients a_1, b_1 and c_1 are determined only by the zeroth-order solution and that the coefficient a_2, b_2 and c_2 depend on the first-order solution as well as the zeroth-order solution. In fact, the first three coefficients, i.e., a_1, b_1 and c_1, give the zeroth-order approximation of the three characteristics which is the same as for the similarity solution of a pure gas. The other three coefficients a_2, b_2 and c_2 represent the first-order modification owing to the presence of the particles. These coefficients can be estimated from the numerical results using eqs. (5.8)-(5.10). In Table 1, the listed values are the coefficients for the case where the flow parameters are Pr = 0.69, Ec = 1.0, ω = 0.67 and T_W = 0.5.

Table 1

Coefficient Values for Boundary-Layer Characteristic Quantities

	Stokes' Case	non-Stokes' Case			
		Re=0.1	Re=1.0	Re=10.0	Re=100.0
a_1	0.5472	0.5472	0.5472	0.5472	0.5472
a_2	1.888	1.599	2.312	3.728	9.870
b_1	0.4382	0.4382	0.4382	0.4382	0.4382
b_2	2.275	2.058	2.827	4.487	11.21
c_1	1.101	1.101	1.101	1.101	1.101
c_2	-0.6672	-0.4515	-0.7152	-1.148	-2.748

From the values given in the above table, it is seen that the shear stress and heat-transfer rate at the wall in the case of dusty gases become greater than those in the case of pure gases and the displacement thickness thinner.

5.2 Small-Slip Limit

The zeroth-order equations for the gas as well as for the particles in the small-slip limit, Eqs. (4.21)-(4.23), are similar to the conservation equations for a pure-gas boundary-layer flow but with modified properties. Physically, the small-slip approximation represents a quasi-equilibrium flow and the zeroth-order problem constitutes the exact equilibrium limit where the particles are 'fixed' to the mass of the gas so that the gas and particles move together like a perfect-gas mixture. For the dilute two-phase system with the approximation of negligible volume fraction of the particles, the particles contribute to the mixture density but not to the viscosity [23]:

$$\bar{\rho}^* = (1+\beta)\,\rho^* \tag{5.11}$$

$$\bar{\mu}^* = \mu^* \tag{5.12}$$

The other thermodynamic properties are given by

$$\bar{c}_p^* = c_p^* \frac{1 + \beta/\alpha}{1 + \beta} \tag{5.13}$$

$$\bar{k}^* = k^* \tag{5.14}$$

Then the modified similarity parameters can be expressed as

$$\overline{Pr} = \frac{\bar{c}_p^*\,\bar{\mu}^*}{\bar{k}^*} = Pr\,\frac{1 + \beta/\alpha}{1+\beta} \tag{5.15}$$

$$\overline{Ec} = \frac{u_\infty^{*2}}{\bar{c}_p^*\,T_\infty^*} = Ec\,\frac{\alpha(1+\beta)}{\alpha+\beta} \tag{5.16}$$

Substituting the modified Prandtl number and Eckert number into Eqs. (3.18)-(3.20), which are exactly the same as the boundary-layer equations for pure gases as mentioned before, the resulting 'modified' equations are just the zeroth-order equations for the small-slip limit, Eqs. (4.21)-(4.23). It implies that in the zeroth-order approximation, the gas-particle mixture behaves like a pure gas with modified thermodynamic properties. In this paper, the numerical solutions in the small-slip limit are calculated for the condition of $\alpha = 1.0$. Under this condition, the zeroth-order equations (4.21)-(4.23) for the small-slip limit reduce to those for the large-slip limit, Eqs. (3.18)-(3.20). The results are given in Figs. 3-5. Clearly, in the small-slip limit, the zeroth-order velocity and temperature for the particles are the same as the ones for the gas. From Eq. (4.24), it is found that the nondimensional density of the particle phase $\rho_p^{(0)}$ is equal to the nondimensional density of the gas phase $\rho^{(0)}$ (or the reciprocal of the nondimensional gas temperature $1/T^{(0)}$). It is seen from Fig. 14 that $\rho_p^{(0)}$, or $\rho^{(0)}$, varies monotonically from its maximum value at the wall to its freestream value at the outer edge. In this report, the constant wall temperature T_w is specified as $T_w = 0.5$ and then the density at the wall is equal to 2, as shown in Fig. 14. From Eqs. (4.9) and (4.10), the densities in the dimensional form are given by

$$\rho^* = \rho_\infty^* \rho, \qquad \rho_p^* = \beta \rho_\infty^* \rho_p \tag{5.17}$$

Neglecting the small quantities of first order, the above gas and particle densities are approximated by

$$\rho^* = \rho_\infty^* \rho^{(0)}, \qquad \rho_p^* = \beta \rho_\infty^* \rho_p^{(0)} \tag{5.18}$$

Therefore, at all points of the boundary layer in the small-slip region,

$$\frac{\rho_p^*}{\rho^*} = \beta \tag{5.19}$$

It means that the constant loading ratio of the particles holds across the whole boundary layer in the small-slip region. In other words, the solid particles remain attached to their original gas mass and always move together with this gas mass. The two-phase system behaves like a gaseous mixture. It is a major feature of the gas-particle flow in the small-slip region.

The slip quantities $u_s^{(1)}$, $v_s^{(1)}$ and $T_s^{(1)}$ are given in Figs. 15 to 17, where the effects of the flow parameters Pr, Ec and ω on the first-order

flow of the particles are shown. In fact, the slip quantities represent the first-order approximation for the particle phase. It is seen that the profile of the normal slip velocity $v_s^{(1)}$ is different from that of the tangential slip velocity $u_s^{(1)}$. At the outer edge of the boundary layer, the tangential slip velocity becomes zero but the normal slip velocity approaches a finite value, since the boundary conditions for the tangential and normal velocities are different in boundary-layer analyses. As in the usual boundary-layer problems, the tangential particle velocity at the outer edge of the boundary layer should be equal to the freestream value and then the slip velocity should become zero at the outer edge. However, no similar boundary conditions at the outer edge can be specified for the normal velocity. The unique boundary condition for the normal velocity is that it is equal to zero at the wall. Owing to the continuity equation, the normal velocity is induced and approaches its maximum value at the outer edge. Therefore, the normal slip velocity at the outer edge takes a finite value which is the difference between the normal velocities of the two phases at the outer edge. In addition, by comparing Fig. 15 with Fig. 11, it is found that there exist significant changes in the first-order profile for the tangential velocity of the particles in the two limiting regions. In the small-slip region, the particle slip velocity at the wall is equal to zero, while in the large-slip region, the first-order velocity of the particles has its maximum value in magnitude at the wall as mentioned earlier. As a result of the maximum slip velocity, the interaction term between the gas and the particles has its maximum value at the wall and then the maximum deceleration of the particles takes place along the wall. Hence, at some distance from the leading edge, the particle velocity at the wall reduces to zero and is equal to that of the gas. After this point the particles keep their zero velocity at the wall because of the zero slip velocity. This special point, where the particle velocity becomes zero at the wall, is defined as the critical point for the gas-particle boundary-layer flow. At the critical point, the dusty-gas boundary layer essentially fulfills the transition from the quasi-frozen flow to the quasi-equilibrium flow. The two-phase flow in the small-slip limit is a typical example of a quasi-equilibrium flow. By comparing Fig. 17 with Fig. 12, the same situation happens to the first-order temperature of the particles in the two limiting regions: at the wall, the first-order temperature has its maximum value in the large-slip region and the temperature defect vanishes in the small-slip region. A detailed discussion is omitted here, since it is similar to the above case of velocity. Similar to the large-slip case, it is interesting to obtain the expressions for the boundary-layer characteristic quantities. However, in the small-slip case, since there are no solutions available to the first-order equations of the gas, they can be expressed only in zeroth order. Similarly, the three boundary-layer characteristics are given in the nondimensional form:

$$\tau_w = \frac{\mu_w}{\sqrt{x}} \left(\sqrt{1+\beta}\, a_1\right) \tag{5.20}$$

$$\dot{q}_w = - \frac{\mu_w}{\sqrt{x}} (\sqrt{1+\beta}\, b_1) \tag{5.21}$$

$$\delta = \sqrt{x}\, \left(\frac{c_1}{\sqrt{1+\beta}}\right) \tag{5.22}$$

The coefficients a_1, b_1 and c_1 in Eqs. (5.20)-(5.22) have the same values as in Table 1. By contrast with the large-slip limit, the zeroth-order expressions for the boundary-layer characteristics in the small-slip limit, Eqs. (5.20)-(5.22), involve the effects of the particles. In fact, the term $\sqrt{1+\beta}$ in Eqs. (5.20)-(5.22) represents the alteration of the boundary layer by the particles. In the small-slip limit, the two-phase system acts like a single gaseous system with modified properties as pointed out before. With Eqs. (5.9)-(5.10), the 'modified' similarity variable $\bar{\eta}$ becomes

$$\bar{\eta} = \sqrt{\frac{u_\infty^*}{2\bar{\nu}_\infty^* x^*}}\, y^* = \sqrt{\frac{(1+\beta)u_\infty^*}{2\nu_\infty^* x^*}}\, y^* = \eta \cdot \sqrt{1+\beta} \tag{5.23}$$

This implies that the boundary-layer flow of a dusty gas in the small-slip limit corresponds to a similarity solution with the normal scale modified by the factor $\sqrt{1+\beta}$, owing to the particles. Consequently, the shear stress and heat-transfer rate at the wall increase and the displacement thickness decreases by the same factor of $\sqrt{1+\beta}$. Therefore, it can be concluded that the presence of particles enhances the shear stress and heat-transfer at the wall and thins the boundary layer in the two limiting regions. This tendency can be seen in Figs. 18 and 19, where the shear stress and heat-transfer rate are shown as functions of the nondimensional distance x for the cases with and without particles. As expected, the results for the large-slip limit and the small-slip limit coincide with the pure-gas results in the limits $x \to 0$ and $x \to \infty$, respectively. Note that the large-slip results when $x > 0.1$ and the small-slip results when $x < 10$ are meaningless since the aysmptotic solutions are not valid. Physically, the changes in the characteristics caused by the particles can be explained as follows. The gas-flow profiles with and without particles are schematically shown in Fig. 20. As a result of the interaction, the gas velocity and temperature increase in the cold-wall case (say, $T_w = 0.5$). Then the derivatives of the gas velocity and temperature with respect to the normal coordinate y^* at the wall become greater than those without particles. These changes result in an increase in the shear stress and heat-transfer at the wall, since they are proportional to those derivatives. In addition, the boundary layer

becomes thinner since the velocity approaches its freestream value more quickly.

The numerical results for the asymptotic solutions using the series-expansion method were compared with the finite-difference solutions in the two limiting regions. The agreement between the asymptotic solutions and the difference solutions was excellent [1].

6.0 CONCLUDING REMARKS

Some general conclusions obtained from the asymptotic solutions of the flat-plate boundary-layer flow of a dilute gas-particle mixture are summarized as follows:

(1) The asymptotic solutions to the dusty-gas boundary-layer equations can be obtained using a series-expansion method. They describe the limiting properties of two-phase flows in the large-slip region and the small-slip region, which are characterized by a frozen flow and an equilibrium flow, respectively. The asymptotic solutions are in excellent agreement with the finite-difference solutions.

(2) The interaction between the gas and particles determines the flow properties of the particle phase, and influences strongly the flow properties of the gas phase in addition to the viscosity. When the particle slip Reynolds number is high, a proper expression for the drag and heat transfer between the two phases should be specified instead of using Stokes' relations. The results when using Stokes' relations are reasonable qualitatively but not correct quantitatively for a Reynolds number greater than unity.

(3) For a given gas-particle system with specified values of the mass loading ratio and the ratio of the specific heats of the two phases, similar to the case of high-velocity viscous flows of a pure gas, all of the following parameters are important for the analysis of compressible laminar boundary-layer flows of gas-particle mixtures: Reynolds, Prandtl and Eckert numbers as well as the transport properties (viscosity and heat conductivity).

(4) For compressible, laminar, boundary-layer flows of dusty gases, the shear stress and the heat-transfer rate at the wall increase and the displacement thickness decreases when compared with the corresponding results for a pure gas. Owing to the presence of the particles, the gas velocity and temperature increase on a flat-plate boundary layer with a cold wall. As a result, the velocity and temperature gradients at the wall for the gas phase increase so that the shear stress and heat transfer are enhanced and the velocity achieves its freestream value at a shorter distance from the wall so that the displacement thickness of the boundary layer is decreased.

REFERENCES

1. Wang, B. Y. and Glass, I. I., "Finite-Difference Solutions for Compressible Laminar Boundary-Layer Flows of a Dusty Gas Over a Semi-Infinite Flat Plate", UTIAS Report No. 311, 1986.

2. Marble, F. E., "Dynamics of a Gas Containing Small Solid Particles", Combustion and Propulsion, 5th AGARD Colloquium, Pergamon Press, 1963.

3. Liu, J. T. C., "Flow Induced by the Impulsive Motion of an Infinite Flat Plate in a Dusty Gas", Astronautica Acta, Vol. 13, No. 4, 1967, pp. 369-377.

4. Soo, S. L., "Non-Equilibrium Fluid Dynamics - Laminar Flow Over a Flat Plate", ZAMP, Vol. 19, No. 4, 1968, pp. 545-563.

5. Zung, L. B., "Flow Induced in Fluid Particle Suspension by an Infinite Rotating Disk", The Physics of Fluids, Vol. 12, No. 1, 1969, pp. 18-23.

6. Otterman, B. and Lee, S. L., "Particulate Velocity and Concentration Profiles for Laminar Flow of a Suspension Over a Flat Plate", Heat Transfer and Fluid Mechanics Institute, Monterey, California, June 10-12, 1970 Proceedings, Stanford University Press, pp. 311-322.

7. Lee, S. L. and Chan, W. K., "Two-Phase Laminar Boundary Layer Along a Vertical Flat Wall", Hydrotransport, Vol. 2, 1972, A4.45-A4.58.

8. DiGiovanni, P. R. and Lee, S. L., "Impulsive Motion in a Particle-Fluid Suspension Including Particulate Volume, Density and Migration Effects", Journal of Applied Mechanics, Vol. 41, No. 1, 1974, pp. 35-41.

9. Soo, S. L., "Fluid Dynamics of Multiphase Systems", Blaisdell Publishing Co., 1967.

10. Tabakoff, W. and Hamed, A., "Analysis of Cascade Particle Gas Boundary Layer Flows with Pressure Gradient", AIAA Paper No. 72-87.

11. Hamed, A. and Tabakoff, W., "The Boundary Layer of Particulate Gas Flow", Zeitschrift fur Flugwissenchaften, Vol. 20, 1972, pp. 373-381.

12. Jain, A. C. and Ghosh, A., "Gas-Particulate Laminar Boundary Layer on a Flat Plate", Z. Flugwise Weltraumersch, Vol. 3, 1979, pp. 379-385.

13. Hamed, A. and Tabakoff, W., "Analysis of Nonequilibrium Particulate Flow", AIAA Paper No. 73-687.

14. Prabha, S. and Jain, A. C., "On the Use of Compatibility Conditions in the Solution of Gas Particulate Boundary Layer Equations", Applied Scientific Research, Vol. 36, No. 2, 1980, pp. 81-91.

15. Osiptsov, A. N., "Structure of the Laminar Boundary Layer of a Disperse Medium on a Flat Plate", Fluid Dynamics, Vol. 15, No. 4, 1980 pp. 512-517.

16. Prabha, S. and Jain, A. C., "On the Nature of Gas-Particulate Flow", 13th International Symposium on Space Technology and Science, Tokyo, Japan, June 28-July 3, 1982, pp. 517-522.

17. Singleton, R. E., "The Compressible Gas-Solid Particle Flow Over a Semi-Infinite Flat Plate", ZAMP, Vol. 16, 1965, pp. 421-429.

18. Chapman, S. and Cowling, T. G., The Mathematical Theory of Non-Uniform Gases, Cambridge University Press, 1961.

19. Gilbert, M. Davis, L. and Altman, D., "Velocity Lag of Particles in Linear Accelerated Combustion Gases", Jet Propulsion, Vol. 25, 1965, pp. 26-30.

20. Knudsen, J. G. and Katz, D. L., Fluid Mechanics and Heat Transfer, McGraw-Hill, 1958.

21. Schlichting, H., Boundary-Layer Theory (Seventh Edition), McGraw-Hill Inc., 1979.

22. Gear, C. W., Numerical Initial Value Problems in Ordinary Differential Equations. Prentice-Hall, Englewood Cliffs, 1971.

23. Rudinger, G., Fundamentals of Gas-Particle Flow, Elsevier Scientific Publishing Co., 1980.

APPENDIX

RELAXATION PROCESS AND VELOCITY EQUILIBRIUM TIME

In gas-particle flows, generally speaking, the gas and the particles may have different velocities and temperatures, and as an immediate consequence the two phases must interact. Every particle experiences a drag force and exchanges heat with the gas. The same happens to the gas but in the opposite direction. Consequently, the velocities and temperatures tend to approach each other, and the instantaneous rate of this approach depends on the instantaneous velocity and temperature differences between the particle and the gas. This phenomenon, which is usually known as the relaxation process, is a major feature of gas-particle flows. A discussion of the viscous drag between the gas and the particles and of the velocity relaxation process will illustrate the relaxation processes in a two-phase system.

For the case of a single spherical particle in a viscous flow, if the particle velocity $\vec{U}_p$ (here the unstarred quantities denote dimensional flow properties) is different from the gas velocity $\vec{U}$, the viscous drag exerted by the gas on the particle depends on the relative, or slip, velocity $(\vec{U}_p - \vec{U})$. As usual in fluid mechanics, the drag $\vec{F}$ is expressed by means of a drag coefficient C_D which is defined in terms of the dynamic head of the relative flow and the frontal area of the particle:

$$\vec{F} = C_D \left\{ \frac{1}{2} \rho (\vec{U} - \vec{U}_p) |\vec{U} - \vec{U}_p| \frac{\pi}{4} d^2 \right\} \tag{A.1}$$

where ρ is the gas density and d is the particle diameter. On the right-hand side of Eq. (A.1), the square of the relative velocity is written in this manner to ensure that the drag force always has the correct sign. The drag coefficient C_D is a function of the particle slip Reynolds number

$$C_D = C_D(Re_s) \tag{A.2}$$

where Re_s is the slip Reynolds number based on the particle diameter

$$Re_s = \frac{\rho |\vec{U}_p - \vec{U}| d}{\mu} \tag{A.3}$$

where μ is the gas viscosity.

For the Stokes case, with a low-slip Reynolds number less than about one, the drag coefficient takes the simple form

$$C_{D_0} = \frac{24}{Re_s} \tag{A.4}$$

This is the Stokes relation for the drag force. For a higher slip Reynolds number ($Re_s > 1$), there are several empirical relations for the drag coefficient given by different investigators. It is convenient to write

$$C_D = C_{D_0} \cdot D(Re_s) \tag{A.5}$$

or

$$D = \frac{C_D}{C_{D_0}} \tag{A.6}$$

where D is the so-called normalized drag coefficient in this analysis. It is clear that $D(Re_s) = 1$ corresponds to Stokes' drag.

The above discussion deals only with isolated particles. Of course, if there is an appreciable number density of particles, the effective, or apparent, drag coefficient may be different from that for a single particle because of some forms of interaction between the particles, such as direct collisions and particle-wake interaction. At present, there are no adequate analytical or experimental results available for these interactions. In this report, the case of a dilute gas-particle mixture is considered, and it is reasonable to assume that the drag coefficient for a single sphere is valid for the particle cloud. Therefore, if the drag coefficient takes the form of the Stokes relation, the drag force on every particle is

$$\vec{F} = \frac{24}{Re_s} \left\{\frac{1}{2} \rho(\vec{U} - \vec{U}_p)|\vec{U} - \vec{U}_p| \frac{\pi}{4} d^2\right\}$$

$$= \frac{24}{\rho|\vec{U}_p - \vec{U}|d/\mu} \left\{\frac{\pi d^2}{8} \rho(\vec{U} - \vec{U}_p)|\vec{U} - \vec{U}_p|\right\}$$

$$= 3\pi\mu d(\vec{U} - \vec{U}_p) \tag{A.7}$$

Let n_p denote the number density of the particles, ρ_p the density of the particle phase, ρ_s the density of the particle material and m the mass of a particle. Then

$$m = \rho_s \cdot \frac{\pi}{6} d^3 \tag{A.8}$$

$$n_p = \frac{\rho_p}{m} = \frac{\rho_p}{\rho_s \cdot \frac{\pi}{6} d^3} \tag{A.9}$$

The force per unit volume of the gas-particle mixture acting on the gas, $\vec{D} = \vec{i}Dx + \vec{j}Dy$, can be given as

$$\vec{D} = -n_p \cdot \vec{F}$$

$$= \frac{\rho_p}{\rho_s \cdot \frac{\pi}{6} d^3} \cdot 3\pi\mu d(\vec{U}_p - \vec{U})$$

$$= \rho_p \frac{\vec{U}_p - \vec{U}}{\tau_v} \tag{A.10}$$

where τ_v is defined as the particle velocity-equilibrium time

$$\tau_v = \frac{\rho_s d^2}{18\mu} \tag{A.11}$$

The velocity-equilibrium time τ_v depends on the density of particle material, the particle diameter and the gas viscosity. Some typical values of the velocity-equilibrium time are given in Table 2, where the particle material density ρ_p = 2.5 g/cm^3 (typical of crown glass).

Table 2

Typical Values of the Particle Velocity Equilibrium Time (ms)

Gas Temperature T (K)	Particle Diameter d (μm)		
	10	20	40
300	0.755	3.02	12.08
400	0.605	2.42	9.68
500	0.510	2.04	8.16

Physically, τ_v is the time required for a particle to reduce the slip velocity to e^{-1} of its initial value. To examine this criteria, consider a flow field with constant gas velocity and temperature. For the particles moving in this flow field, Newton's law of motion becomes

$$m \frac{d\vec{U}_p}{dt} = \vec{F} \tag{A.12}$$

Substituting Eqs. (A.7) and (A.8), Eq. (A.12) becomes

$$\frac{d\vec{U}_p}{dt} = \frac{\vec{F}}{m}$$

$$= \frac{3\pi\mu d(\vec{U} - \vec{U}_p)}{\rho_s \cdot \frac{\pi}{6} d^3}$$

$$= \frac{18\mu}{\rho_s d^2} (\vec{U} - \vec{U}_p)$$

$$= \frac{\vec{U} - \vec{U}_p}{\tau_v} \tag{A.13}$$

Since the gas velocity and temperature are assumed as constant, i.e., $\vec{U}$ and τ_v are constant, Eq. (A.13) is readily integrated with the result

$$\vec{U}_p - \vec{U} = (\vec{U}_{p,o} - \vec{U})e^{-\frac{t}{\tau_v}} \tag{A.14}$$

where $\vec{U}_{p,o}$ is the initial velocity of the particles at t = 0. This result indicates a typical velocity-relaxation process in which the slip velocity decays exponentially. From Eq. (A.14), it is known that the velocity-equilibrium time τ_v is the time elapsed for a particle to reduce its original relative velocity by e^{-1}. It should be pointed out that, in fact, the velocity relaxation process is not completed in the velocity-equilibrium time τ_v, since the slip velocity still has an appreciable value, i.e., about 37% of its original value. In addition, if the gas velocity and temperature are not constant, or Stokes' drag does not apply, Eq. (A.13) becomes more difficult to solve, and the solution is no longer a simple exponential decay of the slip velocity, Eq. (A.14). Nevertheless, the parameter τ_v remains a convenient measure for the tendency of the particles to reach velocity equilibrium with the gas.

For the non-Stokes case, the drag force on every particle is given by

$$\vec{F} = C_{D_0}\{\frac{1}{2}\rho(\vec{U} - \vec{U}_p)|\vec{U} - \vec{U}_p|\frac{\pi}{4}d^2\}D$$

$$= 3\pi\mu d(\vec{U} - \vec{U}_p)D \tag{A.15}$$

The drag force per unit volume exerting on the gas by the particles is obtained as

$$\vec{D} = -n_p \cdot \vec{F}$$

$$= \rho_p \frac{\vec{U}_p - \vec{U}}{\tau_v} D \tag{A.16}$$

or

$$D_x = \rho_p \frac{u_p - u}{\tau_v} D, \qquad D_y = \rho_p \frac{v_p - v}{\tau_v} D \tag{A.17}$$

where u and v are the velocity components for the gas, and u_p and v_p for the particles:

$$\vec{U} = \vec{i}u + \vec{j}v, \qquad \vec{U}_p = \vec{i}u_p + \vec{j}v_p \tag{A.18}$$

The dissipation function due to the relative motion of the particles is

$$\begin{aligned}\phi &= \vec{D} \cdot (\vec{U}_p - \vec{U}) \\ &= (u_p - u)D_x + (v_p - v)D_y \end{aligned} \tag{A.19}$$

The heat transfer from a particle to the gas has the form

$$q = k(\pi d^2)\frac{T_p - T}{d} \cdot Nu$$

where k is the heat conductivity of the gas, Nu is the Nusselt number, and T_p and T are the particle and gas temperatures, respectively. Then the total heat transfer to the gas per unit volume is given by

$$\begin{aligned} Q &= n_p \cdot q \\ &= \frac{\rho_p}{\rho_s \frac{\pi}{6} d^3} k \cdot \pi d^2 \frac{T_p - T}{d} Nu \\ &= \rho_p \frac{12k}{\rho_s d^2}(T_p - T)\frac{Nu}{2} \\ &= \rho_p c_s \frac{T_p - T}{\tau_T}\frac{Nu}{2} \end{aligned} \tag{A.20}$$

where c_s is the specific heat of the particle phase and τ_T is the temperature-equilibrium time:

$$\tau_T = \frac{\rho_s d^2}{12k} c_s \qquad (A.21)$$

The temperature-equilibrium time τ_T can be expressed in terms of the velocity-equilibrium time τ_v:

$$\tau_T = \frac{\rho_s d^2}{18\mu} \frac{18\mu}{12k} \cdot c_s$$

$$= \frac{3}{2} Pr \frac{c_s}{c_p} \tau_v \qquad (A.22)$$

where c_p is the specific heat at constant pressure for the gas and Pr is the gas Prandtl number:

$$Pr = \frac{c_p \mu}{k} \qquad (A.23)$$

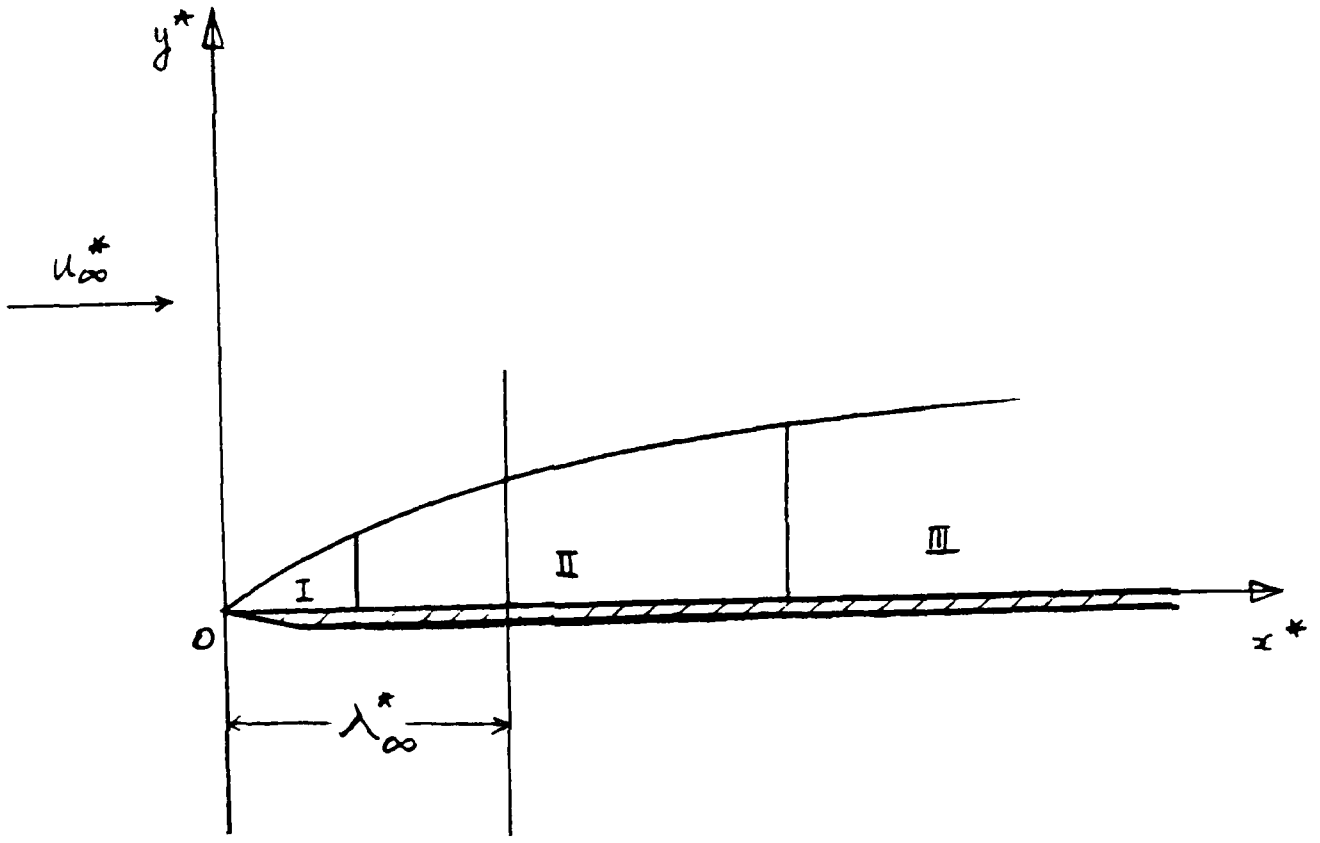

FIGURE 1. SCHEMATIC OF A DUSTY-GAS BOUNDARY-LAYER OVER A SEMI-INFINITE FLAT PLATE. REGION I: LARGE-SLIP REGION. REGION II: MODERATE-SLIP REGION. REGION III: SMALL-SLIP REGION.

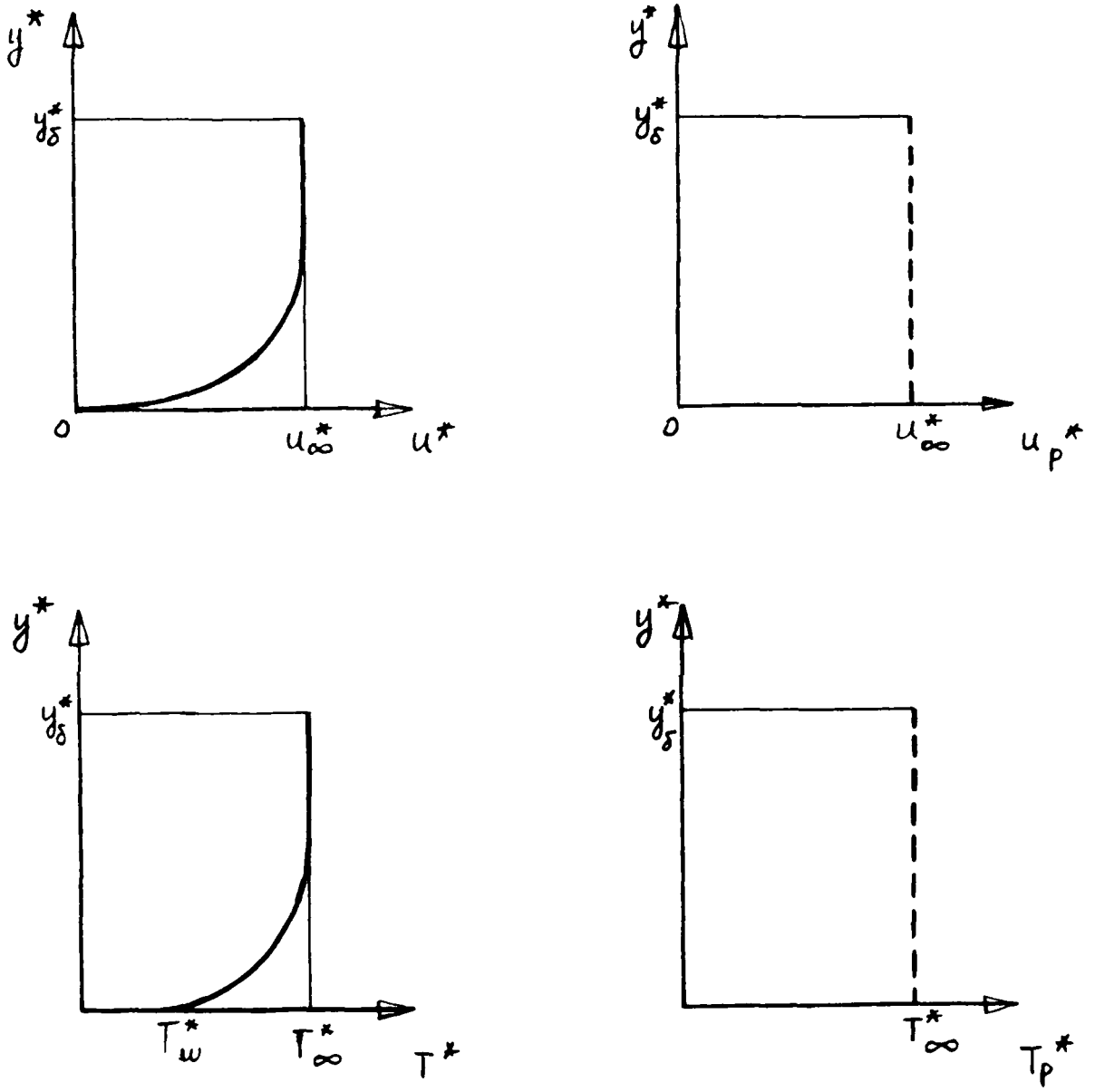

FIGURE 2. ASYMPTOTIC FLOW PROFILES IN THE TWO LIMITING REGIMES.

(a) FROZEN FLOW; (b) EQUILIBRIUM FLOW.
—— GAS; --- PARTICLES.

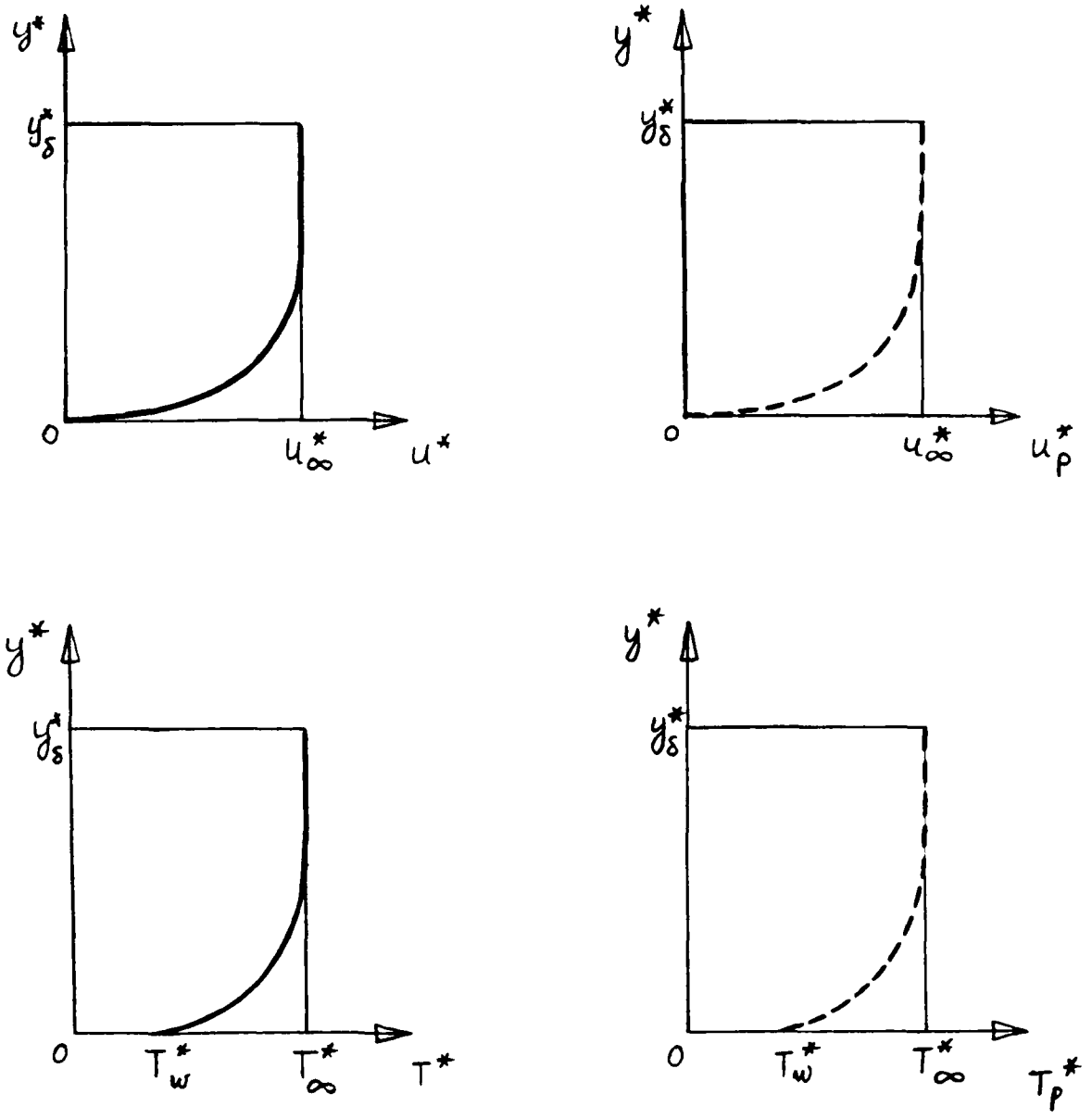

FIGURE 2. ASYMPTOTIC FLOW PROFILES IN THE TWO LIMITING REGIMES.

(a) FROZEN FLOW; (b) EQUILIBRIUM FLOW.
—— GAS; --- PARTICLES.

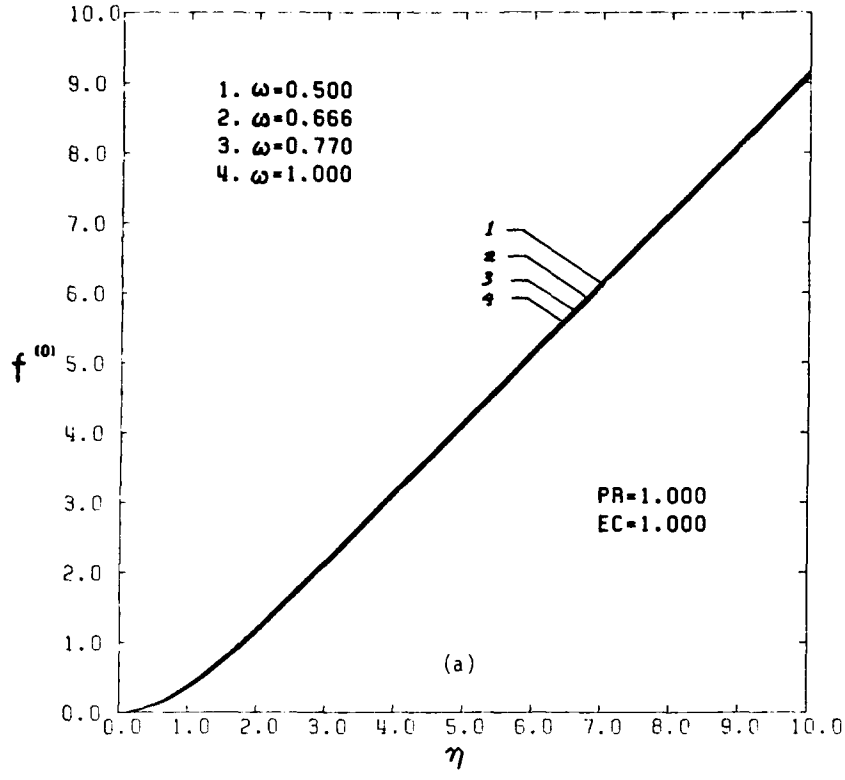

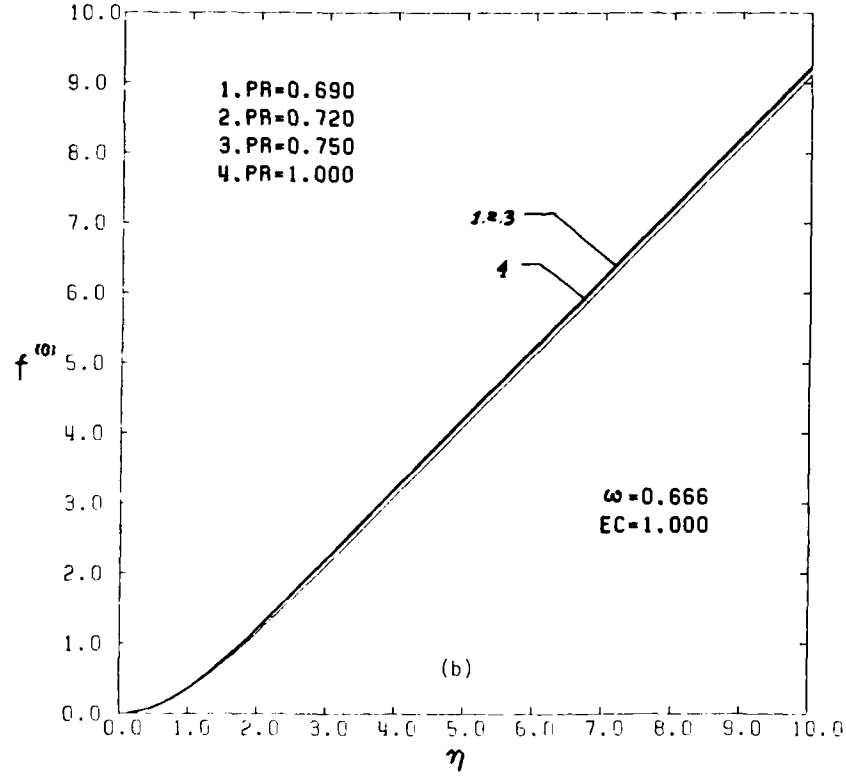

FIGURE 3. THE ZEROTH-ORDER FUNCTION $f^{(0)}$ FOR THE GAS PHASE.

(a) Pr = 1.0, Ec = 1.0 and ω = 0.5, 0.67, 0.77 AND 1.0, RESPECTIVELY.
(b) Ec = 1.0, ω = 0.67 and Pr = 0.69, 0.72, 0.75 AND 1.0, RESPECTIVELY.
(c) Pr = 0.69, ω = 0.67 AND Ec = 0.1, 0.4 AND 1.0, RESPECTIVELY.

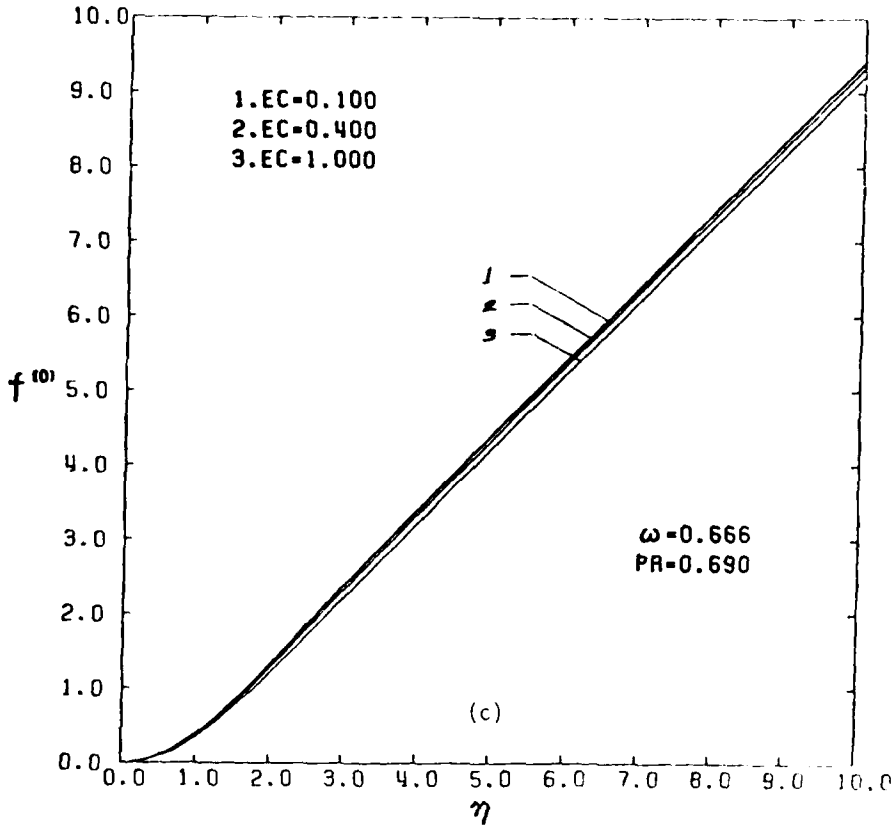

FIGURE 3 - CONTINUED

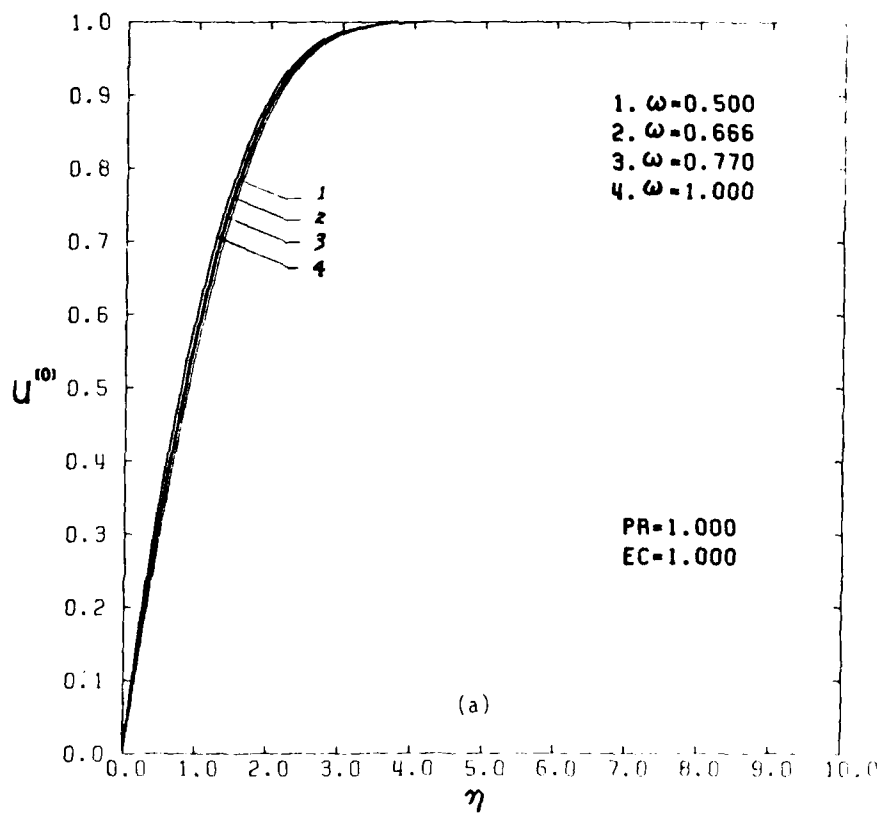

FIGURE 4. THE ZEROTH-ORDER VELOCITY $u^{(0)}$ FOR THE GAS PHASE.

(a) Pr = 1.0, Ec = 1.0 AND ω = 0.5, 0.67, 0.77 AND 1.0, RESPECTIVELY.
(b) Ec = 1.0, ω = 0.67 AND Pr = 0.69, 0.72, 0.75 AND 1.0, RESPECTIVELY.
(c) Pr = 0.69, ω = 0.67 AND Ec = 0.1, 0.4 AND 1.0, RESPECTIVELY.

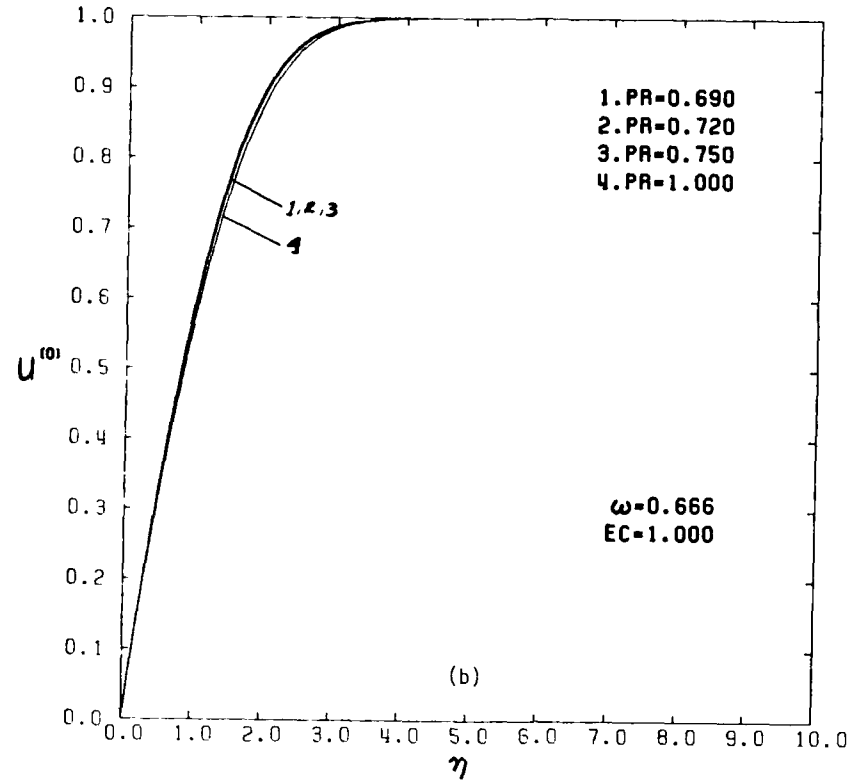

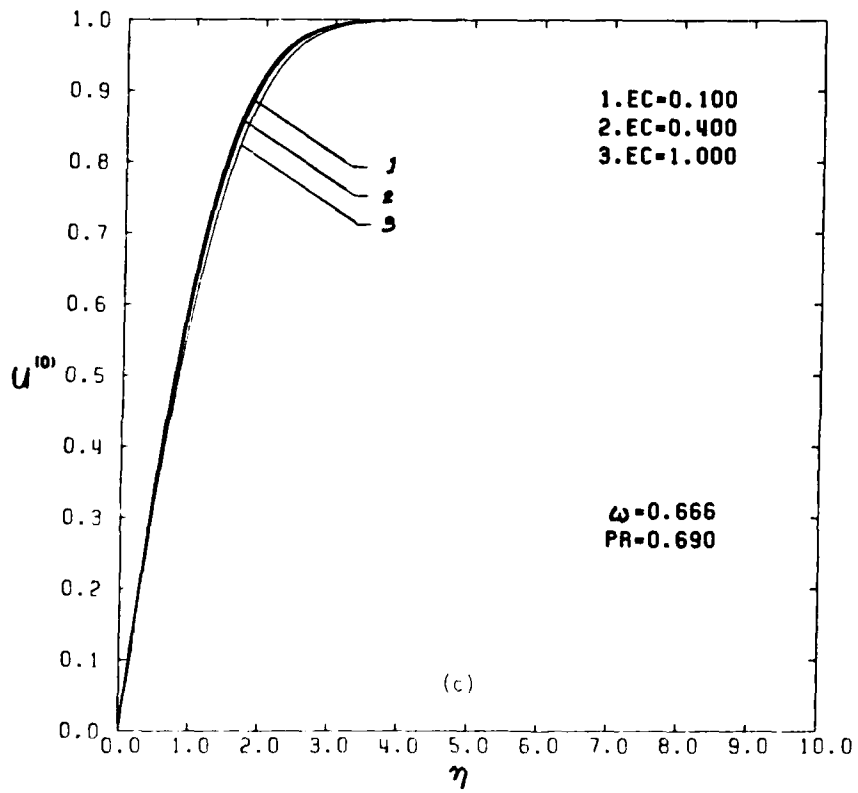

FIGURE 4 - CONTINUED

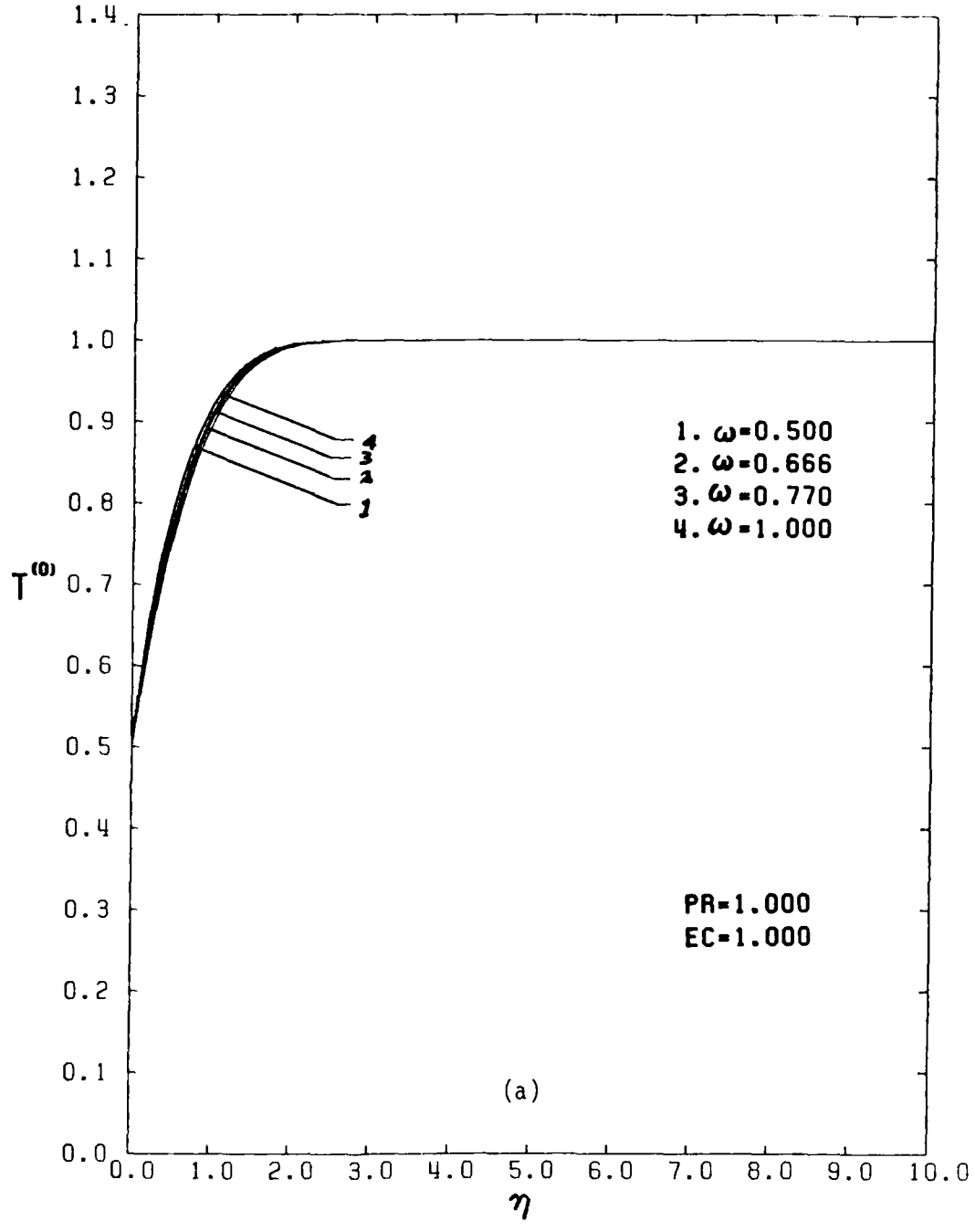

FIGURE 5. THE ZEROTH-ORDER TEMEPRATURE $T^{(0)}$ FOR THE GAS PHASE.

(a) Pr = 1.0, Ec = 1.0 AND ω = 0.5, 0.67, 0.77 AND 1.0, RESPECTIVELY.
(b) Ec = 1.0, ω = 0.67 AND Pr = 0.69, 0.72, 0.75 AND 1.0, RESPECTIVELY.
(c) Pr = 0.69, ω = 0.67 AND Ec = 0.1, 0.4 AND 1.0, RESPECTIVELY.

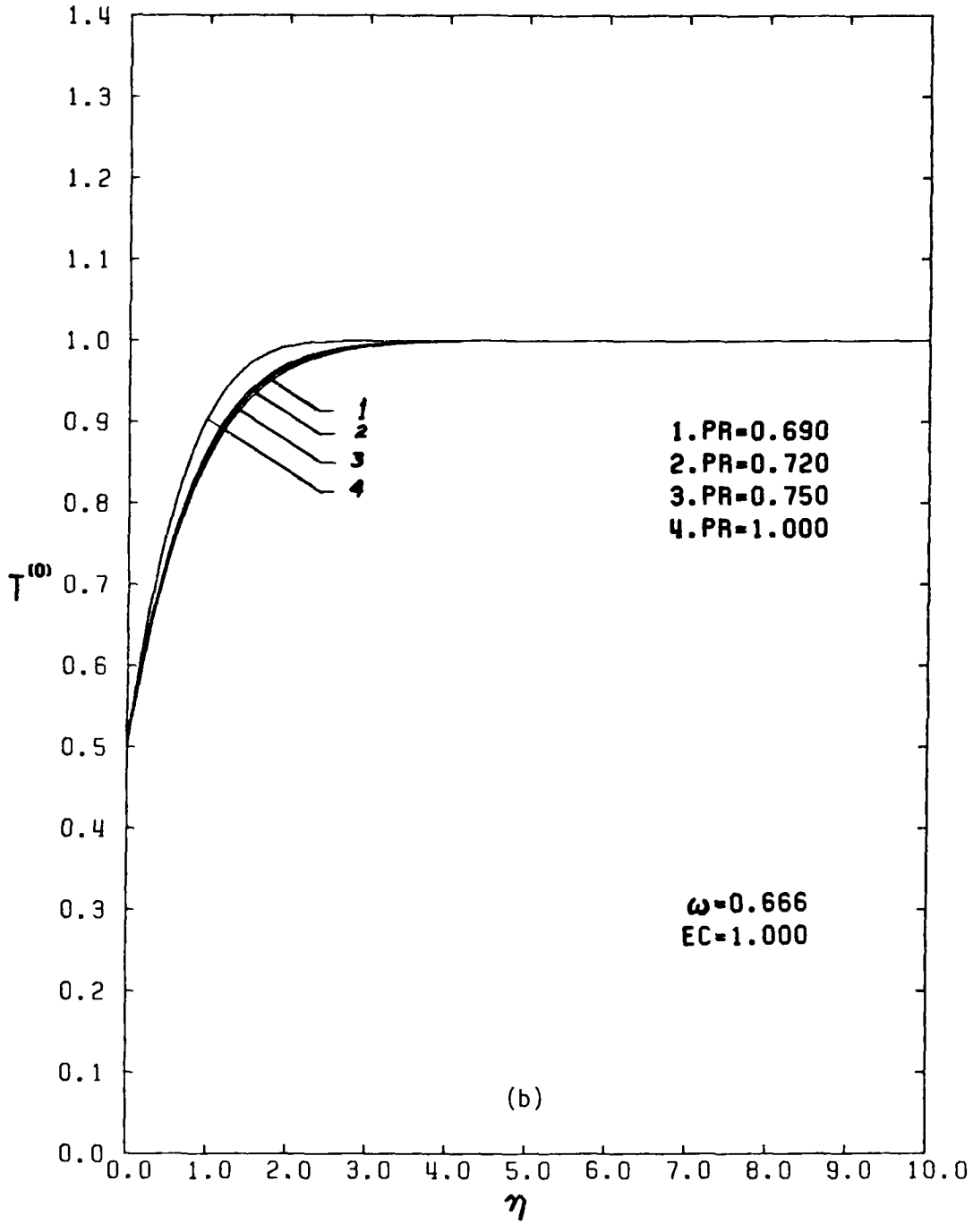
1.4
1.3
1.2
1.1
1.0
0.9
0.8
0.7
0.6
0.5
0.4
0.3
0.2
0.1
0.0
T(0)
0.0
1.0
2.0
3.0
4.0
5.0
6.0
7.0
8.0
9.0
10.0
η
1
2
3
4
1.PR=0.690
2.PR=0.720
3.PR=0.750
4.PR=1.000
ω=0.666
EC=1.000
(b)

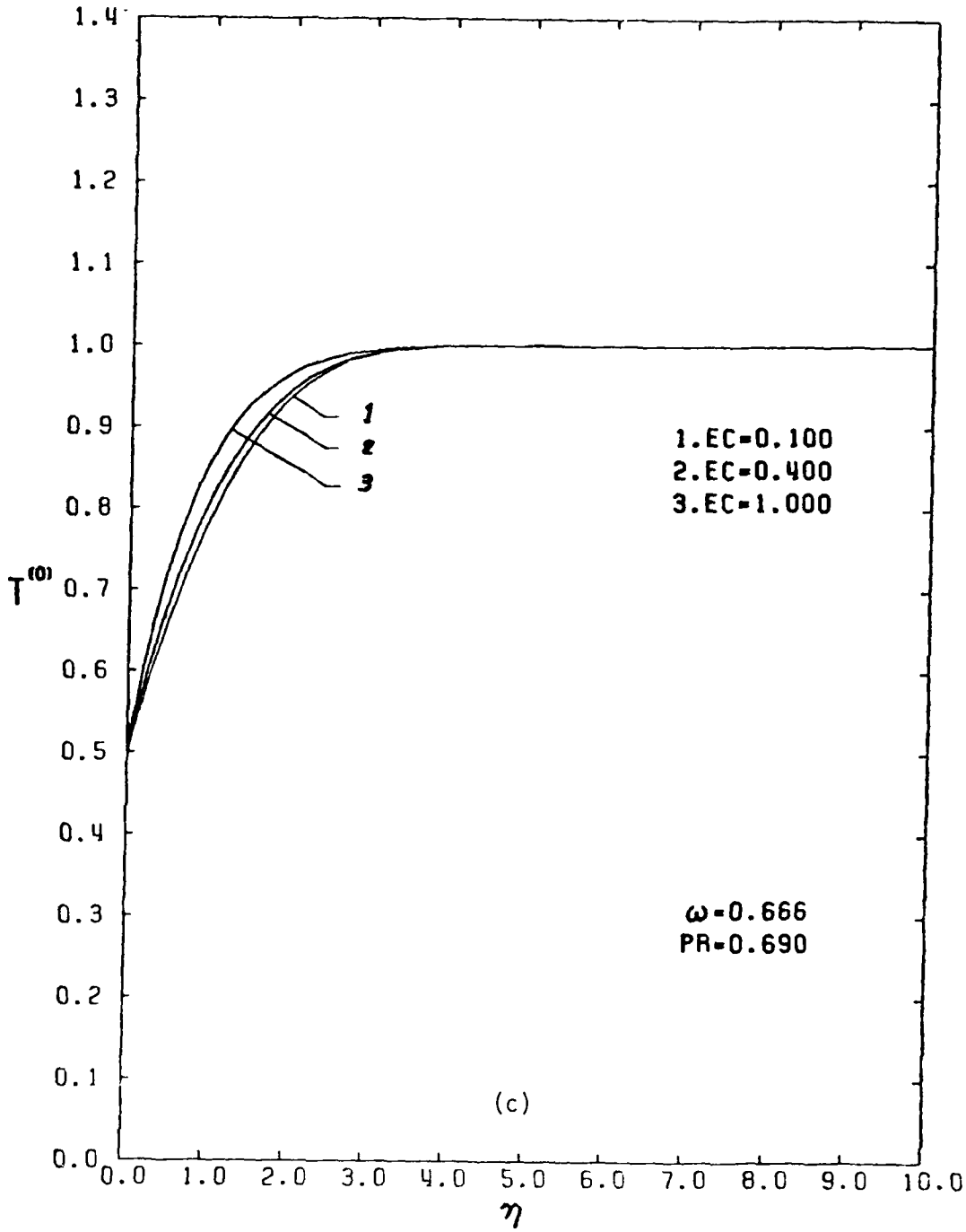

FIGURE 5 - CONTINUED

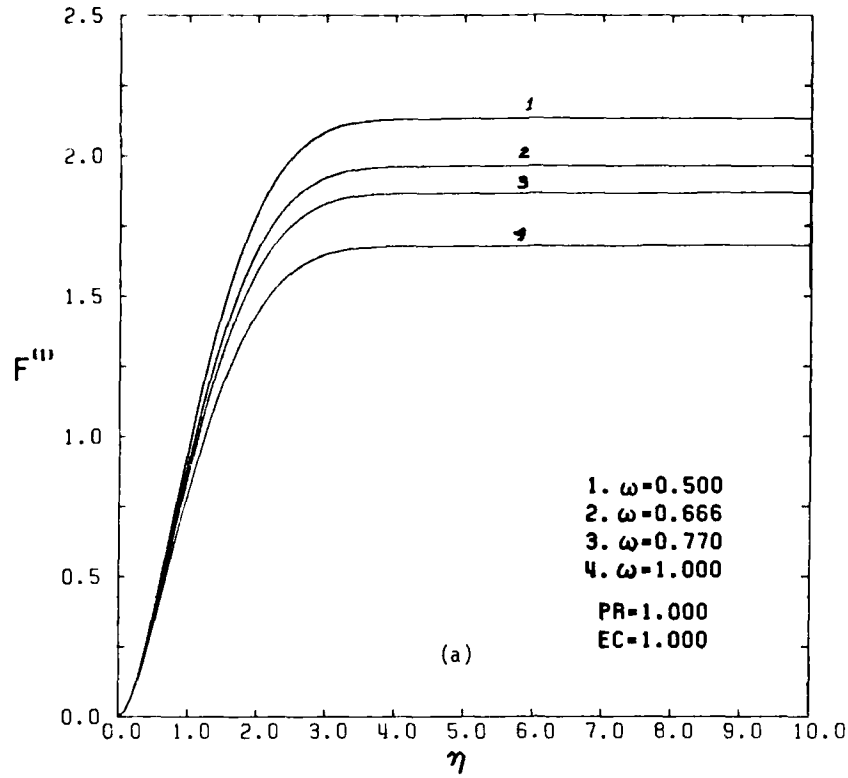

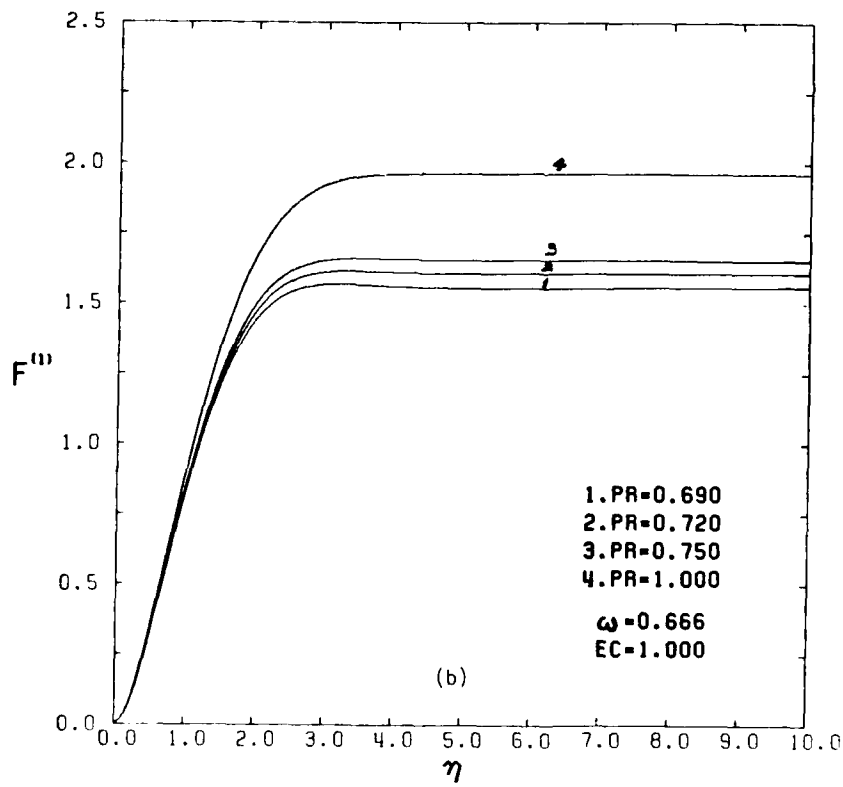

FIGURE 6. FIRST-ORDER FUNCTION $F^{(1)}$ FOR THE GAS PHASE IN THE LARGE-SLIP LIMIT FOR THE STOKES CASE.

(a) Pr = 1.0, Ec = 1.0 AND ω = 0.5, 0.67, 0.77 AND 1.0, RESPECTIVELY.
(b) Ec = 1.0, ω = 0.67 AND Pr = 0.69, 0.72, 0.75 AND 1.0, RESPECTIVELY.
(c) Pr = 0.69, ω = 0.67 AND Ec = 0.1, 0.4 and 1.0, RESPECTIVELY.

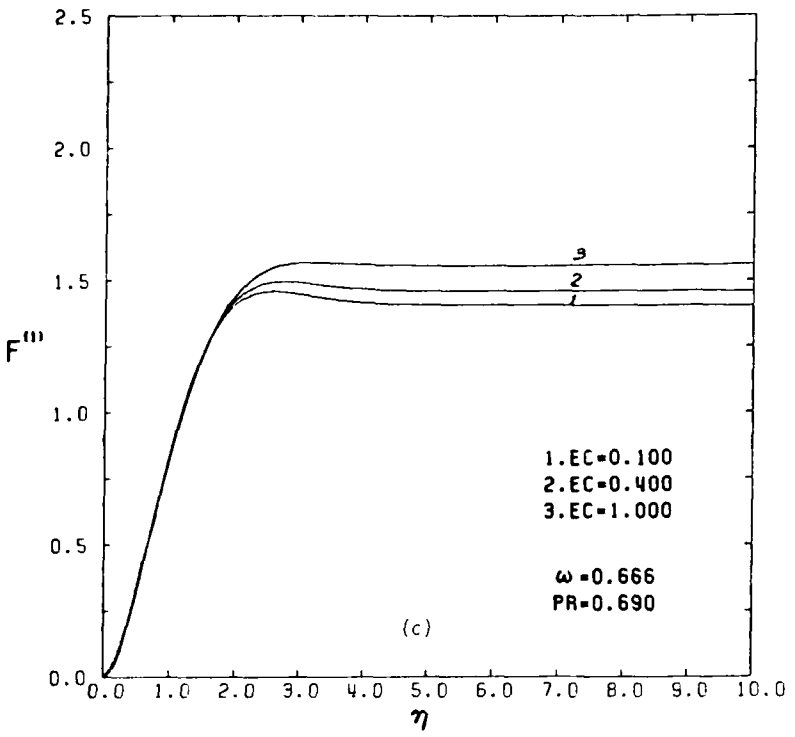

FIGURE 6 - CONTINUED

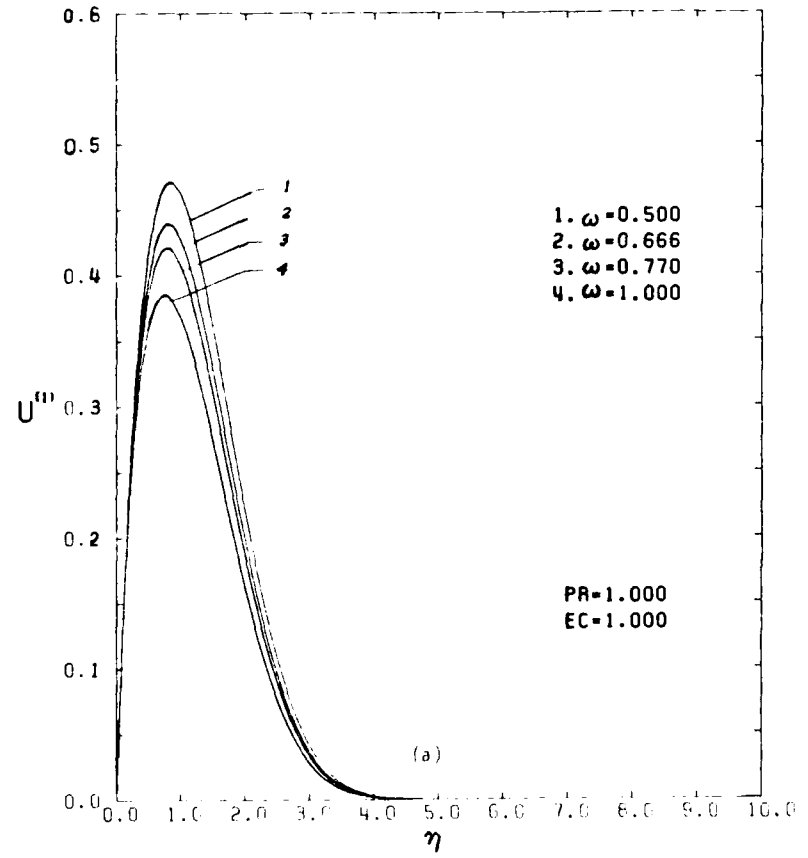

FIGURE 7. FIRST-ORDER VELOCITY $U^{(1)}$ FOR THE GAS PHASE IN THE LARGE-SLIP LIMIT FOR THE STOKES CASE.

(a) Pr = 1.0, Ec = 1.0 AND ω = 0.5, 0.67, 0.77 AND 1.0, RESPECTIVELY.
(b) Ec = 1.0, ω = 0.67 AND Pr = 0.69, 0.72, 0.75 AND 1.0, RESPECTIVELY.
(c) Pr = 0.69, ω = 0.67 AND Ec = 0.1, 0.4, AND 1.0, RESPECTIVELY.

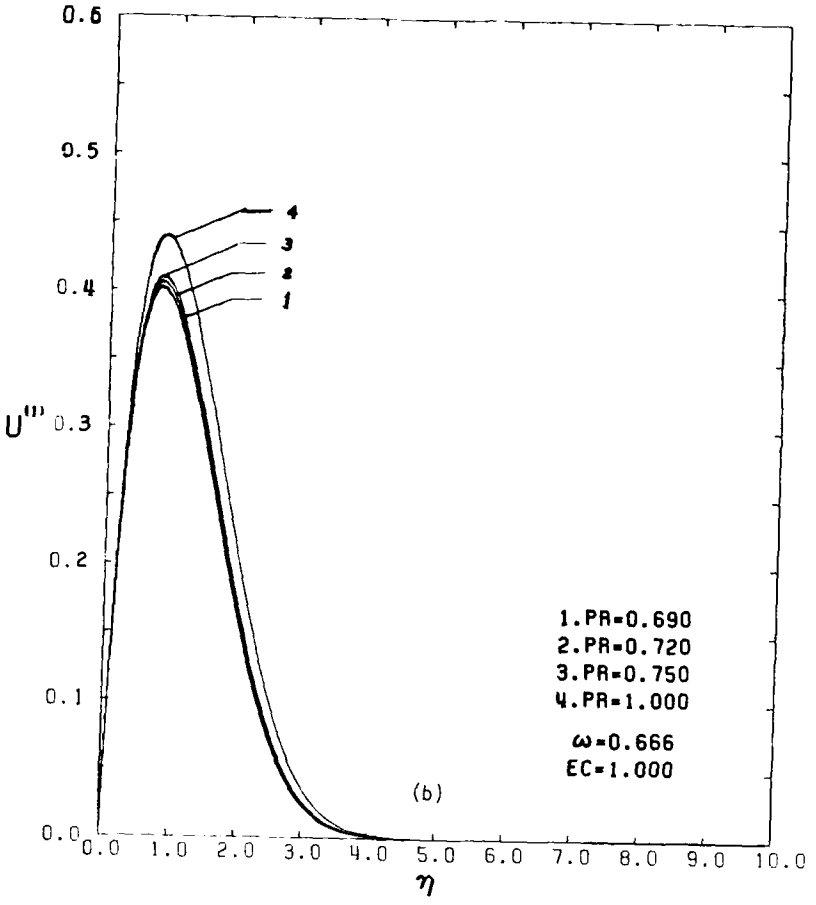

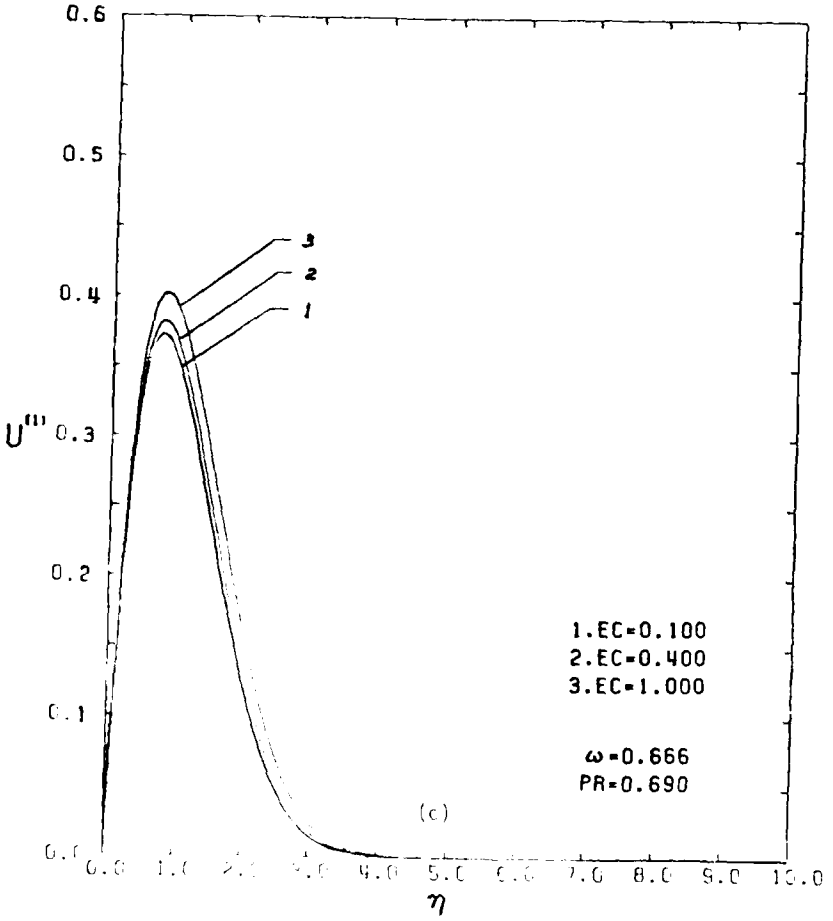

FIGURE 7 - CONTINUED

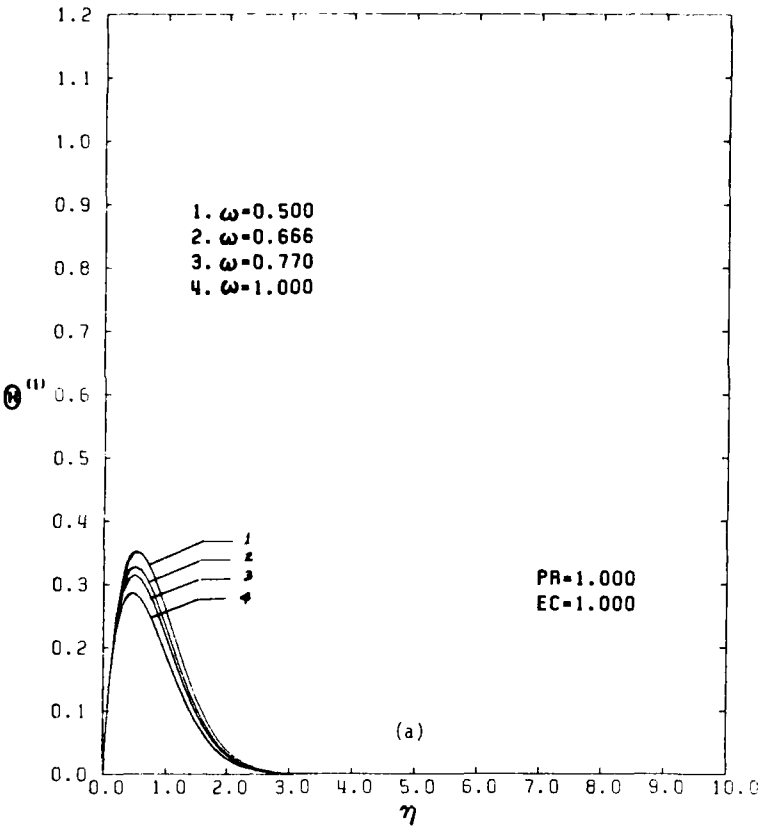

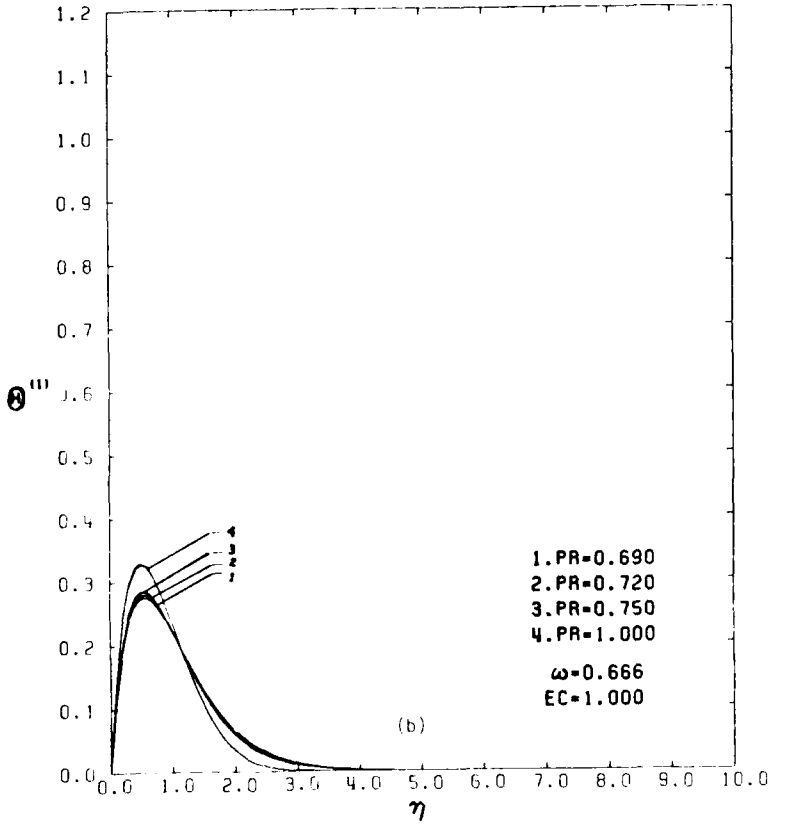

FIGURE 8. FIRST-ORDER TEMPERATURE $^{(1)}$ FOR THE GAS PHASE IN THE LARGE-SLIP LIMIT FOR THE STOKES CASE.

(a) Pr = 1.0, Ec = 1.0 AND ω = 0.5, 0.67, 0.77 AND 1.0, RESPECTIVELY.
(b) Ec = 1.0, ω = 0.67 AND Pr = 0.69, 0.72, 0.75 AND 1.0, RESPECTIVELY.
(c) Pr = 0.69, ω = 0.67 AND Ec = 0.1, 0.4 AND 1.0, RESPECTIVELY.

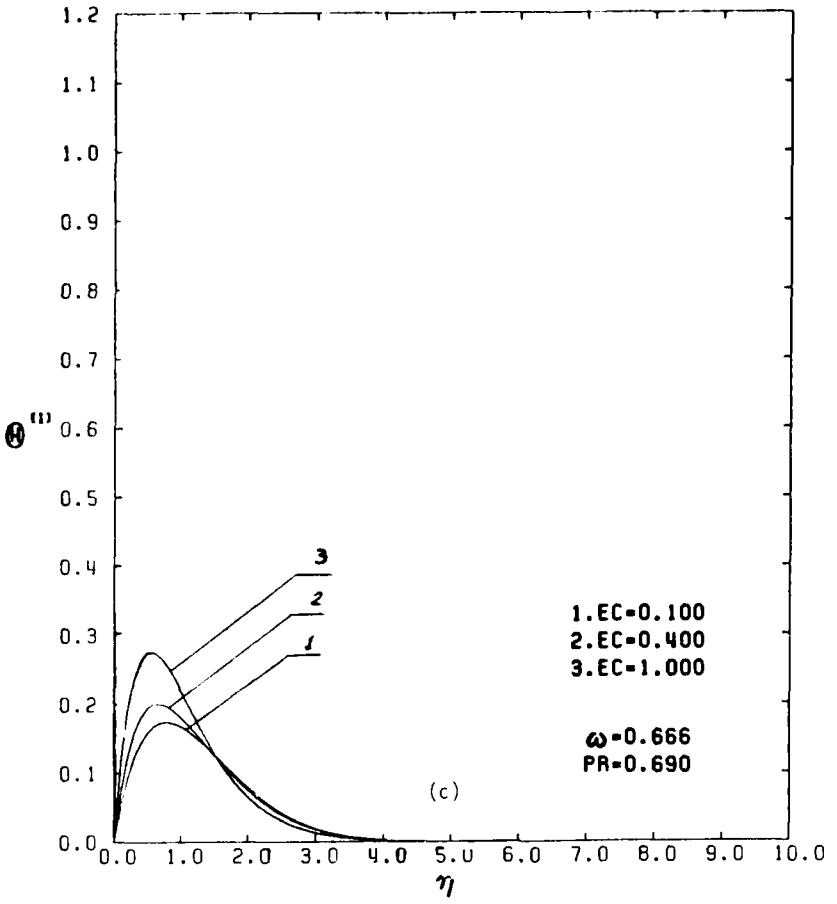

FIGURE 8 - CONTINUED

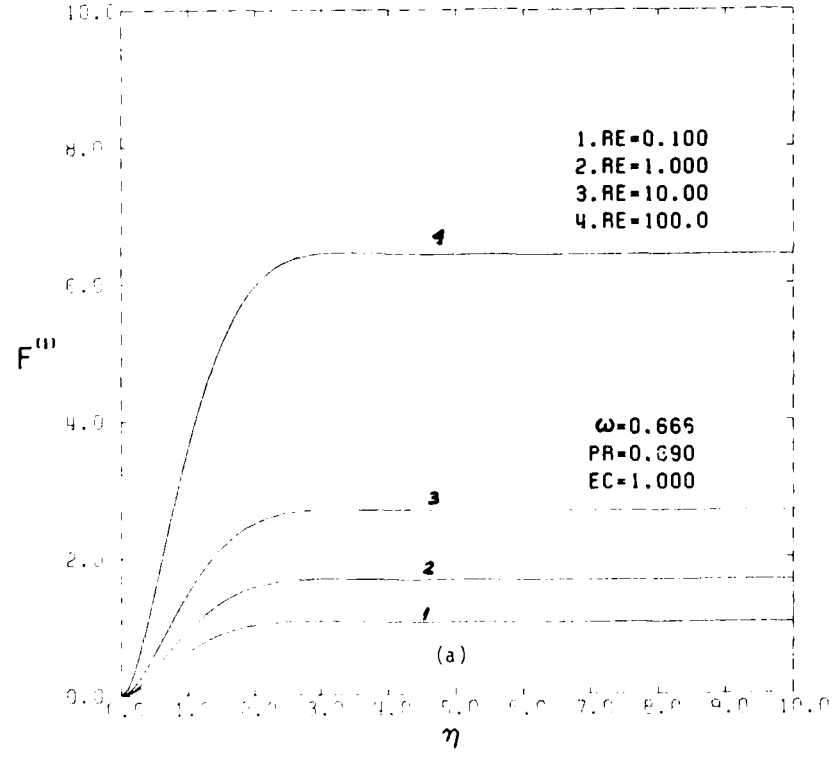

FIGURE 9. FIRST-ORDER SOLUTIONS FOR THE GAS PHASE IN THE LARGE-SLIP LIMIT FOR THE NON-STOKES CASE WITH Pr = 0.69, Ec = 0.67 AND Re_p = 0.1, 1.0, 10.0 AND 100.0, RESPECTIVELY.

(a) FUNCTION $F^{(1)}$; (b) VELOCITY $U^{(1)}$ (c) TEMPERATURE $\Theta^{(1)}$.

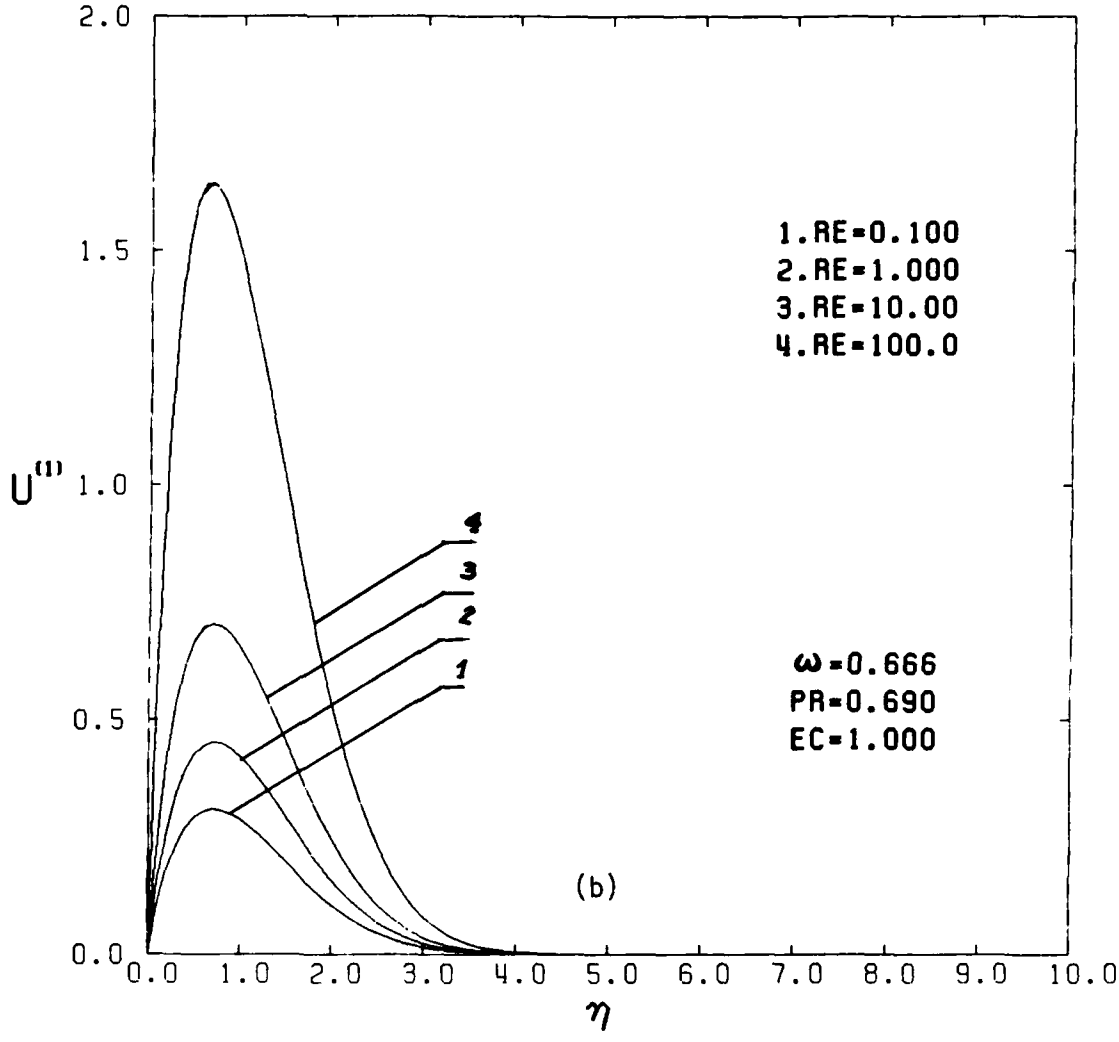
2.0
1.5
1.0
0.5
0.0
$U^{(1)}$
0.0
1.0
2.0
3.0
4.0
5.0
6.0
7.0
8.0
9.0
10.0
η
1.RE=0.100
2.RE=1.000
3.RE=10.00
4.RE=100.0
ω=0.666
PR=0.690
EC=1.000
(b)

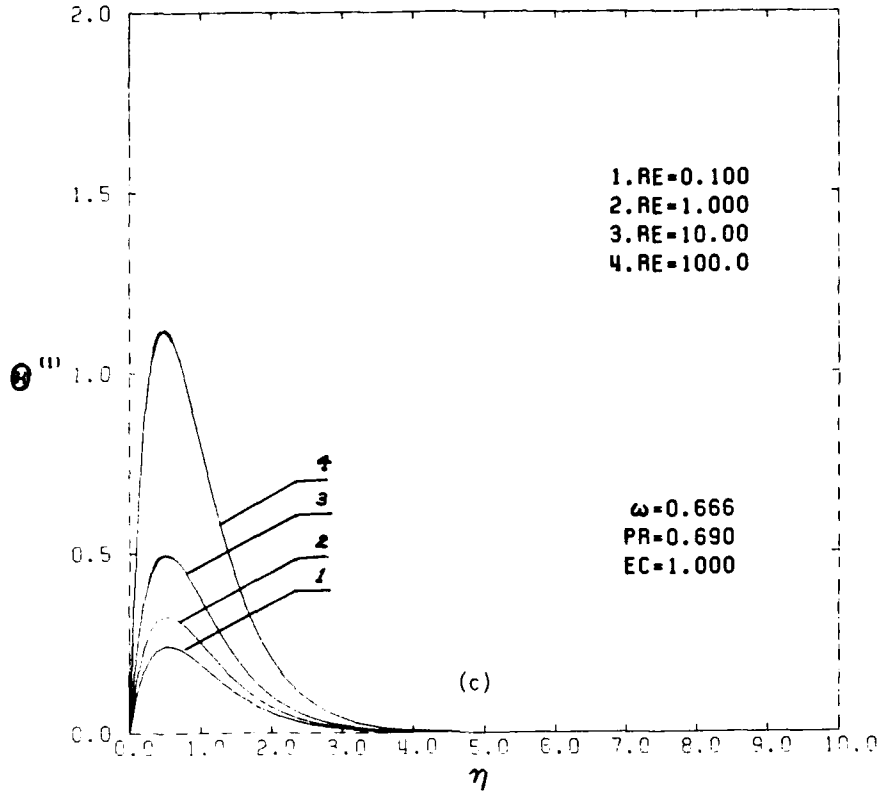

FIGURE 9 - CONTINUED

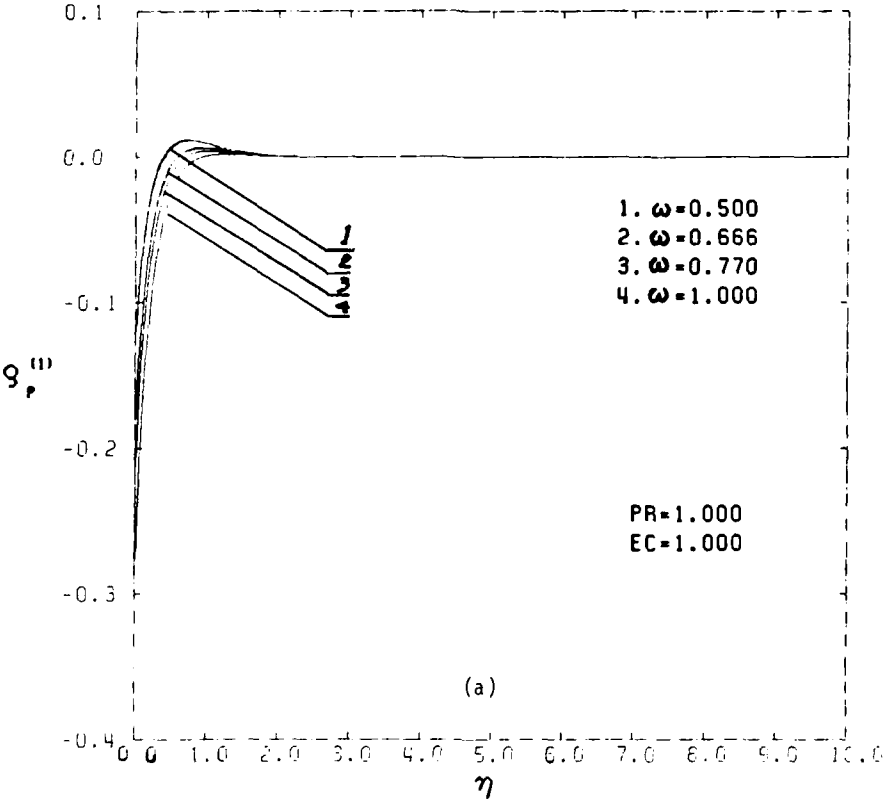

FIGURE 10. FIRST-ORDER DENSITY $\rho_p^{(1)}$ FOR THE PARTICLE PHASE IN THE LARGE-SLIP LIMIT FOR THE STOKES CASE.

(a) Pr = 1.0, Ec = 1.0 AND ω = 0.5, 0.67, 0.77 AND 1.0, RESPECTIVELY.
(b) Ec = 1.0, ω = 0.67 AND Pr = 0.69, 0.72, 0.75 AND 1.0, RESPECTIVELY.
(c) Pr = 0.69, ω = 0.67 AND Ec = 0.1, 0.4 AND 1.0, RESPECTIVELY.

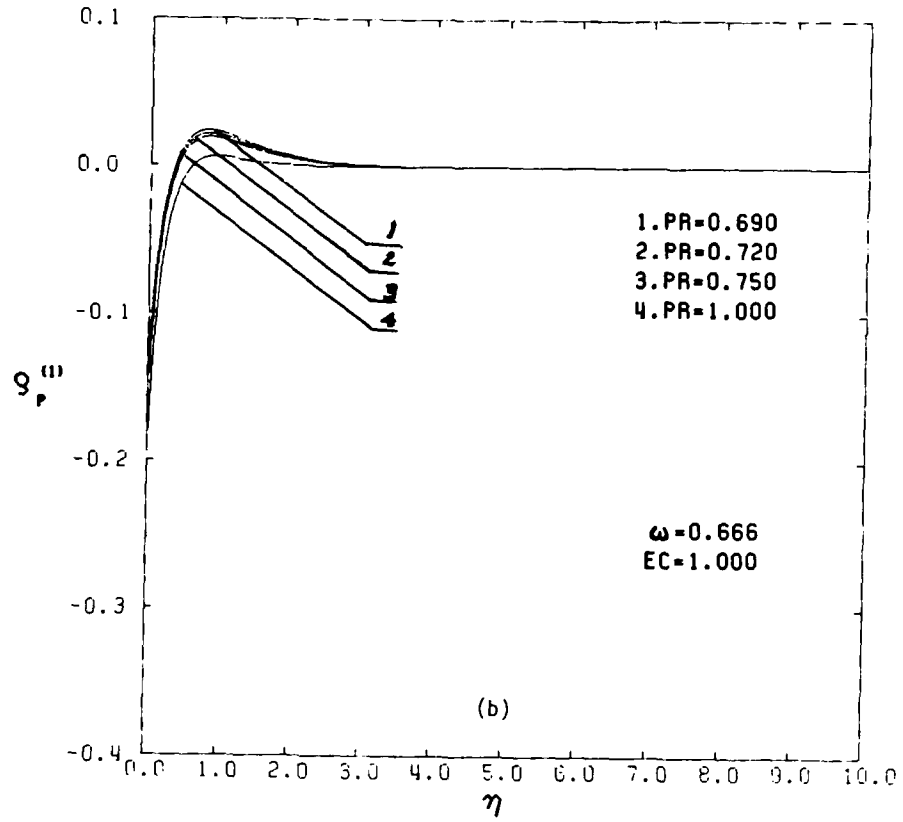

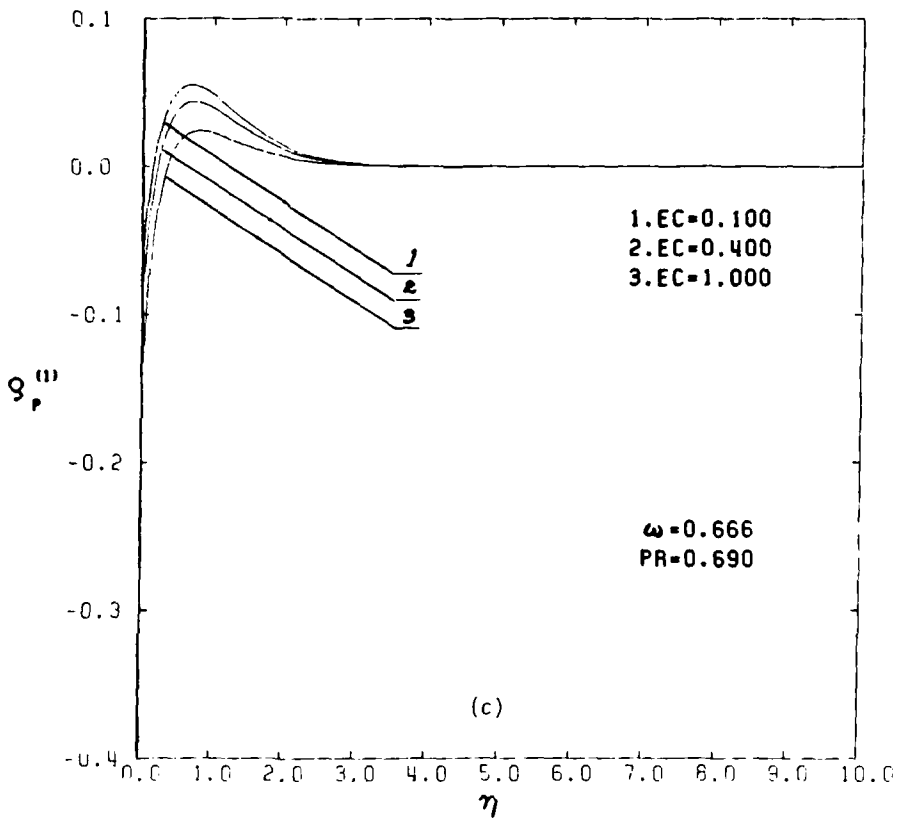

FIGURE 10 - CONTINUED

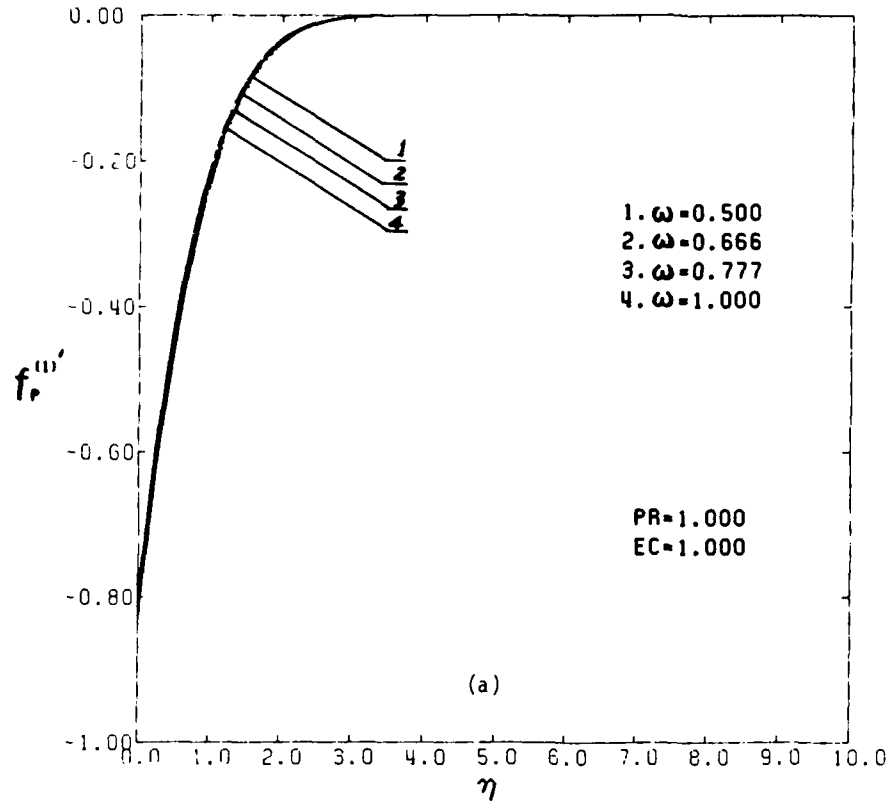

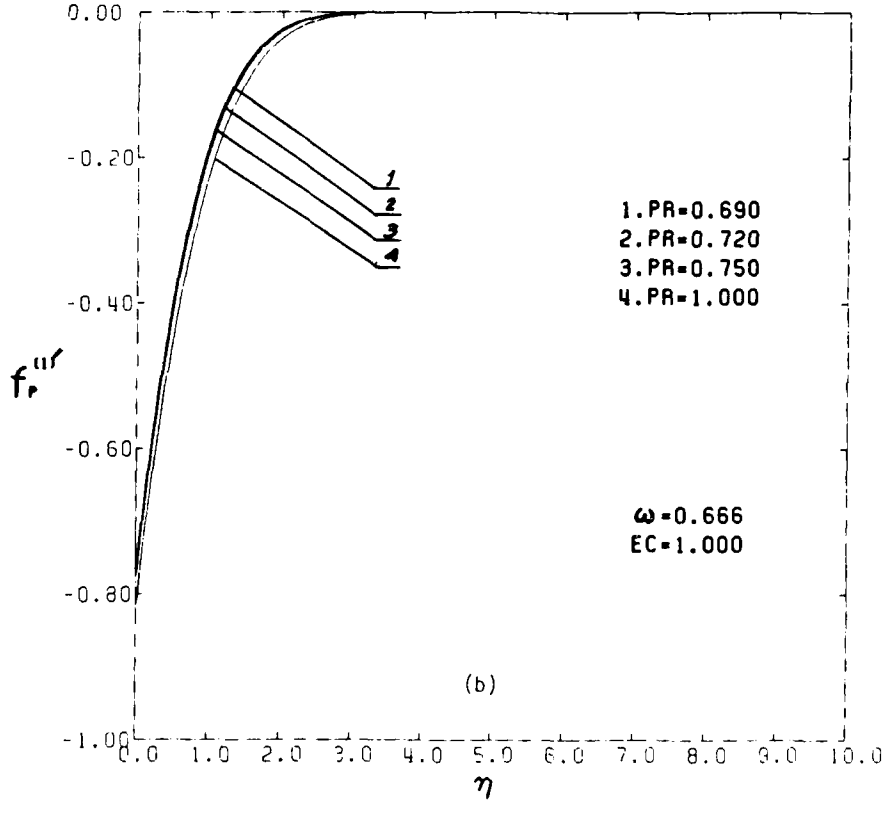

FIGURE 11. FIRST-ORDER VELOCITY $f_p^{(1)'}$ FOR THE PARTICLE PHASE IN THE LARGE-SLIP LIMIT FOR THE STOKES CASE.

(a) Pr = 1.0, Ec = 1.0 AND ω = 0.5, 0.67, 0.77 AND 1.0, RESPECTIVELY.
(b) Ec = 1.0, ω = 0.67 AND Pr = 0.69, 0.72, 0.75 AND 1.0, RESPECTIVELY.
(c) Pr = 0.69, ω = 0.67 AND Ec = 0.1, 0.4 AND 1.0, RESPECTIVELY.

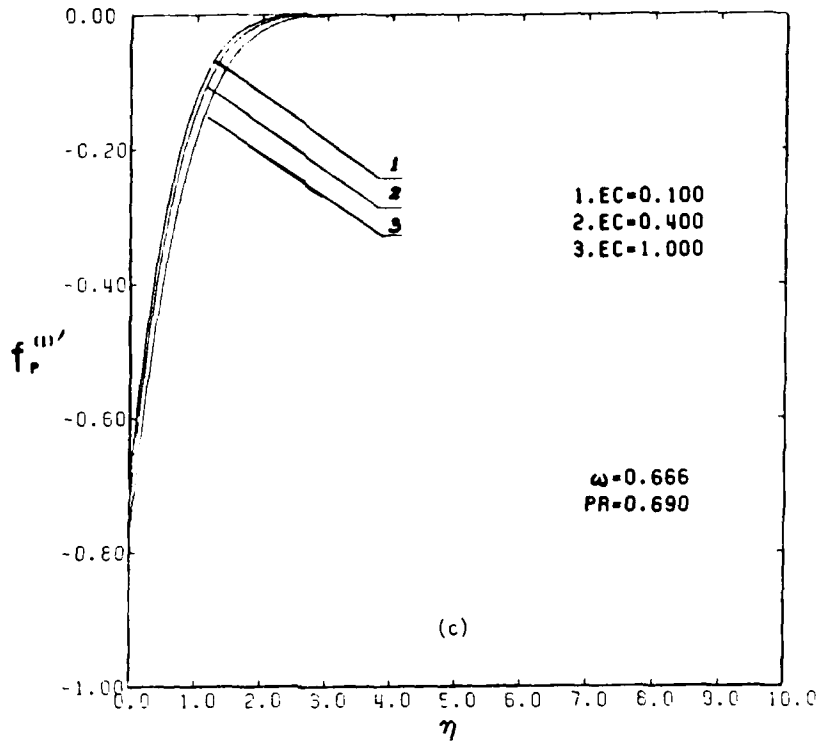

FIGURE 11 - CONTINUED

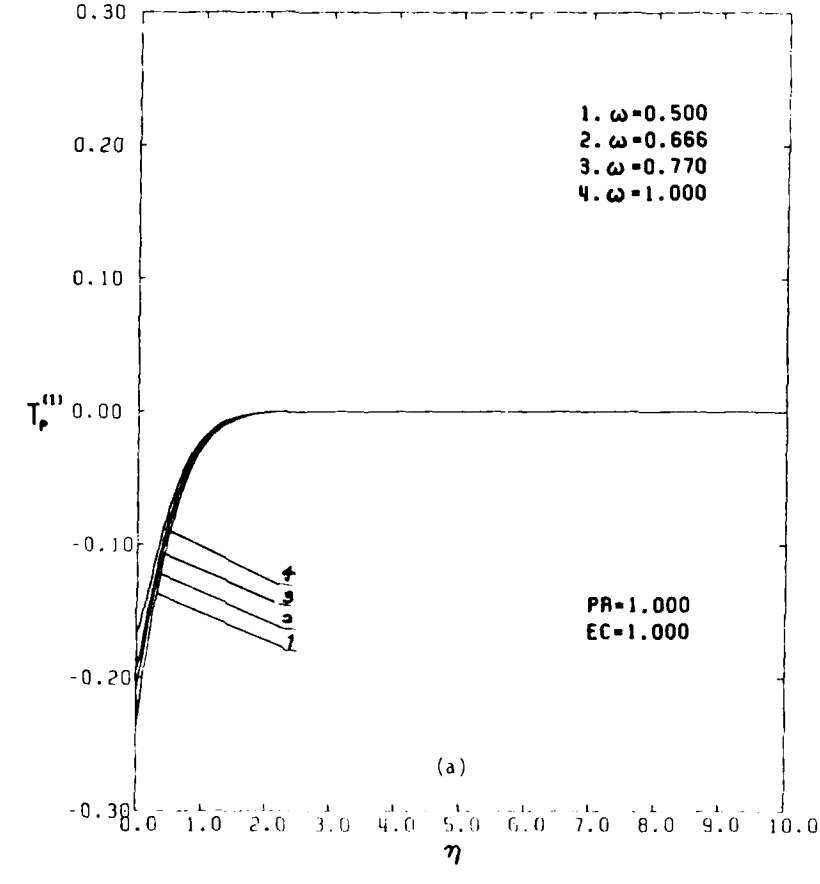

FIGURE 12. FIRST-ORDER TEMPERATURE $T_p^{(1)}$ FOR THE PARTICLE PHASE IN THE LARGE-SLIP LIMIT FOR THE STOKES CASE.

(a) Pr = 1.0, Ec = 1.0 AND ω = 0.5, 0.67, 0.77 AND 1.0, RESPECTIVELY.
(b) Ec = 1.0, ω = 0.67 AND Pr = 0.69, 0.72, 0.75 AND 1.0, RESPECTIVELY.
(c) Pr = 0.69, ω = 0.67 AND Ec = 0.1, 0.4 AND 1.0, RESPECTIVELY.

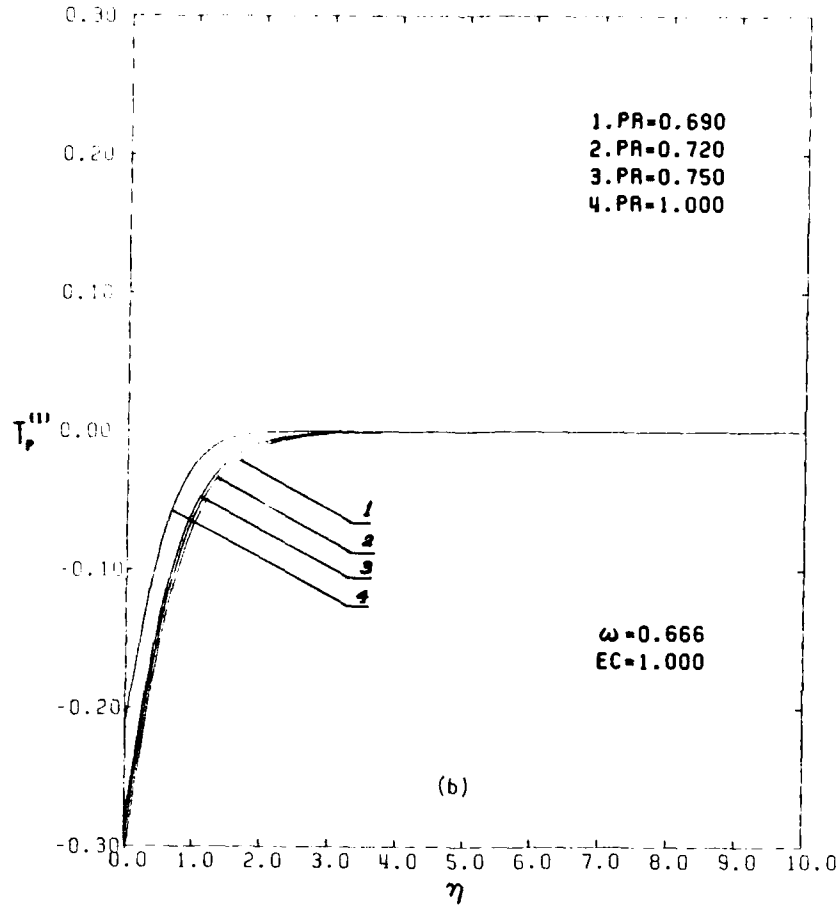

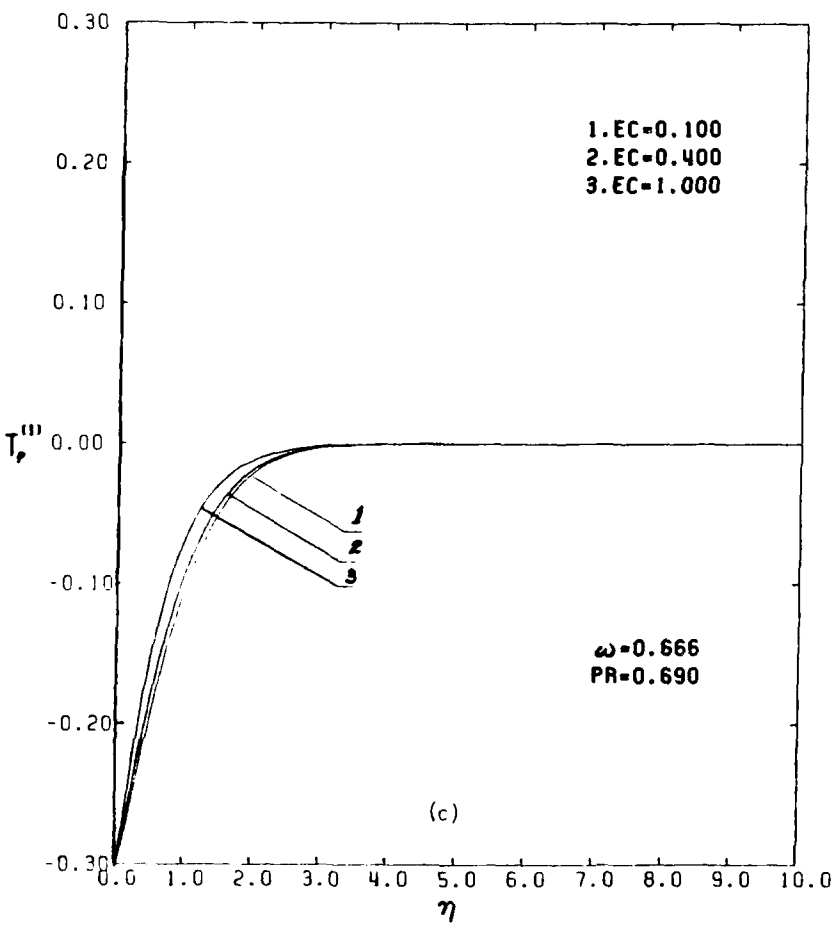

FIGURE 12 - CONTINUED

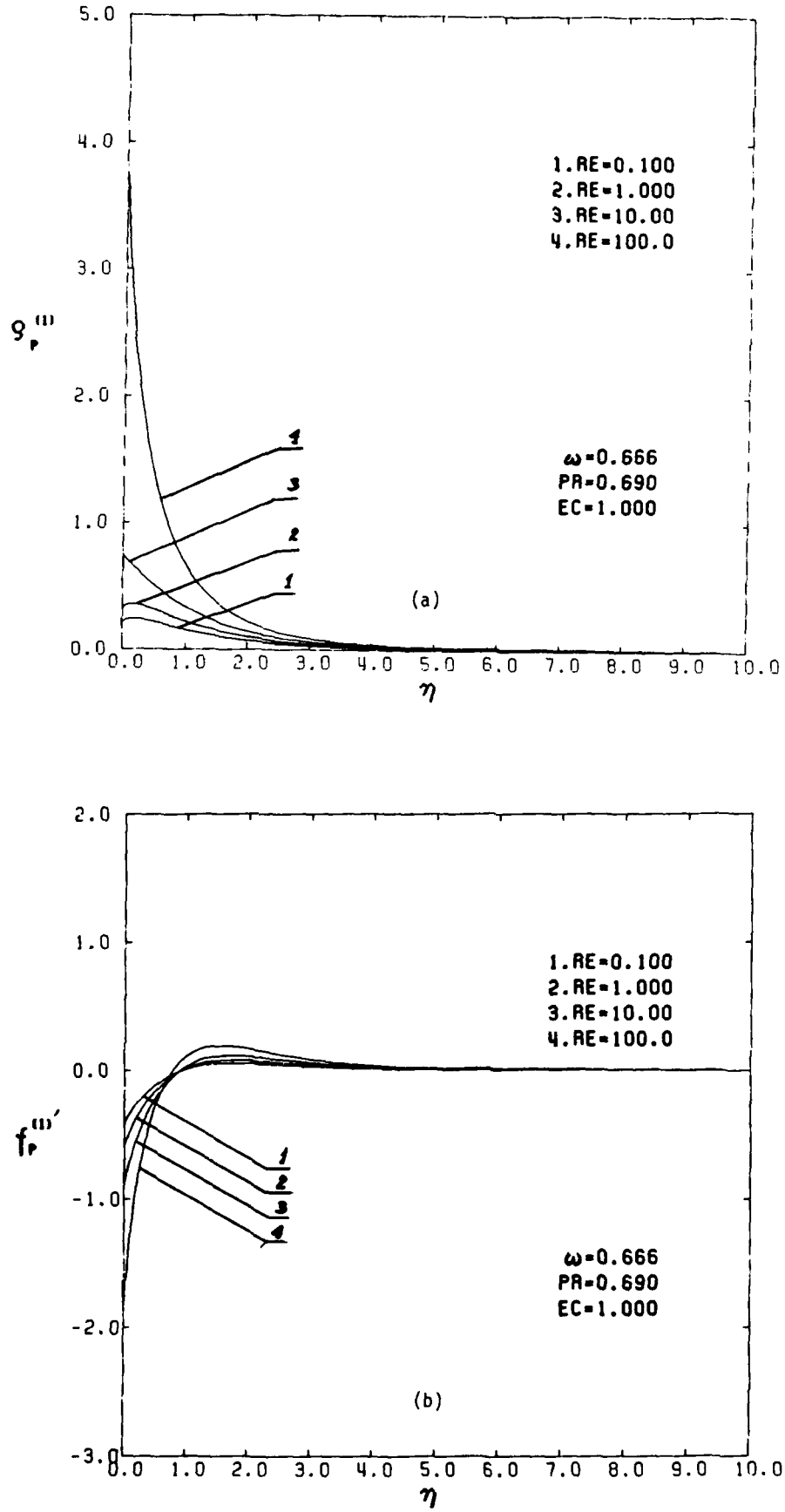

FIGURE 13. FIRST-ORDER SOLUTIONS FOR THE PARTICLE PHASE IN THE LARGE-SLIP LIMIT FOR THE NON-STOKES CASE WITH Pr = 0.69, Ec = 1.0, ω = 0.67 AND Re_p = 0.1, 1.0, 10.0 AND 100.0, RESPECTIVELY.

(a) DENSITY $\rho_p^{(1)}$; (b) VELOCITY $f_p^{(1)'}$; (c) TEMPERATURE $T_p^{(1)}$.

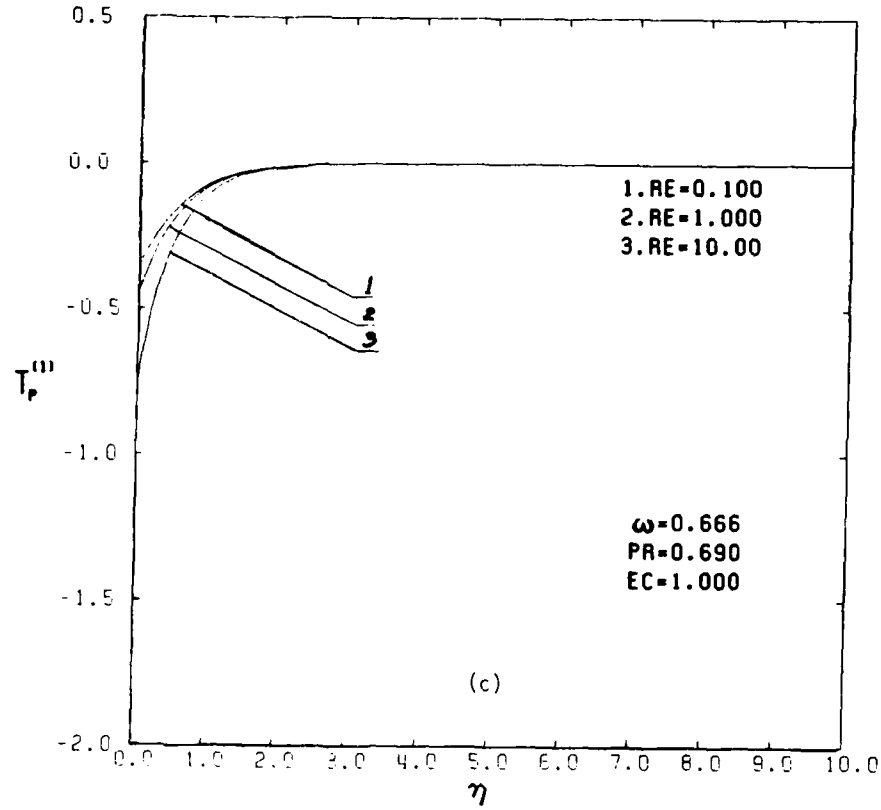

FIGURE 13 - CONTINUED

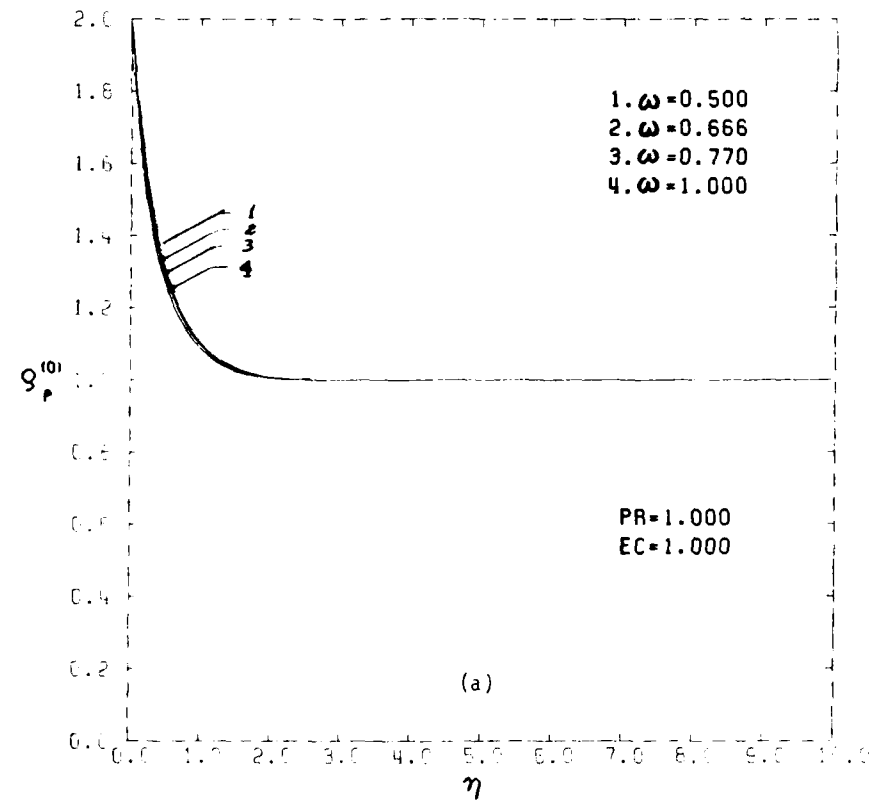

FIGURE 14. ZEROTH-ORER DENSITY $\rho_p^{(0)}$ FOR THE PARTICLE PHASE IN THE SMALL-SLIP LIMIT.

(a) Pr = 1.0, Ec = 1.0 AND ω = 0.5, 0.67, 0.77 AND 1.0, RESPECTIVELY.
(b) Ec = 1.0, ω = 0.67 AND Pr = 0.69, 0.72, 0.75 AND 1.0, RESPECTIVELY.
(c) Pr = 0.69, ω = 0.67 AND Ec = 0.1, 0.4 AND 1.0, RESPECTIVELY.

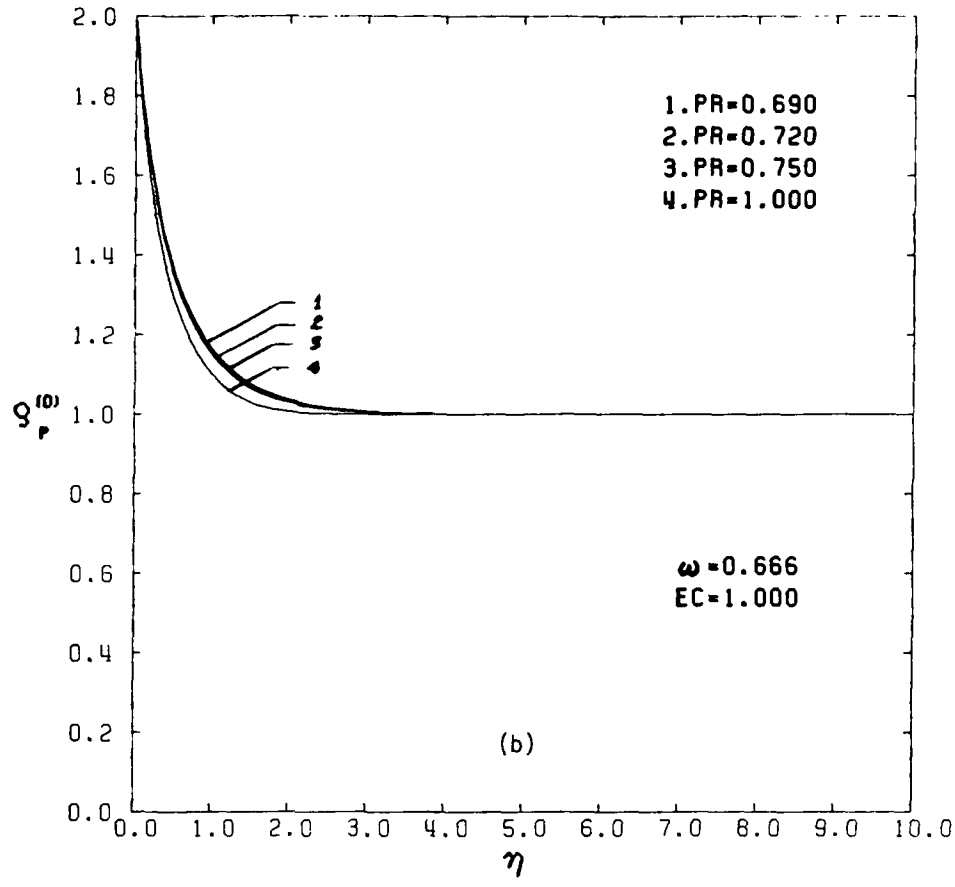

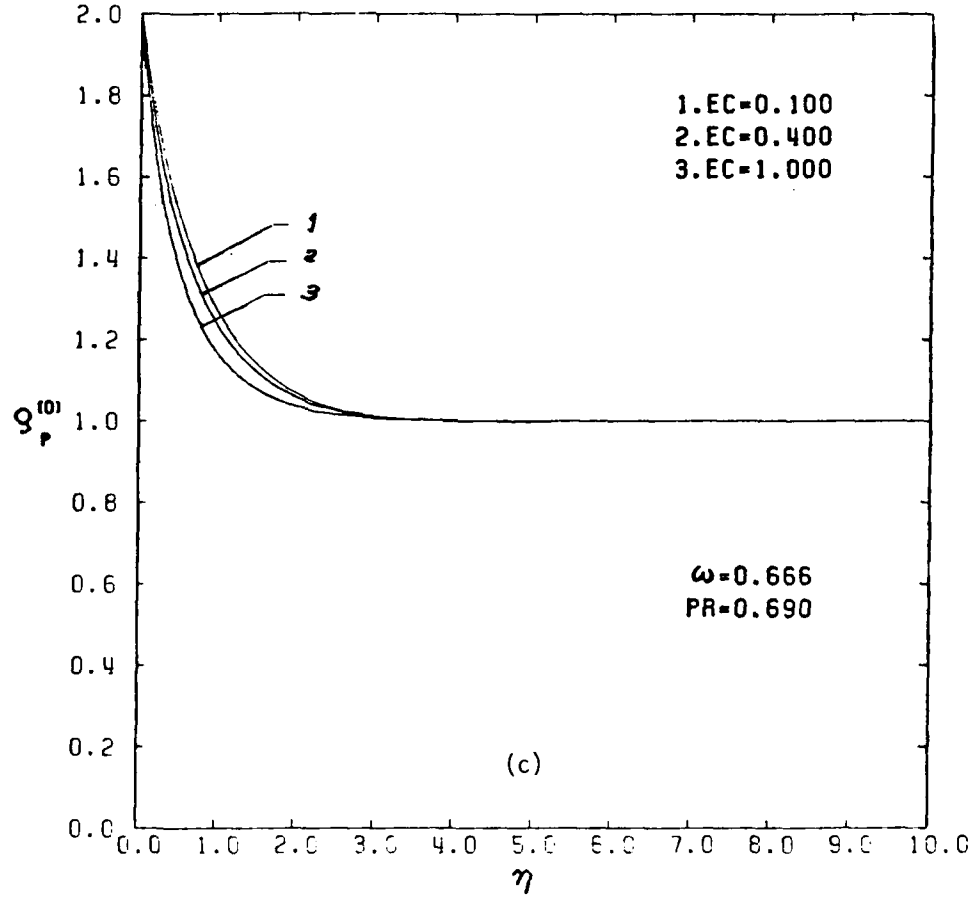

FIGURE 14 - CONTINUED

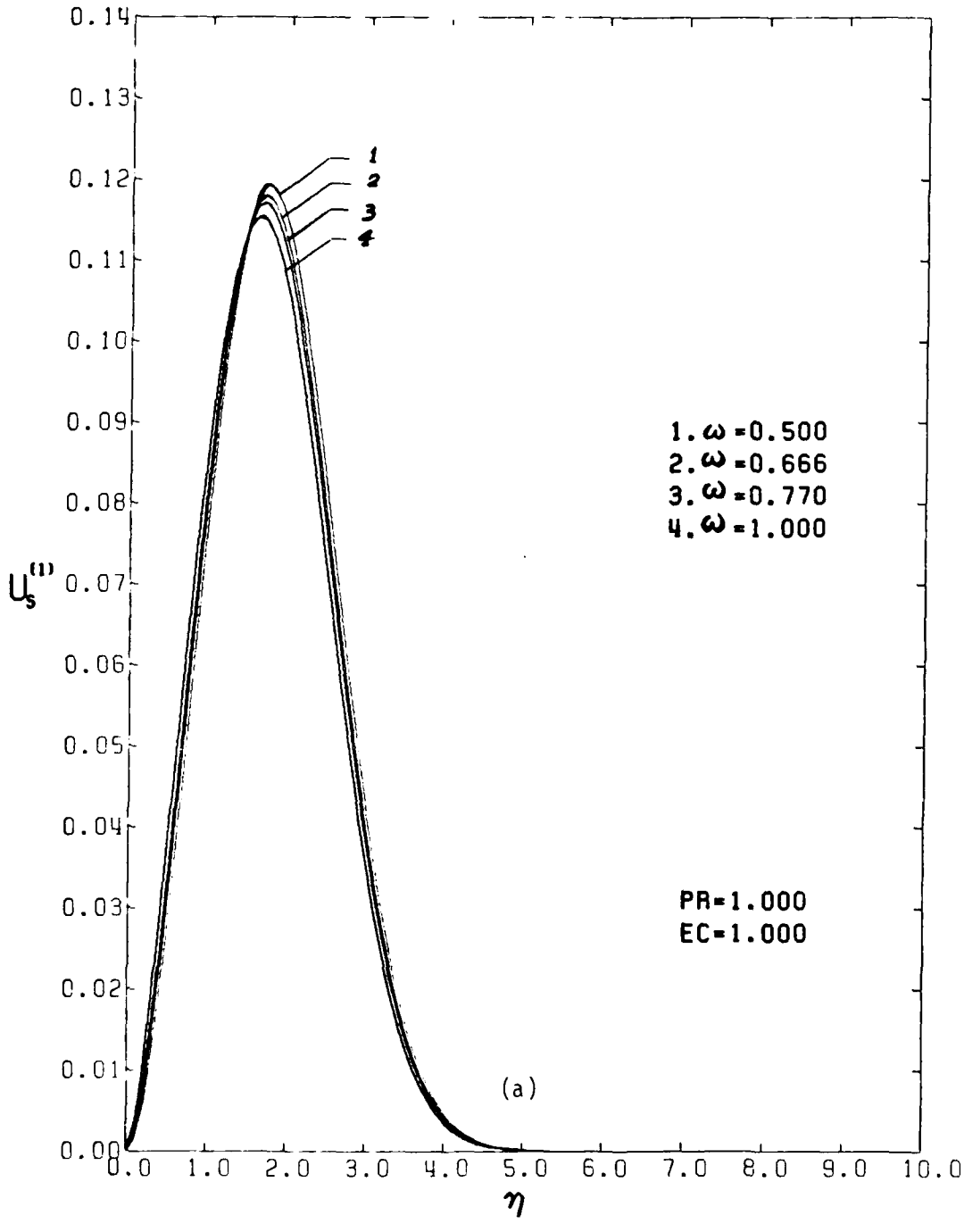

FIGURE 15. TANGENTIAL SLIP-VELOCITY $u_s^{(1)}$ IN THE SMALL-SLIP LIMIT.

(a) Pr = 1.0, Ec = 1.0 AND ω = 0.5, 0.67, 0.77 AND 1.0, RESPECTIVELY.
(b) Ec = 1.0, ω = 0.67 AND Pr = 0.69, 0.72, 0.75 AND 1.0, RESPECTIVELY.
(c) Pr = 0.69, ω = 0.67 AND Ec = 0.1, 0.4 AND 1.0, RESPECTIVELY.

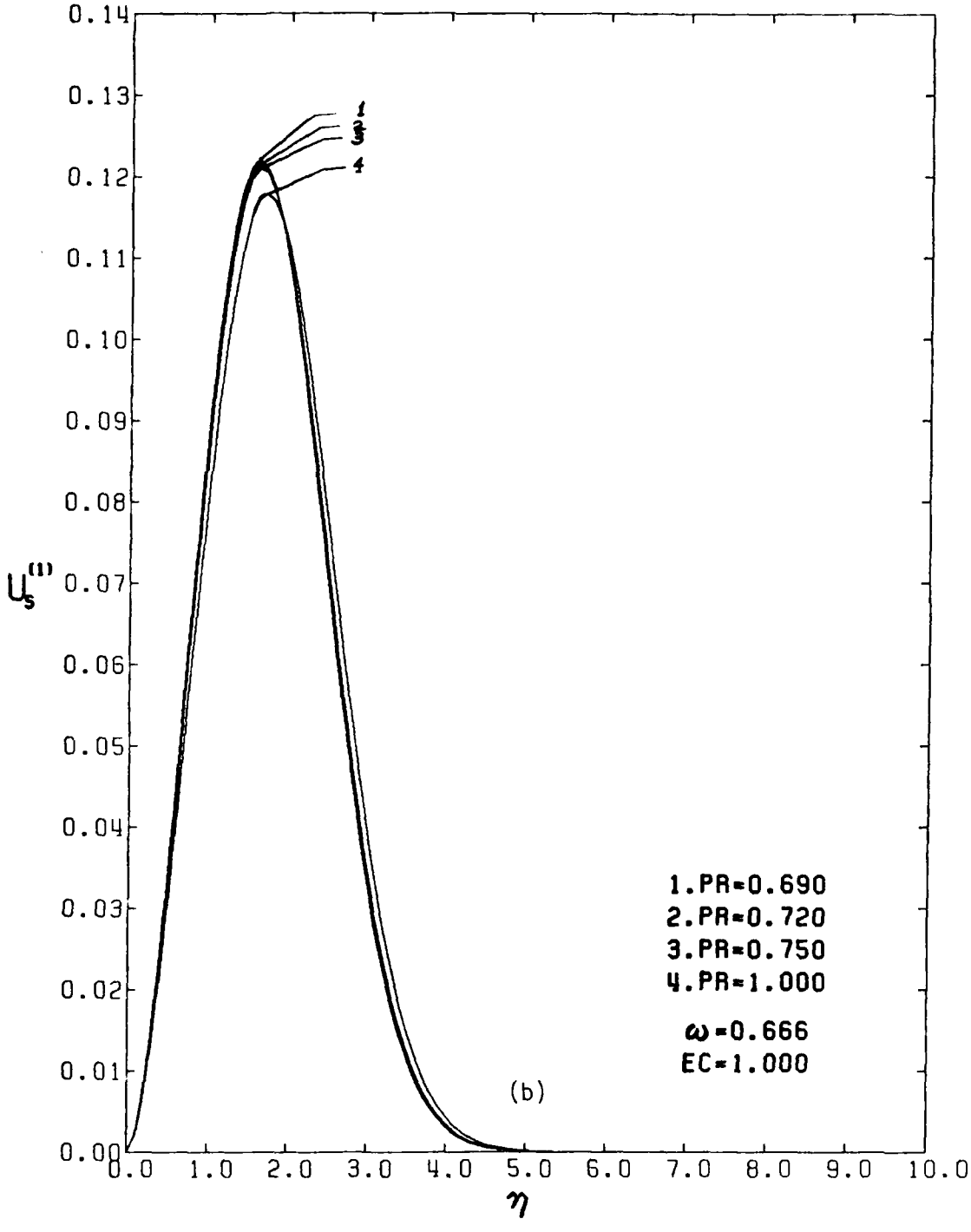
0.14
0.13
0.12
0.11
0.10
0.09
0.08
0.07
0.06
0.05
0.04
0.03
0.02
0.01
0.00
$U_s^{(1)}$
0.0
1.0
2.0
3.0
4.0
5.0
6.0
7.0
8.0
9.0
10.0
η
1
2
3
4
1.PR=0.690
2.PR=0.720
3.PR=0.750
4.PR=1.000
ω=0.666
EC=1.000
(b)

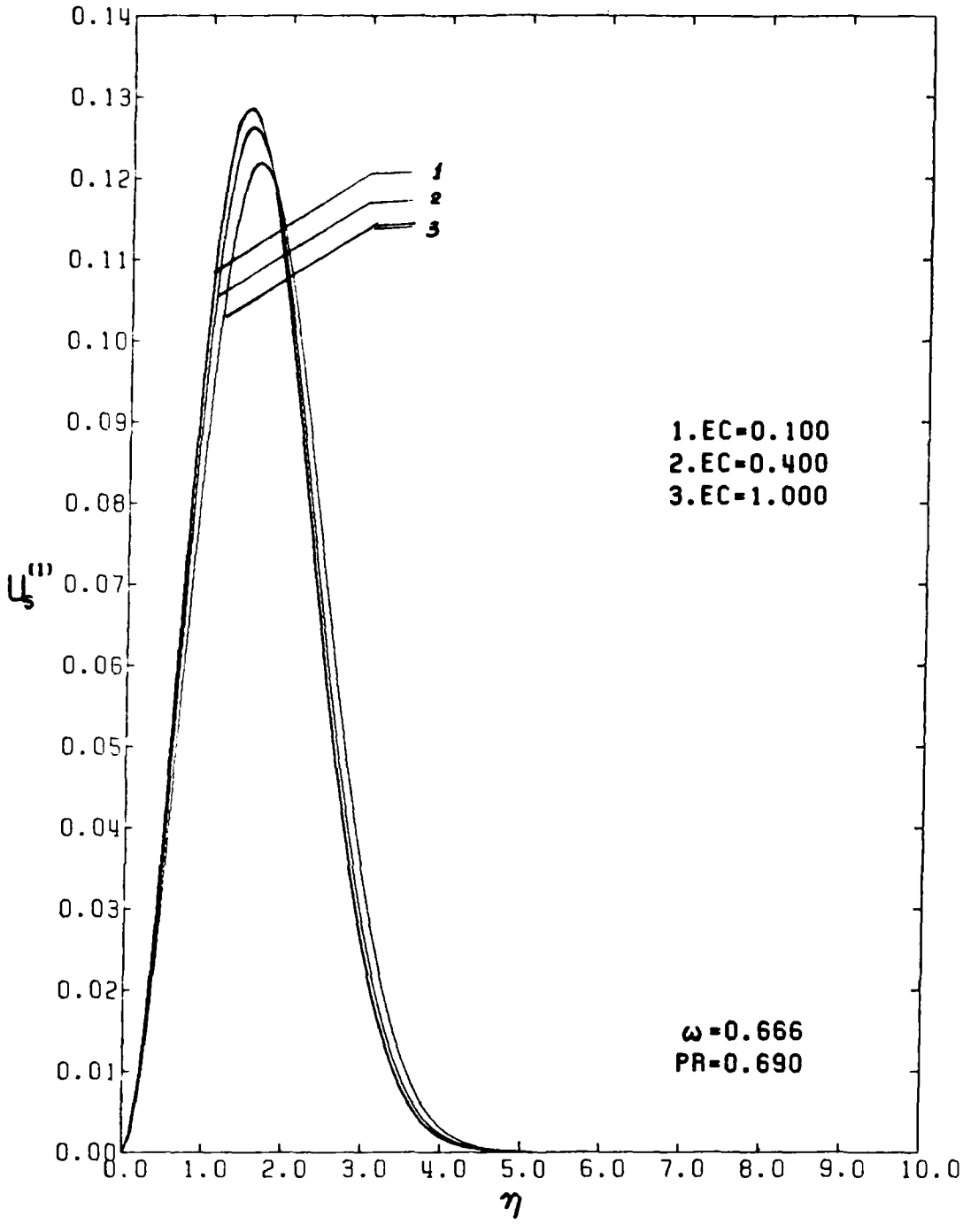

FIGURE 15 - CONTINUED

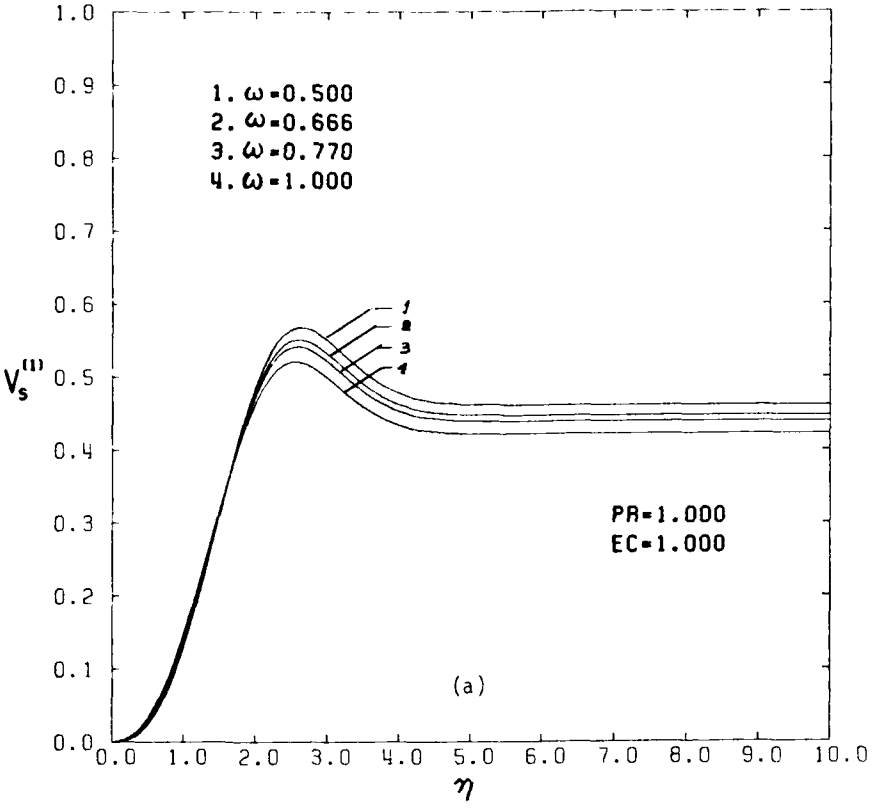

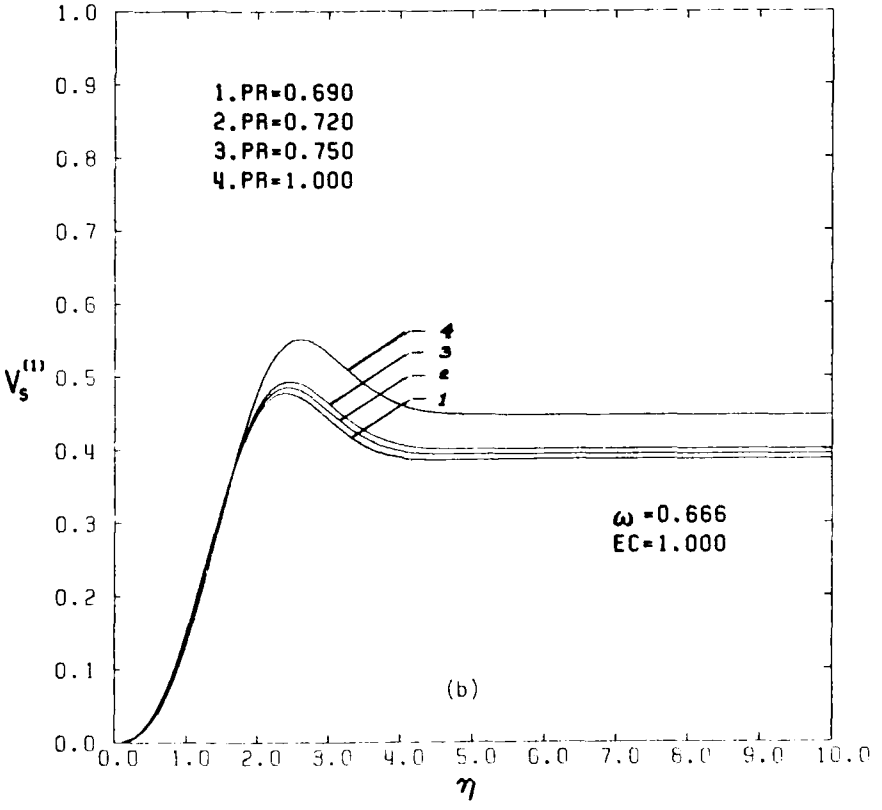

FIGURE 16. NORMAL SLIP-VELOCITY $v_s^{(1)}$ IN THE SMALL-SLIP LIMIT.

(a) Pr = 1.0, Ec = 1.0 AND ω = 0.5, 0.67, 0.77 AND 1.0, RESPECTIVELY.
(b) Ec = 1.0, ω = 0.67 AND Pr = 0.69, 0.72, 0.75 AND 1.0, RESPECTIVELY.
(c) Pr = 0.69, ω = 0.67 AND Ec = 0.1, 0.4 AND 1.0, RESPECTIVELY.

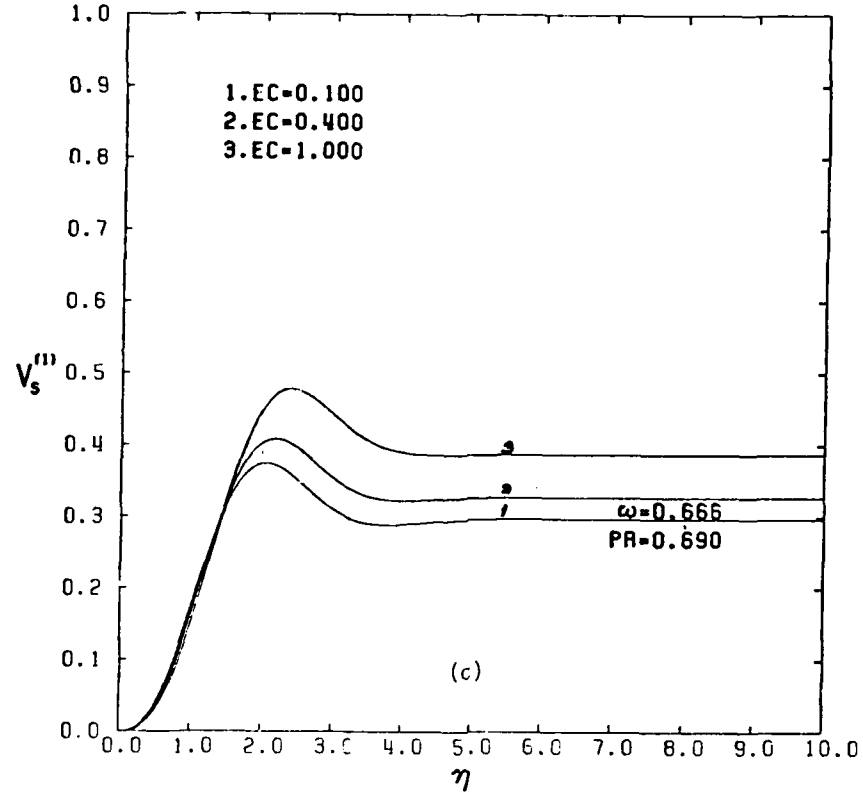

FIGURE 16 - CONTINUED

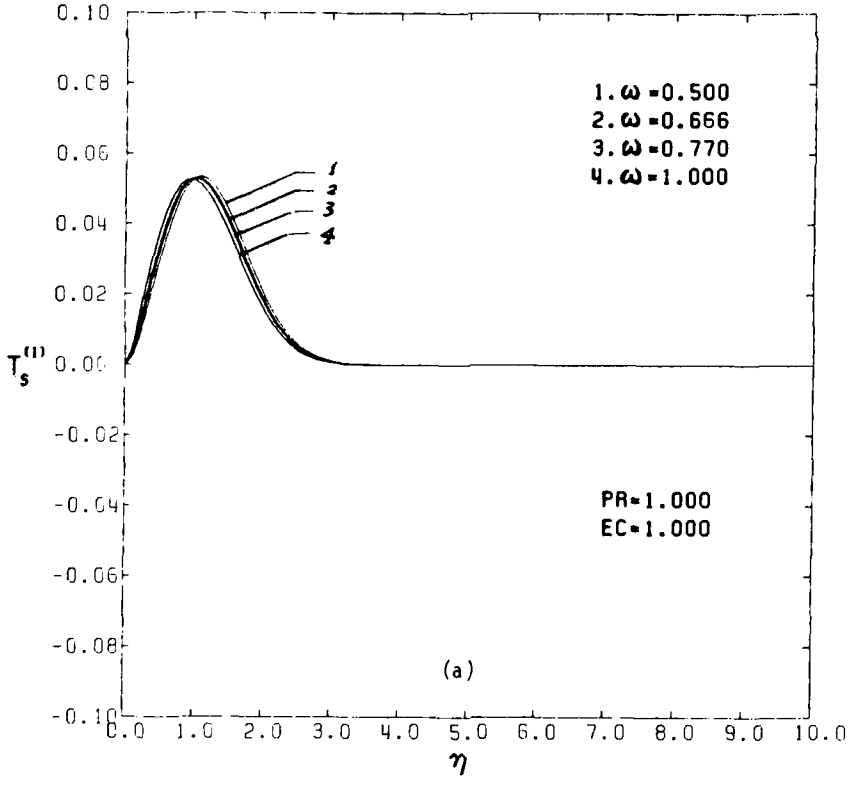

FIGURE 17. TEMPERATURE DEFECT $T_s^{(1)}$ IN THE SMALL-SLIP LIMIT.

(a) Pr = 1.0, Ec = 1.0 AND ω = 0.5, 0.67, 0.77 AND 1.0, RESPECTIVELY.
(b) Ec = 1.0, ω =0.67 AND Pr = 0.69, 0.72, 0.75 AND 1.0, RESPECTIVELY.
(c) Pr = 0.69, ω = 0.67 AND Ec = 0.1, 0.4 AND 1.0, RESPECTIVELY.

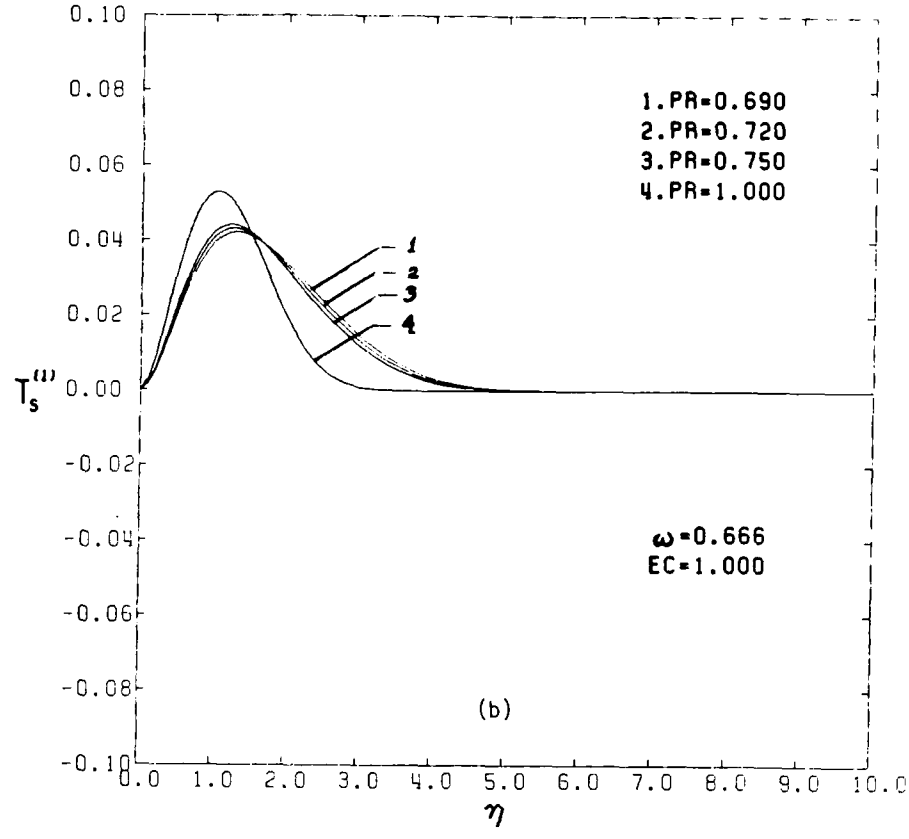

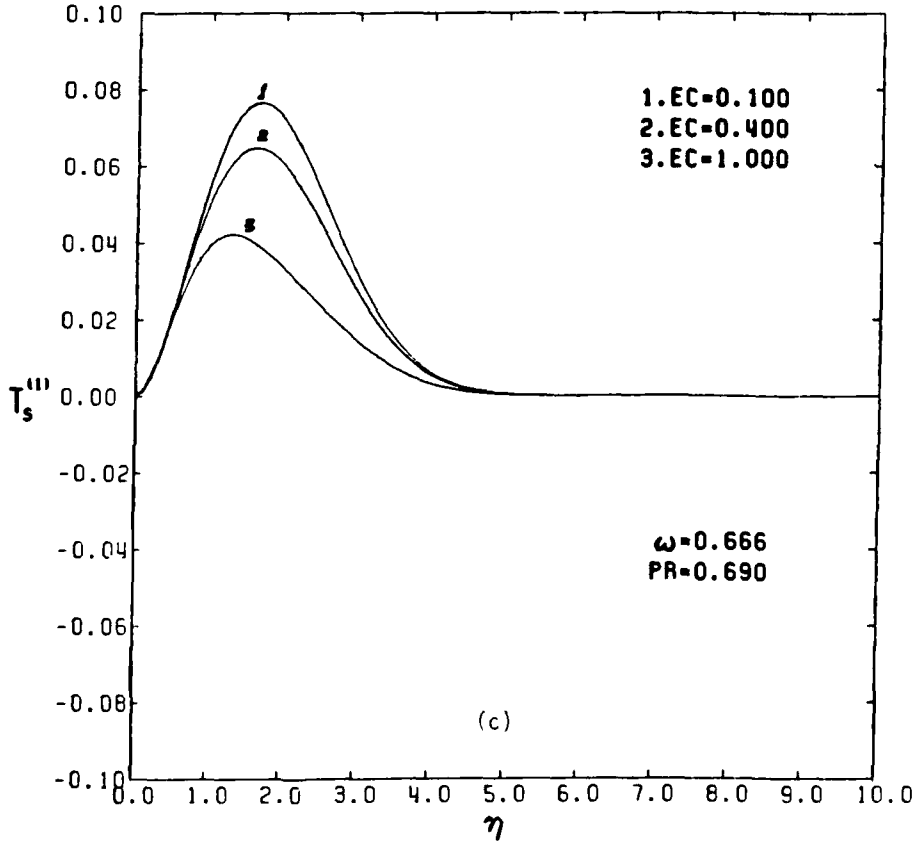

FIGURE 17 - CONTINUED

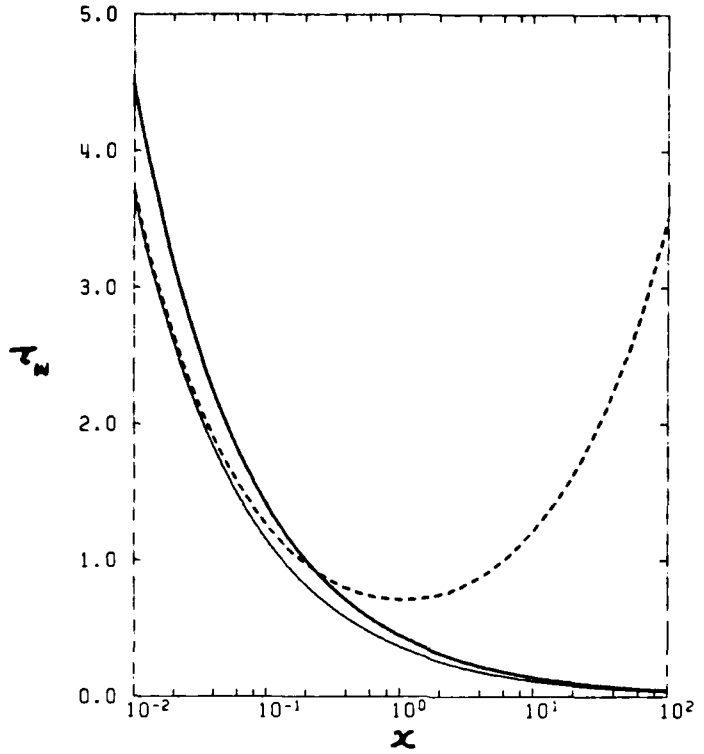

FIGURE 18. NONDIMENSIONAL SHEAR STRESS AT THE WALL AS A FUNCTION OF THE NONDIMENSIONAL DISTANCE x.

——— PURE-GAS SOLUTION; --- LARGE-SLIP SOLUTION FOR THE DUSTY GAS; ——— SMALL-SLIP SOLUTION FOR THE DUSTY GAS.

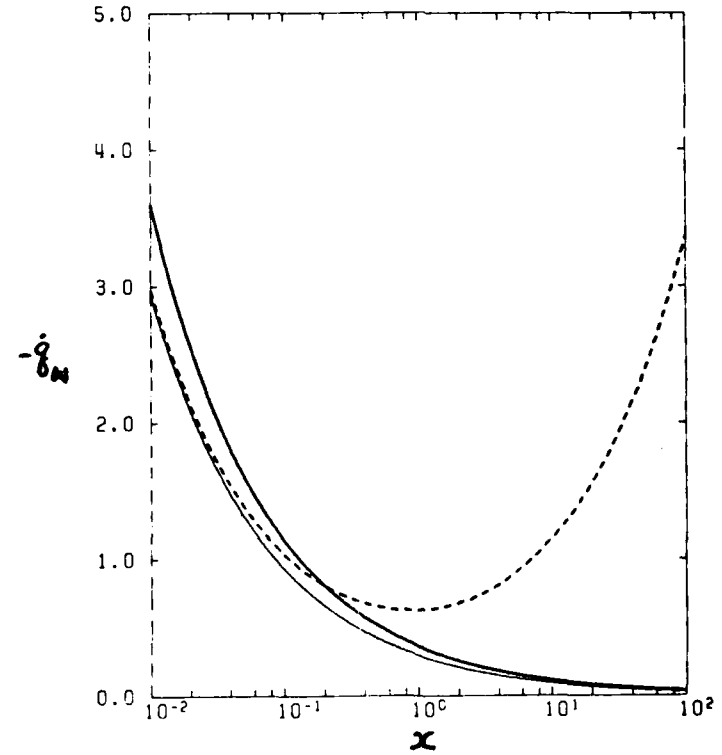

FIGURE 19. NONDIMENSIONAL HEAT-TRANSFER RATE AT THE WALL AS A FUNCTION OF THE NONDIMENSIONAL DISTANCE x.

——— PURE-GAS SOLUTION; --- LARGE-SLIP SOLUTION FOR THE DUSTY GAS; ——— SMALL-SLIP SOLUTION FOR THE DUSTY GAS.

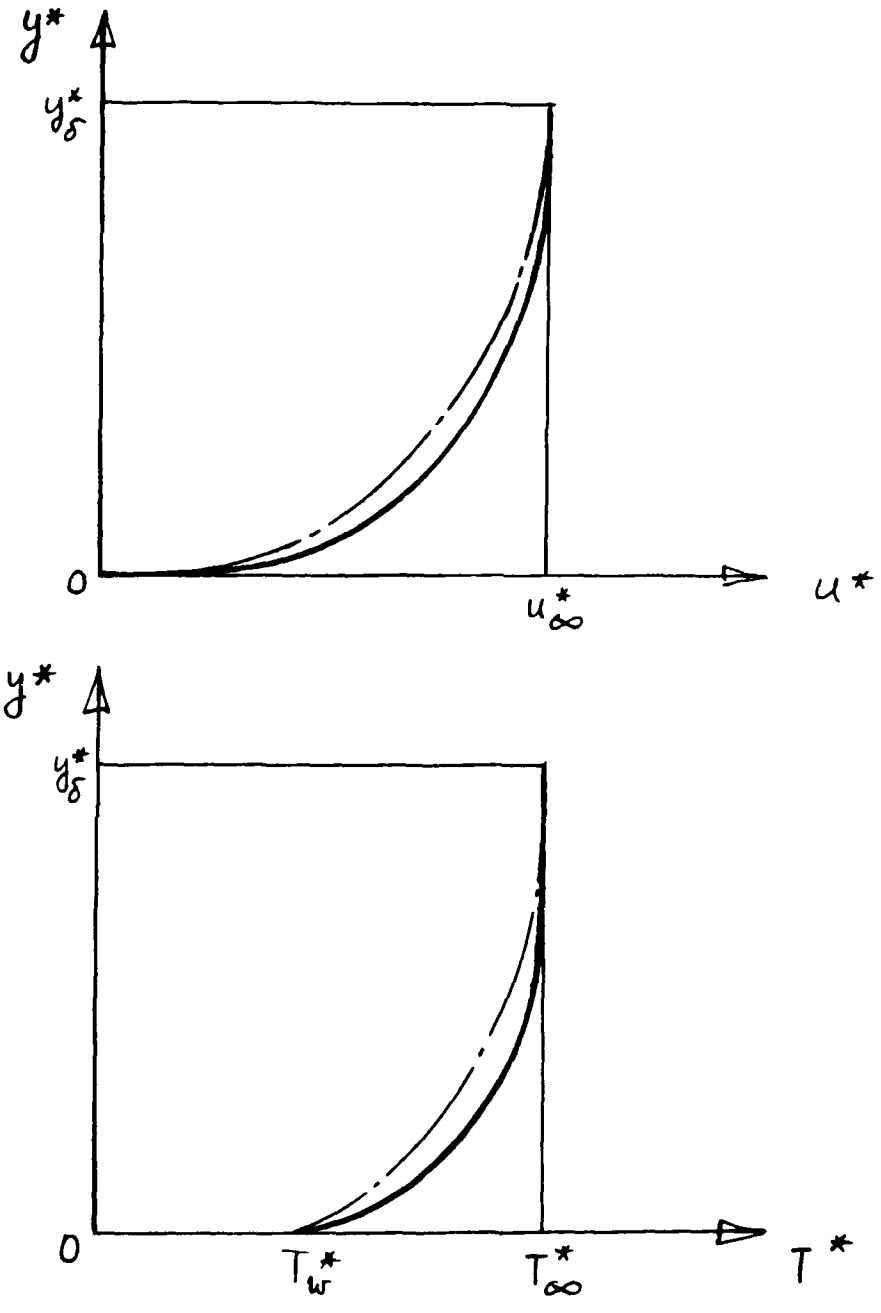

FIGURE 20. COMPARISON BETWEEN THE FLOW PROFILES OF THE GAS WITH AND WITHOUT PARTICLES.

(a) VELOCITY; (b) TEMPERATURE.
—•— WITHOUT PARTICLES; —— WITH PARTICLES.

UTIAS Report No. 310

University of Toronto, Institute for Aerospace Studies (UTIAS)
4925 Dufferin Street, Downsview, Ontario, Canada, M3H 5T6

ASYMPTOTIC SOLUTIONS TO COMPRESSIBLE LAMINAR BOUNDARY-LAYER EQUATIONS FOR DUSTY-GAS FLOW OVER A SEMI-INFINITE FLAT PLATE

Wang, B. Y., Glass, I. I.

1. Dusty-gas flows 2. Two-phase flows 3. Boundary-layer flows
4. Partial differential equations 5. Numerical analysis

I. UTIAS Report No. 310 II. Wang, B. Y., Glass, I. I.

An asymptotic analysis is given of the compressible, laminar boundary-layer flow of a dilute gas-particle mixture over a semi-infinite flat plate. The analysis extends existing work by considering more realistic drag and heat-transfer relations than those provided by Stokes. A more general viscosity-temperature expression is also incorporated into the analysis. The solution involves a series expansion in terms of the slip parameter of the particles. The numerical results, including the zeroth and first-order approximations for the gas and particle phases, are presented for the two limiting regimes: the large-slip limit near the leading edge and the small-slip limit far downstream. Significant effects on the flow produced by the particles with Stokes' and non-Stokes' relations are studied and clarified. The effects of some nondimensional similarity parameters, such as the Reynolds, Prandtl and Eckert numbers, on the two-phase boundary-layer flow are discussed.

Available copies of this report are limited. Return this card to UTIAS, if you require a copy.

UTIAS Report No. 310

University of Toronto, Institute for Aerospace Studies (UTIAS)
4925 Dufferin Street, Downsview, Ontario, Canada, M3H 5T6

ASYMPTOTIC SOLUTIONS TO COMPRESSIBLE LAMINAR BOUNDARY-LAYER EQUATIONS FOR DUSTY-GAS FLOW OVER A SEMI-INFINITE FLAT PLATE

Wang, B. Y., Glass, I. I.

1. Dusty-gas flows 2. Two-phase flows 3. Boundary-layer flows
4. Partial differential equations 5. Numerical analysis

I. UTIAS Report No. 310 II. Wang, B. Y., Glass, I. I.

An asymptotic analysis is given of the compressible, laminar boundary-layer flow of a dilute gas-particle mixture over a semi-infinite flat plate. The analysis extends existing work by considering more realistic drag and heat-transfer relations than those provided by Stokes. A more general viscosity-temperature expression is also incorporated into the analysis. The solution involves a series expansion in terms of the slip parameter of the particles. The numerical results, including the zeroth and first-order approximations for the gas and particle phases, are presented for the two limiting regimes: the large-slip limit near the leading edge and the small-slip limit far downstream. Significant effects on the flow produced by the particles with Stokes' and non-Stokes' relations are studied and clarified. The effects of some nondimensional similarity parameters, such as the Reynolds, Prandtl and Eckert numbers, on the two-phase boundary-layer flow are discussed.

Available copies of this report are limited. Return this card to UTIAS, if you require a copy.

UTIAS Report No. 310

University of Toronto, Institute for Aerospace Studies (UTIAS)
4925 Dufferin Street, Downsview, Ontario, Canada, M3H 5T6

ASYMPTOTIC SOLUTIONS TO COMPRESSIBLE LAMINAR BOUNDARY-LAYER EQUATIONS FOR DUSTY-GAS FLOW OVER A SEMI-INFINITE FLAT PLATE

Wang, B. Y., Glass, I. I.

1. Dusty-gas flows 2. Two-phase flows 3. Boundary-layer flows
4. Partial differential equations 5. Numerical analysis

I. UTIAS Report No. 310 II. Wang, B. Y., Glass, I. I.

An asymptotic analysis is given of the compressible, laminar boundary-layer flow of a dilute gas-particle mixture over a semi-infinite flat plate. The analysis extends existing work by considering more realistic drag and heat-transfer relations than those provided by Stokes. A more general viscosity-temperature expression is also incorporated into the analysis. The solution involves a series expansion in terms of the slip parameter of the particles. The numerical results, including the zeroth and first-order approximations for the gas and particle phases, are presented for the two limiting regimes: the large-slip limit near the leading edge and the small-slip limit far downstream. Significant effects on the flow produced by the particles with Stokes' and non-Stokes' relations are studied and clarified. The effects of some nondimensional similarity parameters, such as the Reynolds, Prandtl and Eckert numbers, on the two-phase boundary-layer flow are discussed.

Available copies of this report are limited. Return this card to UTIAS, if you require a copy.

UTIAS Report No. 310

University of Toronto, Institute for Aerospace Studies (UTIAS)
4925 Dufferin Street, Downsview, Ontario, Canada, M3H 5T6

ASYMPTOTIC SOLUTIONS TO COMPRESSIBLE LAMINAR BOUNDARY-LAYER EQUATIONS FOR DUSTY-GAS FLOW OVER A SEMI-INFINITE FLAT PLATE

Wang, B. Y., Glass, I. I.

1. Dusty-gas flows 2. Two-phase flows 3. Boundary-layer flows
4. Partial differential equations 5. Numerical analysis

I. UTIAS Report No. 310 II. Wang, B. Y., Glass, I. I.

An asymptotic analysis is given of the compressible, laminar boundary-layer flow of a dilute gas-particle mixture over a semi-infinite flat plate. The analysis extends existing work by considering more realistic drag and heat-transfer relations than those provided by Stokes. A more general viscosity-temperature expression is also incorporated into the analysis. The solution involves a series expansion in terms of the slip parameter of the particles. The numerical results, including the zeroth and first-order approximations for the gas and particle phases, are presented for the two limiting regimes: the large-slip limit near the leading edge and the small-slip limit far downstream. Significant effects on the flow produced by the particles with Stokes' and non-Stokes' relations are studied and clarified. The effects of some nondimensional similarity parameters, such as the Reynolds, Prandtl and Eckert numbers, on the two-phase boundary-layer flow are discussed.

Available copies of this report are limited. Return this card to UTIAS, if you require a copy.

END

7-87

DTIC